BAW-2439
May 2003

Analysis of the B&W Owners Group Capsule TMI2-LG2

-- Master Integrated Reactor Vessel Surveillance Program --

by

J. B. Hall
J. W. Newman, Jr.

Framatome ANP Document No. 43-2439-00
(See Section 9 for document signatures.)

Prepared for

B&W Owners Group
Reactor Vessel Working Group

Dominion Energy
Duke Energy Corporation
Entergy Operations, Inc.
Exelon Nuclear Corporation
FirstEnergy Nuclear Operating Company
Florida Power Corporation
Florida Power & Light Company
Nuclear Management Company

Prepared by

Framatome ANP, Inc.
3315 Old Forest Road
P. O. Box 10935
Lynchburg, Virginia 24506-0935

FRAMATOME ANP

Executive Summary

This report describes the results of the testing of the specimens from the B&W Owners Group TMI2-LG2 capsule as part of the B&W Owners Group Master Integrated Reactor Vessel Surveillance Program (MIRVP). The objective of the MIRVP program is to monitor the effects of neutron irradiation on the mechanical properties of their reactor vessel materials. The TMI2-LG2 capsule was inserted into the Crystal River Unit 3 reactor vessel at the end of cycle 6 and removed at the end of cycle 12. The TMI2-LG2 capsule contained irradiated tensile, Charpy V-notch, and compact fracture specimens of three sources of Linde 80-weld metal all fabricated with the 299L44 weld wire heat. The specimens were irradiated to a fluence between 1.17 to 2.01 x 10^{19} n/cm^2 (E > 1.0 MeV).

The measured Charpy V-notch upper-shelf energies for the three 299L44 welds tested are less than the required 50 ft-lbs limit per 10 CFR 50 Appendix G "Fracture Toughness Requirements," as expected. The upper-shelf fracture toughness tests conducted on the three 299L44 welds demonstrate that the current model in use for justifying continued operation per 10 CFR 50 Appendix G conservatively represents this test data.

On average the shift in the master curve fracture toughness based reference temperature (T_0) for all 299L44 welds measured to date are less than the predicted Charpy impact transition temperature shift based on 10 CFR 50.51 "Fracture Toughness Requirements for Protection Against Pressurized Thermal Shock Events" and NRC Regulatory Guide 1.99, Revision 2, Position 1. In addition, the average shift and scatter in the fracture toughness based reference temperature for all 299L44 welds measured to date are less than the measured Charpy impact transition temperature shift.

The irradiation embrittlement results reported herein measure the shift in the ductile-to-brittle transition temperature using the master curve methodology per ASTM E 1921. This shift measurement technique is not the same as that specified in 10CFR50.61 and 10CFR50 Appendix G, therefore current licensed pressurized thermal shock and adjusted reference temperatures (used in establishing operating pressure-temperature curves) are not affected. However, each licensee can use the embrittlement measurements reported herein to improve pressurized thermal shock values and adjusted reference temperatures as part of a separate submittal using the master curve methodology.

Table of Contents

Appendices

List of Tables

List of Tables (Continued)

List of Figures

List of Figures (Continued)

List of Figures (Continued)

1.0 Introduction

The B&W Owners Group (B&WOG) Master Integrated Reactor Vessel Surveillance Program (MIRVP) is designed to provide the data required for continued licensability of 13 reactor vessels fabricated by Babcock & Wilcox (B&W).[1, 2] These reactor vessels include seven B&W-designed 177-Fuel Assembly (FA) plants and six Westinghouse-designed plants with B&W-fabricated reactor vessels. The MIRVP is built upon the integrated surveillance program developed by the B&WOG for the B&W 177-FA plants.[2]

The MIRVP combines the separate plant-specific reactor vessel surveillance programs (RVSPs) and, where appropriate or necessary, provides for sharing of irradiation sites. The MIRVP consists of three parts: plant-specific RVSP capsules, supplementary weld metal surveillance capsules (SUPCAPs), and higher fluence supplementary weld metal surveillance capsules (HUPCAPs). The first part of the MIRVP is the continuation of the plant-specific RVSPs that monitor the irradiation damage to selected materials, as originally planned. The plant-specific RVSP capsules are being irradiated either in the original plant intended or in a B&W 177-FA host reactor. The second part of the MIRVP consists of a series of specially designed supplementary weld metal surveillance capsules (SUPCAPs) to study the effect of irradiation on a number of weld metals, which are anticipated to be highly sensitive to irradiation damage because of their chemical composition and low initial Charpy upper-shelf energies. The third part of the MIRVP consists of higher fluence supplementary weld metal surveillance capsules (HUPCAPs) to obtain irradiated weld metal data (primarily fracture toughness properties) to satisfy the requirements of 10 CFR 50, Appendix G, "Fracture Toughness Requirements," [3] and 10 CFR 50, Appendix H, "Reactor Vessel Material Surveillance Program Requirements," [4] for the current license and license renewal of the plants involved in this program.

The HUPCAPs were prepared to (1) provide for additional B&W-design irradiation capsules to expand and enlarge the compact fracture toughness database for Linde 80-weld metals; (2) provide an irradiation capsule of Westinghouse-design for correlation of irradiation data in the Westinghouse neutronic environment with the B&W 177-FA environment; and (3) provide capsules for a weld metal annealing response investigation.

The TMI2-LG2 capsule was irradiated in the Three Mile Island Unit 2 (TMI-2) reactor from start-up until the incident of March 29, 1979, which caused the closure of the unit. Both the TMI-2

specific and the B&WOG SUPCAP capsules were withdrawn from the TMI-2 reactor vessel. Through a capsule re-qualification program, it was determined that the capsules were briefly heated to temperatures in the range of 621°F and 700°F. The re-qualification effort concluded that the capsules could continue being irradiated in the B&WOG MIRVP.[5] The TMI2-D, TMI2-LG1, and TMI2-LG2 were transferred to and inserted into the Crystal River Unit 3 reactor vessel at the end of cycle 6 and removed at the end of cycle 12. This schedule allowed testing of specimens ahead of the B&WOG Reactor Vessel Working Group (RVWG) reactor vessel needs. This report presents the examination results of the SUPCAP TMI2-LG2 capsule.

2.0 Background

The ability of the reactor vessel to resist fracture is a primary factor in ensuring the safety of the primary coolant system in light water reactors. The reactor vessel beltline region is the most critical region of the vessel because it is exposed to the highest level of neutron-irradiation. The general effects of fast neutron-irradiation on the mechanical properties of weld metals used in the fabrication of reactor vessels are well characterized and documented. Weld metals used in the beltline region of reactor vessels exhibit an increase in ultimate and yield strength properties with a corresponding decrease in ductility after irradiation. The most significant mechanical property change in reactor vessel steels is the increase in the ductile-to-brittle transition temperature accompanied by a reduction in the upper-shelf fracture toughness.

10 CFR 50, Appendix G, "Fracture Toughness Requirements," specifies minimum fracture toughness requirements for the ferritic materials of the pressure-retaining components of the reactor coolant pressure boundary (RCPB) of commercial light water reactors and provides specific guidelines for determining the pressure-temperature limitations for operation of the RCPB. The fracture toughness and operational requirements are specified to provide adequate safety margins during normal operation, including anticipated operational occurrences and system hydrostatic tests, to which the pressure boundary may be subjected over its lifetime. The requirements of 10 CFR 50, Appendix G, became effective on August 16, 1973. These requirements are applicable to all boiling and pressurized light water nuclear power reactors, including those under construction or in operation on the effective date.

10 CFR 50, Appendix H, "Reactor Vessel Material Surveillance Program Requirements," defines the material surveillance program required to monitor changes in the fracture toughness properties of ferritic materials in the reactor vessel beltline region of light water-cooled reactors resulting from exposure to neutron-irradiation and the thermal environment. Fracture toughness test data are obtained from material specimens contained in capsules that are periodically withdrawn from the reactor vessel. These data permit determination of the conditions under which the vessel can be operated with adequate safety margins against nonductile fracture throughout its service life.

A method for guarding against nonductile fracture in reactor vessels is described in Appendix G of the American Society for Mechanical Engineering (ASME) Boiler and Pressure Vessel (B&PV) Code, Section III, "Nuclear Power Plant Components"[6] and Section XI, "Rules for Inservice

Inspection."[7] This method uses fracture mechanics concepts and the reference nil-ductility temperature, RT_{NDT}, which is defined as the greater of the drop weight nil-ductility transition temperature (in accordance with ASTM Standard E 208-81[8]) or the temperature that is 60°F below that at which the material exhibits 50 ft-lbs of impact energy and 35 mils lateral expansion. The RT_{NDT} of a given material is used to index that material to a reference stress intensity factor curve (K_{IR} curve), which appears in Appendix G of the ASME B&PV Code Section III and Section XI. The K_{IR} curve is a lower bound of dynamic and crack arrest fracture toughness data obtained from several heats of pressure vessel steel. When a given material is indexed to the K_{IR} curve, allowable stress intensity factors can be obtained for the material as a function of temperature. The operating pressure-temperature limits can then be determined using these allowable stress intensity factors.

The RT_{NDT} and, in turn, the pressure/temperature limits of a nuclear power plant, are adjusted to account for the effects of irradiation on the fracture toughness of the reactor vessel materials. The irradiation embrittlement and the resultant changes in mechanical properties of a given pressure vessel steel can be monitored by a surveillance program in which surveillance capsules containing prepared specimens of the reactor vessel materials are periodically removed from the operating nuclear reactor and the specimens are tested. The increase in the Charpy V-notch 30 ft-lb temperature is added to the original RT_{NDT} to adjust it for irradiation embrittlement. The adjusted RT_{NDT} is used to index the material to the K_{IR}* curve which, in turn, is used to set operating pressure-temperature limits for the nuclear power plant. These new limits take into account the effects of irradiation on the reactor vessel materials.

10 CFR 50, Appendix G, also requires a minimum initial Charpy upper-shelf energy (C_VUSE) of 75 ft-lbs for all beltline region materials unless it is demonstrated that lower values of upper-shelf fracture energy will provide an adequate margin of safety against fracture equivalent to those required by ASME Section XI, Appendix G. No action is required for a material that does not meet the initial 75 ft-lbs requirement provided that the irradiation embrittlement does not cause the C_VUSE to drop below 50 ft-lbs. The regulations specify that if the C_VUSE drops below 50 ft-lbs, it must be demonstrated, in a manner approved by the Office of Nuclear Reactor Regulation, that the lower values will provide adequate margins of safety.

Prior to irradiation, the beltline region Linde 80-weld metals exhibit C_VUSE levels in the range of 66 to 94 ft-lbs and average copper contents in the range of 0.15 to 0.35 wt%. Plant specific RVSP results and the predictive techniques developed by Framatome ANP, Inc., formerly Framatome Technologies, Inc. (FTI), B&W Nuclear Technologies (BWNT), and Babcock & Wilcox Co., Nuclear Power Division, indicate that these weld metals will have C_VUSE values of less than 50 ft-

* With the issuance of the 1999 ASME Section XI Code Addenda, the K_{Ic} curve can be used.

lbs during the latter half of the reactor vessel design life. In accordance with 10 CFR 50, Appendix G, alternative actions have been taken by the B&WOG to address the low upper-shelf fracture toughness issue for these Linde 80-weld metals. These actions include the accumulation of fracture toughness data and performing fracture mechanics analyses. Analyses performed by Framatome ANP, Inc. demonstrated adequate fracture toughness for service level A, B, C, and D loads through the original design life for all participants of the B&WOG RVWG. Using RVWG data and analytical methods, these fracture toughness analyses have been approved by the Nuclear Regulatory Commission (NRC).[9, 10] This analysis was performed for 48 EFPY for the B&W designed reactor vessels incorporating new data and has been approved by the NRC.[11]

Recently, the Nuclear Management Company, was granted an exemption from the requirements of 10 CFR part 50, Appendix G, Appendix H and Section 50.61 for the Kewaunee Nuclear Power Plant.[12] This exception is based on fracture toughness data performed to American Society for Testing and Materials (ASTM) Standard Test Method E 1921-97[13] and ASME Code Case N-629.[14] The transition temperature fracture toughness testing conducted as part of the MIRVP program is conducted in order to evaluate reactor vessel weld fracture toughness changes due to neutron-irradiation using this fracture toughness based reference temperature.

3.0 Supplemental Weld Metal Surveillance Capsules

3.1. Introduction

The SUPCAPs are included in the MIRVP for the irradiation and testing of eight Linde 80 weld metals [SA-1135, SA-1526, SA-1585, WF-25(6),* WF-25(9),** WF-67, WF-70(N),*** and WF-112] that are contained in six capsules. The capsules are being irradiated in two B&W 177-FA host reactors (Crystal River-3 and Davis-Besse). The six SUPCAPs are designated TMI2-LG2, TMI2-LG2, CR3-LG1, CR3-LG2, DB1-LG1, and DB1-LG2. Each SUPCAP contains Charpy V-notch, tension test, and compact fracture specimens from three weld metals. There are two capsule designs, type R-1 and R-2. The R-2 capsule represents an improved design over the R-1 since it utilizes subsize (Charpy size) tension test specimens. The subsize tension test specimens allow the addition of five more tension test specimens and three more compact fracture specimens per capsule. In addition, there are small variations between types R-1 and R-2 in the location of thermal monitors and neutron dosimeters.

The SUPCAPs are cylindrical; the unique advantage of the cylindrical capsule is that it allows easy capsule replacement and uniform specimen temperatures. Aluminum alloy spacers hold the specimens, neutron dosimeters, and thermal monitors in place and fill the gaps within the capsule. The remaining spaces are helium-filled. The capsules are locked in place in a holder tube assembly.

The SUPCAPs are designed to maintain specimens within ±25°F of the reactor vessel temperature at the ¼-thickness (¼T) vessel wall location.[15]

This report describes the analysis of the SUPCAP designated TMI2-LG2, removed from the Crystal River Unit 3 reactor vessel at the end of cycle 12. All the MIRVP SUPCAPs have been

* The (6) indicates that the material was taken from NSS-6 (Three Mile Island Unit 2) nozzle dropout.

** The (9) indicates that the material was taken from NSS-9 (Oconee Unit 3) nozzle dropout.

*** The (N) indicates that the material was taken from NSS-12 (Midland Unit 1) nozzle dropout.

withdrawn. SUPCAP Capsules CR3-LG1[16], CR3-LG2[17], DB1-LG1[18], and TMI2-LG1[19] have been tested and the results reported. DB1-LG2 is currently in storage. HUPCAPs A1, A2, A4, and L2 continue to be irradiated in either the Crystal River Unit 3 or the Davis-Besse reactor vessel.

3.2. SUPCAP TMI2-LG2 Description

The SUPCAP TMI2-LG2 is a type R-1 capsule. The TMI2-LG2 capsule contains Charpy V-notch, full size tension test, and compact fracture specimens of three Linde 80 weld metals. The Linde 80 weld metals and distribution of the specimens for each weld are described in Table 3-1. In addition, the TMI2-LG2 capsule contains neutron dosimeters to measure fluence and thermal monitors to measure the maximum irradiation temperature. The weld metal characterization, neutron dosimeters, and thermal monitors are described below. The arrangements of the specimens, dosimeters, and temperature monitors within the capsule are shown in Figure 3-1.

3.2.1. Weld Metal Characteristics

The three Linde 80 weld metals included in the capsule were all fabricated from the 299L44 weld wire heat. The three welds are from three different nozzle dropouts as shown in Table 3-1. The nozzle dropouts are actual vessel weld cutouts (dropouts) removed from the nozzle belt region of the vessel during fabrication. The nozzle dropouts (ND) were removed for subsequent attachment of the nozzles. The nozzle dropout welds consist of a thicker section (12" versus 8") than the beltline and RVSP block welds. In addition, all the nozzle dropouts received 50 to 53 hours of stress relief, which is greater than the stress relief time received by the same weld wire heats contained in the vessels. The quantity of specimens for each weld contained in the capsule are shown in Table 3-1. The chemical compositions and post weld stress relief times of the Linde 80 weld metals contained in the TMI2-LG2 capsule are described in Table 3-2.

3.2.2. Dosimetry

The TMI2-LG2 capsule contains seven dosimeter tubes, which contain neutron dosimeter wires of a sufficient variety to measure fast neutron fluence (time integrated flux), fast neutron spectrum, and thermal neutron fluence. A variety of neutron dosimeters were chosen in accordance with ASTM Standard Recommended Practices E 419-73[20] and E 482-82[21]. The neutron dosimeters are distributed throughout the capsule to measure the neutron fluence at various locations.

Table 3-3 lists the neutron dosimetry for the TMI2-LG2 capsule and provides energy range and shielding. The gadolinium (shield) thickness of 20 to 50 mils was sized to provide sufficient

neutron absorption to effectively eliminate competing reactions (lower bound) and to prevent significant absorption of fast neutrons (upper bound). The neutron dosimeters, along with their shielding, are then stacked in aluminum alloy holder tubes.

3.2.2. Thermal Monitors

Thermal monitors are distributed throughout the capsule to measure specimen temperatures. Capsule TMI2-LG2 contains seven sets of three to five low-melting-point element or eutectic alloy thermal monitors whose melting points range from 580 to 621F. By determining which monitors have melted, the peak temperature within the capsule can normally be determined. Table 3-4 lists the thermal monitors and their melting temperatures.

3.3. Holder Tube and Capsule Location

The surveillance capsule holder tubes are attached to the thermal shield and position the capsules in the downcomer annulus near the reactor wall. The holder tube is located so that the midspan elevation of the tube is at the core midplane. The azimuthal locations of the holder tubes at Crystal River Unit 3 are shown in Figure 3-2. The location of the TMI2-LG2 capsule during the time of irradiation was in the bottom location of the YZ surveillance capsule holder tube.

Table 3-1. Specimens and Weld Metals in SUPCAP TMI2-LG2 Capsule[1]

Weld Metal	Number of Specimens				
	Tensile (Transverse)	Charpy V-Notch	0.394 TC(T)	0.500 TC(T)	0.936 DC(T)
SA-1526 (CR-3 nozzle drop-out) (Wire Heat 299L44 / Flux Lot 8596)	2	12	2	4	3
WF-25(6) (TMI-2 nozzle drop-out) (Wire Heat 299L44 / Flux Lot 8650)	2	12	2	4	3
WF-25(9) (OC-3 nozzle drop-out) (Wire Heat 299L44 / Flux Lot 8650)	3	12	2	4	3

Table 3-2. Chemical Composition of SUPCAP TMI2-LG2 Capsule Surveillance Weld Metals[1]

Element	Chemical Composition, wt%		
	Weld Metal SA-1526(a)	Weld Metal WF-25(6)(b)	Weld Metal WF-25(9)(c)
C	0.09	0.09	0.09
Mn	1.53	1.58	1.55
P	0.013	0.015	0.014
S	0.017	0.016	0.015
Si	0.53	0.54	0.55
Ni	0.70(d)	0.67(d)	0.70(d)
Cr	0.08	0.09	0.08
Mo	0.42	0.42	0.41
Cu	0.37(d)	0.33(d)	0.36(d)
Post-Weld Heat Treatment			
Weld Metal Identification	Stress Relief Temp., ºF	Stress Relief Time, hours	Cooling Rate, ºF/hour
SA-1526	1100-1150	51	10
WF-25(6)	1100-1150	50	10
WF-25(9)	1100-1150	50	10

(a) Weld material from a Crystal River Unit 3 nozzle dropout.
(b) Weld material from a Three Mile Island Unit 2 nozzle dropout.
(c) Weld material from a Oconee Unit 3 nozzle dropout.
(d) Average of RVSP material source chemical compositions as reported in BAW-2325, Revision 1.[22]

Table 3-3. SUPCAP TMI2-LG2 Capsule Dosimetry[1]

Neutron-Sensitive Element	Shield	Reaction Cross-Section Threshold Energy	Half-Life and Product Isotope
Short Tube			
^{237}Np	Gd	0.5 MeV	Appropriate fission products
^{238}U	Gd	1.1 MeV	Appropriate fission products
^{54}Fe	Gd	2.5 MeV	314 days ^{54}Mn
Long Tube			
^{59}Co	Cd-foil	0.5 eV	5.3 years ^{60}Co
^{237}Np	Gd	0.5 MeV	Appropriate fission products
^{238}U	Gd	1.1 MeV	Appropriate fission products
^{58}Ni	Gd	2.3 MeV	71 days ^{58}Co
^{54}Fe	Gd	2.5 MeV	314 days ^{54}Mn
^{63}Cu	Gd	6.1 MeV	5.3 years ^{60}Co
^{59}Co	None	Thermal	5.3 years ^{60}Co

Table 3-4. SUPCAP TMI2-LG2 Capsule Thermal Monitor Wires[1]

Material Composition, wt%	Approximate Melting Point, °F
97.5 Pb-2.5 Ag	580
97.5 Pb-1.5 Ag-1.0 Sn	588
98.8 Cd-1.2 Cu	598
100 Cd	610
100 Pb	621

Figure 3-1. General Arrangement of Specimens, Dosimeters, and Thermal Monitors in the TMI2-LG2 Capsule[1]

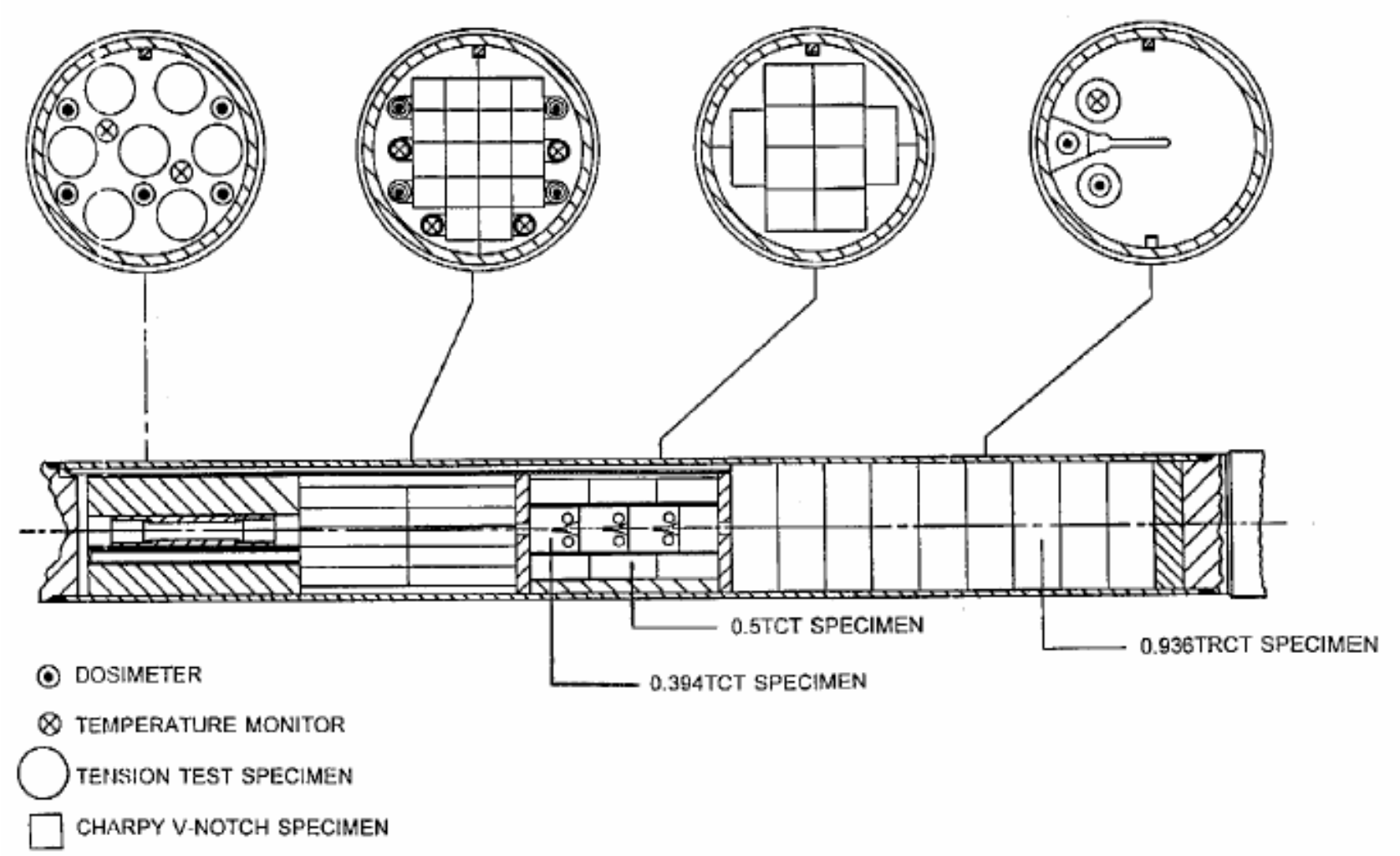

Figure 3-2. Surveillance Capsule Holder Tube Locations and Identifications for the Crystal River Unit 3 Reactor Vessel[1]

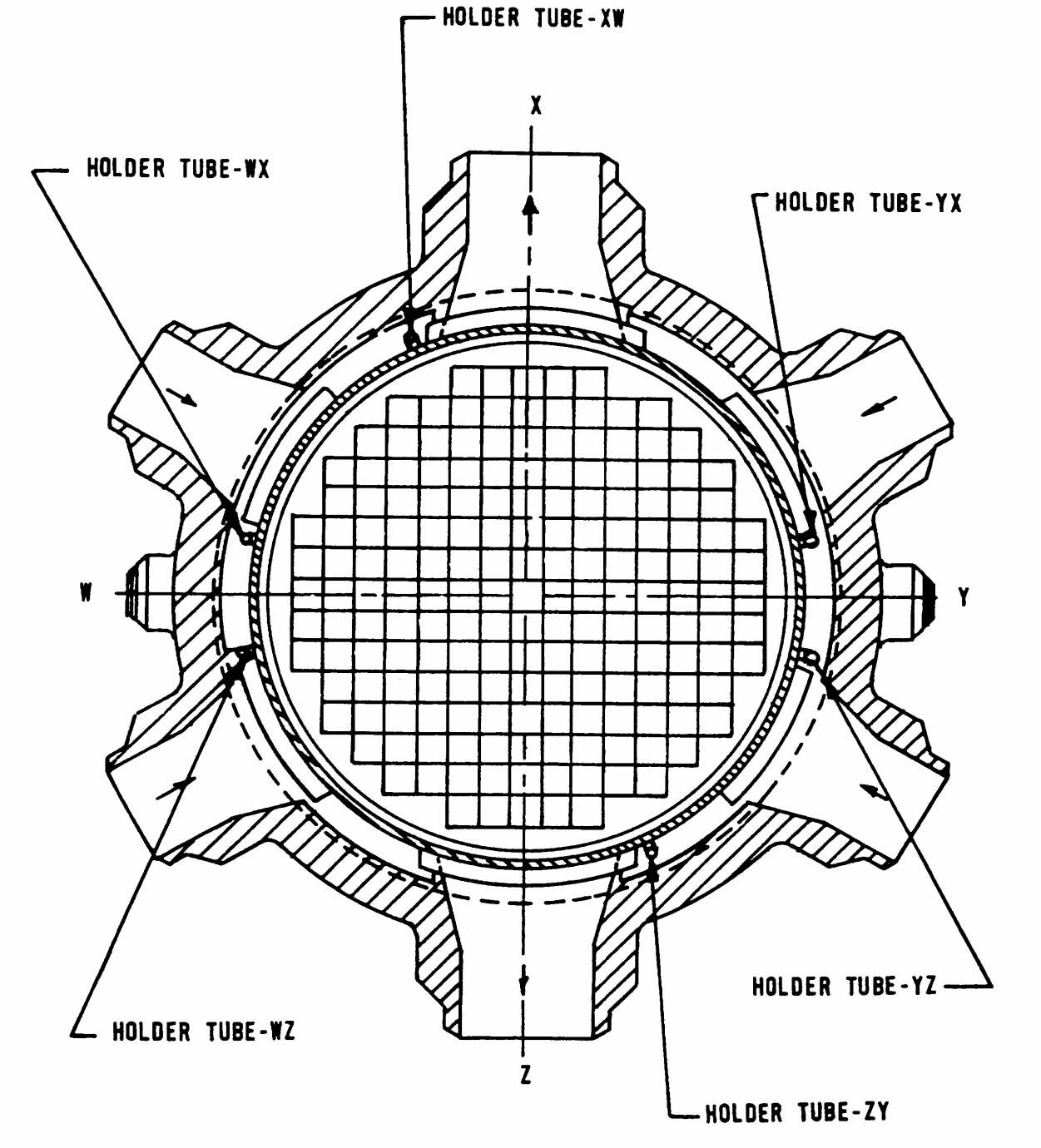

4.0 Post-Irradiation Testing for TMI2-LG2 Capsule

The post-irradiation testing of the tensile specimens, Charpy V-notch impact specimens, the three point bend fracture specimens (using modified precracked Charpy specimens), 0.936 inch thick disk-shaped compact DC(T) fracture specimens, thermal monitors, and dosimeters for the TMI2-LG2 capsule was performed at the BWXT Services Inc. Lynchburg Technology Center (LTC).[23]

4.1. Visual Examination and Inventory

After capsule disassembly, the contents of the TMI2-LG2 capsule were removed, inspected, and inventoried. The contents of the TMI2-LG2 capsule were found to be consistent with the surveillance program report inventory. There was no evidence of rust or penetration of reactor coolant into the capsule. Two 0.936 DC(T) specimens from each of the three welds and one WF-25(9) tensile specimen were not tested and stored in long term retrievable storage at the LTC.

4.2. Thermal Monitors

The TMI2-LG2 capsule contained seven sets of temperature monitors, each containing five fusible alloy wires with melting points at 580°F, 588°F, 598°F, 610°F and 621°F. The monitors were x-rayed to inspect for evidence of melting, irregular bending, and/or slumping. All of the temperature monitors were melted as indicated by the alloys having accumulated at the bottom of each tube. The temperature monitor inspection results are tabulated in Table 4-1. This data agrees with the gamma ray radiograph taken during the re-qualification of the capsule after the TMI-2 incident.[5] Since the thermal monitors had melted during the TMI-2 incident, nothing can be concluded from this examination concerning the peak temperature of the capsule during irradiation in Crystal River Unit 3.

4.3. Tension Test Results

Two tension tests from each weld metal were conducted in accordance with the applicable requirements of ASTM Standard E 8-94[24] and E 21-92[25]. The remaining WF-25(9) tension specimen was placed into long term retrievable storage for possible future testing. The results of the tensile tests are summarized in Tables 4-2 through 4-4. The stress-strain curves are presented in Appendix A.

4.4. Upper-Shelf Charpy V-Notch Impact Test Results

The Charpy V-notch impact testing was performed in accordance with the applicable requirements of ASTM Standard E 23-94a[26] for three specimens from each weld. Impact energy, lateral expansion, and percent shear fracture were measured at upper-shelf test temperature of 400°F and recorded for each specimen. The impact energy was measured using a certified Satec S1-1K Impact tester (traceable to NIST Standard) with a striker velocity of 16.90 ft/sec and 240 ft-lb of available energy. The lateral expansion was measured using a certified dial indicator. The specimen percent shear was estimated by video examination and comparison with the visual standards presented in ASTM Standard E 23-94a.

The results of the Charpy V-notch impact testing are shown in Table 4-5. These values are used to determine upper-shelf energy value in accordance with ASTM Standard E 185-82.[27] Photographs of the Charpy V-notch specimen fracture surfaces are presented in Figure 4-1.

4.4. Upper-Shelf Fracture Toughness Test Results

One 0.936 TDC(T) specimen was selected from each weld metal for upper-shelf fracture toughness testing. The specimens were precracked before insertion into the capsule for irradiation. The final precrack stress intensity factor did not exceed 32 ksi$\sqrt{in}$. The specimens were side-grooved (10% of thickness each side) prior to testing. The fracture toughness testing was performed in compliance with the requirements of ASTM Standards E 813-89[28] and E 1152-87[29] on a servo-hydraulic test machine equipped with a 50-kip load cell. A 25,000-pound range was used to increase the resolution since the maximum force needed for the test was estimated not to exceed 25,000 lbs. The tests were conducted at 550°F using 20% unloading compliance to measure the crack length at defined steps throughout the test. A load versus Crack Opening Displacement (COD) plot for each toughness test is shown in Appendix B.

The crack length was measured optically at nine locations across the precrack front as specified in ASTM E 813-89. All precracks complied with the ASTM Standard E 813-89 crack front straightness criteria. The optical crack length measurements were consistent with those determined from the compliance method. Appendix D contains the optical crack length averages and specimen dimension measurements.

The test results of the upper-shelf fracture toughness tests are shown in Table 4-6. The J values at 0.1" crack extension ($J_{0.1}$) are also presented. The $J_{0.1}$ values are used for justification of the Linde 80 low upper-shelf materials. All three tests meet the validity criteria of ASTM E 813-89. The J-R (J-Δa) curves are presented in Figures 4-2 through 4-4.

4.5. Transition Temperature Fracture Toughness Test Results

Two 0.394 TC(T), four 0.500 TC(T), and nine modified Charpy V-notch specimens from each weld metal removed from the TMI2-LG2 capsule were selected for transition temperature fracture toughness testing.

4.5.1. Modified Charpy V-notch Specimens

Several selected specimens were of the Type A Charpy V-notch geometry. Modification of the existing V-notch was required for fracture toughness testing. The notch was modified using a wire Electro Discharge Machining (EDM) operation resulting in a 0.165-inch deep and 0.012 inch wide notch. At the completion of the modified notch machining, the specimens were precracked in compliance with ASTM Standard E 1921-97[13]. The specimens were precracked using a decreasing ΔK technique beginning at 19 ksi$\sqrt{in}$ and ending with a stress intensity factor of about 15 ksi$\sqrt{in}$ with an R-ratio of 0.05. The Charpy-size single edge notch bend, SE(B), fracture toughness testing was performed in compliance with the requirements of ASTM Standard E 1921 on a servohydraulic test machine equipped with a 3-kip load cell. A 1,500-pound range was used to increase the resolution since the maximum force needed for the test was estimated not to exceed 1,500 lbs. A load versus COD plot for each SE(B)-fracture toughness test is shown in Appendix B. The typical stress intensity factor-loading rate for the Charpy-size SE(B)-fracture toughness tests was 1.3 ksi$\sqrt{in}$/second through the linear portion of the load-COD curve. Upon completion of the SE(B)-fracture toughness testing, the specimens were heat-tinted to facilitate crack length measurement.

4.5.2 0.394 T and 0.500 T Compact Specimens

The 0.394 TC(T) and 0.500 TC(T) compact fracture specimens were precracked before insertion into the capsule for irradiation. The final precrack stress intensity factor did not exceed 17 ksi$\sqrt{in}$. The fracture toughness testing was performed in compliance with the requirements of ASTM Standards E 1921-97 on a servo-hydraulic test machine equipped with a 50-kip load cell. A 25,000-pound range was used to increase the resolution since the maximum force needed for the test was estimated not to exceed 25,000 lbs. A load versus COD plot for each toughness test is shown in Appendix B. Upon completion of the toughness testing, the specimens were heat-tinted to facilitate crack length measurement.

4.5.3. Crack Length Verification

The crack length was measured optically at nine locations across the precrack front as specified in ASTM E1921-97. All precracks complied with the ASTM Standard E 1921 crack front straightness criteria. No crack growth was observed on any of the fracture toughness test specimens. The optical crack length measurements were consistent with those determined from

the compliance method. Appendix D contains the optical crack length averages and specimen dimension measurements.

4.5.4. Calculation of K_{Jc}

The elastic-plastic equivalent stress intensity factor, K_{Jc}, is calculated from the J-integral at the point of cleavage fracture, J_c. This calculation is performed according to ASTM E1921-97:

$$K_{Jc} = \sqrt{J_c E}$$

where E = elastic modulus

The J_c and K_{Jc} value for each test are listed in Tables 4-7 through 4-12. The K_{Jc} value of each test was evaluated to determine whether it exceeded the K_{Jc} limit.

$$K_{Jc(limit)} = \sqrt{\frac{E b_o \sigma_{ys}}{30}}$$

where b_0 = initial remaining ligament
σ_{ys} = yield strength at the test temperature

K_{Jc} values are dependent on the size of the test specimen, therefore, the K_{Jc} values were converted to an equivalent standard fracture toughness value for a 1T specimen size. This conversion (prediction) uses a weakest link theory based on the statistical dependence of fracture toughness data on specimen size. This prediction is only accurate in the transition region and is calculated as follows per ASTM E1921-97:

$$K_{Jc(1T)} = 20 + [K_{Jc} - 20]\left(\frac{B_{XT}}{B_{1T}}\right)^{1/4}, \text{Mpa}\sqrt{\text{m}}$$

where B_{XT} = test specimen thickness with the presence of side grooves ignored
B_{1T} = 1T specimen thickness (1 inch)
K_{Jc} = fracture toughness of XT specimen.

4.5.5 T_0 Determination

The ASTM E1921-97 method requires the testing of a minimum number of fracture toughness specimens of the material of interest at a single temperature. All the K_{Jc} values from each weld

and common geometry type (i.e. modified PCVN and compact) with the same temperature were used to calculate the reference temperature (T_0) per the ASTM E1921-97 procedure. The procedure is briefly described below.

Through the use of Weibull statistics it has been determined that ferritic steels within a certain yield strength range have fracture toughness cumulative probability distribution of the same shape, independent of specimen shape, size and temperature. The Weibull scale parameter, K_o, can be calculated as follows for a group of six or more valid K_{Jc} tests:

$$K_o = \left[\sum_{I=1}^{N} \frac{\left(K_{Jc(I)} - 20 \right)^4}{r - 0.3068} \right]^{1/4} + 20, \quad Mpa\sqrt{m}$$

where N= total number of data points and
r = total number of valid data points.

The estimated median value of the population can be obtained from K_o using the following equation[1]:

$$K_{Jc(med)} = (K_o - 20)(0.9124) + 20 \quad Mpa\sqrt{m}$$

The master curve reference temperature is calculated as follows:

$$T_o = T - \frac{1}{0.019} \ln \left[\frac{K_{Jc(med)} - 30}{70} \right], \quad {}^oC$$

where T = test temperature (°C).

The ASTM E1921-02[30] standard can also be used. This new revision contains the ability to calculate a reference temperature from a multi-temperature data set. The T_0 results obtained using the new E1921-02 standard are within 3°F of the results reported here using the single temperature calculation procedure specified in the E1921-97 standard.

4.5.6 T_0 Result

The T_0 results for the three welds and for each geometry type are presented in Table 4-13. Two of the data sets have an insufficient number of uncensored data points for a valid T_0 as defined by ASTM E 1921-97. Since the data is short of the number required by one, the T_0 could be used with the understanding that the T_0 uncertainty is increased.

Table 4-1. Conditions of Thermal Monitors in TMI2-LG2 Capsule[23]

Temperature Monitor	Melt Temperature	Post-Irradiation Condition
ST7	580°F 598°F 610°F	Melted Melted Melted
ST8	580°F 598°F 610°F	Melted Melted Melted
ST9	580°F 598°F 610°F	Melted Melted Melted
ST10	580°F 598°F 610°F	Melted Melted Melted
ST11	580°F 598°F 610°F	Melted Melted Melted
ST12	580°F 598°F 610°F	Melted Melted Melted
LT2	580°F 588°F 598°F 610°F 621°F	Melted Melted Melted Melted Melted

Table 4-2. Tensile Data for Weld Metal SA-1526 (Wire Heat 299L44 / Flux Lot 8596) Irradiated in the TMI2-LG2 Capsule[23]

Specimen No.	Fluence x 10^{19} n/cm^2 (E > 1 MeV)	Test Temp. (°F)	Strength		Fracture Properties			Elongation		Reduction in Area (%)
			Yield (ksi)	Ultimate (ksi)	Load (lb)	Stress (ksi)	Strength (ksi)	Uniform (%)	Total (%)	
PP004	1.984	70	87.0	102.6	7551	180.2	75.4	10.5	21.3	58.1
PP003	1.734	580	79.4	96.7	8468	141.5	84.6	8.9	15.8	40.2

Table 4-3. Tensile Data for Weld Metal WF-25(6) (Wire Heat 299L44 / Flux Lot 8650) Irradiated in the TMI2-LG2 Capsule[23]

Specimen No.	Fluence x 10^{19} n/cm^2 (E > 1 MeV)	Test Temp. (°F)	Strength		Fracture Properties			Elongation		Reduction in Area (%)
			Yield (ksi)	Ultimate (ksi)	Load (lb)	Stress (ksi)	Strength (ksi)	Uniform (%)	Total (%)	
QQ004	1.580	70	94.0	108.9	7957	187.4	79.5	11.7	24.5	57.6
QQ003	1.689	580	82.4	100.0	8029	158.5	80.2	8.9	17.4	49.4

Table 4-4. Tensile Data for Weld Metal WF-25(9) (Wire Heat 299L44 / Flux Lot 8650) Irradiated in the TMI2-LG2 Capsule[23]

Specimen No.	Fluence x 10^{19} n/cm^2 (E > 1 MeV)	Test Temp. (°F)	Strength		Fracture Properties			Elongation		Reduction in Area (%)
			Yield (ksi)	Ultimate (ksi)	Load (lb)	Stress (ksi)	Strength (ksi)	Uniform (%)	Total (%)	
JJ011	1.299	70	92.8	106.9	7813	181.7	78.1	11.2	24.6	57.0
JJ010	1.253	580	80.8	97.7	8460	138.9	84.5	8.7	15.8	39.1

Table 4-5. Upper-Shelf Charpy V-Notch Impact Data with a Test Temperature of 400°F for Wire Heat 299L44 Irradiated in the TMI2-LG2 Capsule[23]

Weld	Average Fluence x 10^{19} n/cm^2 (E>1 MeV)	Specimen No.	Impact Energy (ft-lb)	Lateral Expansion (mils)	Shear Fracture (%)	Average Impact Energy (ft-lb)
SA-1526 (CR-3 nozzle drop-out)	1.998	PP023	41.5	39	100	42.5
		PP025	43.5	42	100	
		PP026	42.5	42	100	
WF-25(6) (TMI-2 nozzle drop-out)	1.716	QQ022	39	42	100	38.7
		QQ023	39.5	35	95	
		QQ024	37.5	34	95	
WF-25(9) (OC-3 nozzle drop-out)	1.433	JJ011	42.5	40	100	41.7
		JJ012	41	39	100	
		JJ013	41.5	39	100	

Table 4-6. Upper-Shelf Fracture Toughness Data with a Test Temperature of 550°F Wire Heat 299L44 Irradiated to 1.585×10^{19} n/cm^2 (E > 1 MeV) in the TMI2-LG2 Capsule[23]

Weld	Specimen No.	J_{IC} (in-lb/in^2)	K_J (ksi√in)	$J_{0.1"}$ (lb/in)	ASTM E813 Validity
SA-1526 (CR-3 nozzle drop-out)	PP004	372	99.7	766	Valid
WF-25(6) (TMI-2 nozzle drop-out)	QQ002	395	102.7	819	Valid
WF-25(9) (OC-3 nozzle drop-out)	JJ002	363	98.5	770	Valid

Table 4-7. Fracture Toughness Data from TMI2-LG2 Capsule for Weld Metal SA-1526 (Wire Heat 299L44 / Flux Lot 8596) Irradiated to an Average Fluence of 1.812×10^{19} n/cm^2 (E > 1 MeV) in the TMI2-LG2 Capsule[23]

Specimen Identification	Specimen Geometry	Test Temperature (°F)	J_c (in-lb/in^2)	K_{Jc}[31] (ksi√in)	Violations
PP014	PCS(a)	100	247	84.6	
PP015	PCS	100	543	125.4	$K_{Jc(limit)}$(b)
PP016	PCS	100	133	62.1	
PP017	PCS	100	394	106.8	
PP018	PCS	100	385	105.6	
PP019	PCS	100	363	102.6	
PP020	PCS	100	469	116.6	
PP021	PCS	100	381	105.1	
PP022	PCS	100	354	101.3	

(a) Precracked Charpy-size single edge notch bend, SE(B), specimen.
(b) $K_{Jc(limit)}$ defined in 4.5.4.

Table 4-8. Fracture Toughness Data from TMI2-LG2 Capsule for Weld Metal SA-1526 (Wire Heat 299L44 / Flux Lot 8596) Irradiated to an Average Fluence of 1.628×10^{19} n/cm^2 (E > 1 MeV) in the TMI2-LG2 Capsule[23]

Specimen Identification	Specimen Geometry	Test Temperature (°F)	J_c (in-lb/in^2)	K_{Jc}[31] (ksi√in)	Violations
PP006	0.5 TC(T) (a)	120	410	108.8	
PP009	0.5 TC(T)	120	247	84.4	
PP013	0.5 TC(T)	120	211	78.1	
PP015	0.5 TC(T)	120	155	66.9	
PP007	0.394 TC(T)	120	173	70.7	
PP010	0.394 TC(T)	120	998	169.8	

(a) Compact Fracture specimen.

Table 4-9. Fracture Toughness Data from TMI2-LG2 Capsule for Weld Metal WF-25(6) (Wire Heat 299L44 / Flux Lot 8650) Irradiated to an Average Fluence of 1.595×10^{19} n/cm^2 (E > 1 MeV) in the TMI2-LG2 Capsule[23]

Specimen Identification	Specimen Geometry	Test Temperature (°F)	J_c (in-lb/in^2)	K_{Jc}[31] (ksi√in)	Violations
QQ013	PCS(a)	130	463	115.5	
QQ014	PCS	130	529	123.5	
QQ015	PCS	130	123	59.5	
QQ016	PCS	130	433	111.7	
QQ017	PCS	130	205	76.9	
QQ018	PCS	100(b)	122	59.3	
QQ019	PCS	100(b)	147	65.3	
QQ020	PCS	130	207	77.2	
QQ021	PCS	130	75.3	46.6	

(a) Precracked Charpy-size single edge notch bend, SE(B), specimen.
(b) Excluded from the single temperature T_0 calculation.

Table 4-10. Fracture Toughness Data from TMI2-LG2 Capsule for Weld Metal WF-25(6) (Wire Heat 299L44 / Flux Lot 8650) Irradiated to an Average Fluence of 1.545×10^{19} n/cm^2 (E > 1 MeV) in the TMI2-LG2 Capsule[23]

Specimen Identification	Specimen Geometry	Test Temperature (°F)	J_c (in-lb/in^2)	K_{Jc}[31] (ksi√in)	Violations
QQ002	0.5 TC(T) (a)	170	129	60.8	
QQ003	0.5 TC(T)	170	348	99.8	
QQ005	0.5 TC(T)	170	432	111.2	
QQ008	0.5 TC(T)	170	115	57.4	
QQ001	0.394 TC(T)	170	166	68.9	
QQ002	0.394 TC(T)	170	209	77.3	

(a) Compact Fracture specimen.

Table 4-11. Fracture Toughness Data from TMI2-LG2 Capsule for Weld Metal WF-25(9) (Wire Heat 299L44 / Flux Lot 8650) Irradiated to an Average Fluence of 1.235×10^{19} n/cm^2 (E > 1 MeV) in the TMI2-LG2 Capsule[23]

Specimen Identification	Specimen Geometry	Test Temperature (°F)	J_c (in-lb/in^2)	K_{Jc}[31] (ksi√in)	Violations
JJ001	PCS(a)	100	347	100.3	
JJ002	PCS	100	603	132.2	$K_{Jc(limit)}$(c)
JJ003	PCS	100	778	150.1	$K_{Jc(limit)}$
JJ004	PCS	100	192	74.6	
JJ005	PCS	100	96.6	52.9	
JJ006	PCS	130(b)	1010	170.6	$K_{Jc(limit)}$
JJ007	PCS	100	209	77.8	
JJ008	PCS	100	269	88.3	
JJ010	PCS	100	960	166.8	$K_{Jc(limit)}$

(a) Precracked Charpy-size single edge notch bend, SE(B), specimen.
(b) Excluded from the single temperature T_0 calculation.
(c) $K_{Jc(limit)}$ defined in 4.5.4.

Table 4-12. Fracture Toughness Data from TMI2-LG2 Capsule for Weld Metal WF-25(9) (Wire Heat 299L44 / Flux Lot 8650) Irradiated to an Average Fluence of 1.463×10^{19} n/cm^2 (E > 1 MeV) in the TMI2-LG2 Capsule[23]

Specimen Identification	Specimen Geometry	Test Temperature (°F)	J_c (in-lb/in^2)	K_{Jc}[31] (ksi√in)	Violations
JJ004	0.5 TC(T) (a)	110	114	57.4	
JJ005	0.5 TC(T)	110	192	74.5	
JJ006	0.5 TC(T)	110	470	116.6	
JJ007	0.5 TC(T)	110	333	98.1	
JJ007	0.394 TC(T)	110	177	71.6	
JJ010	0.394 TC(T)	110	323	96.7	

(a) Compact Fracture specimen.

Table 4-13. Master Curve Reference Temperature (T_0) Data for Wire Heat 299L44 Irradiated in the TMI2-LG2 Capsule[31]

Weld	Average Fluence x 10^{19} n/cm^2 (E > 1 MeV)	Specimen Type	$K_{Jc(med)}$ (ksi$\sqrt{in}$)	Number of Uncensored Specimens/ Minimum Required	T_0 (°F)	E1921-97 Validity
SA-1526 (CR-3 nozzle drop-out)	1.812	PCS	84	8/6	111	
	1.628	C(T)	94	6/6	116	
WF-25(6) (TMI-2 nozzle drop-out)	1.595	PCS	78	7/6	151	
	1.545	C(T)	72	6/7	203	Invalid
WF-25(9) (OC-3 nozzle drop-out)	1.235	PCS	93	5/6	97	Invalid
	1.463	C(T)	76	6/6	135	

Figure 4-1. Photographs of Charpy Impact Specimen Fracture Surfaces for Wire Heat 299L44 Irradiated in the TMI2-LG2 Capsule[23]

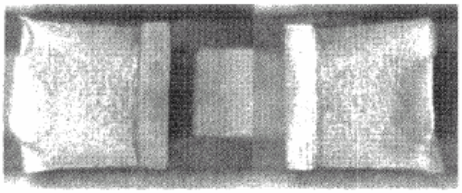

Specimen No. JJ013 test temp. 400° F

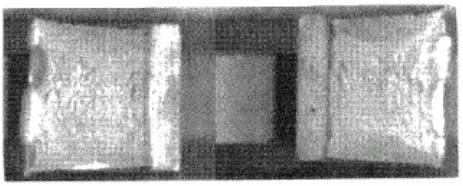

Specimen No. PP023 test temp. 400° F

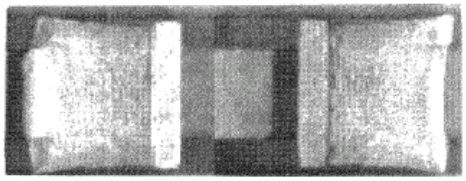

Specimen No. JJ012 test temp. 400° F

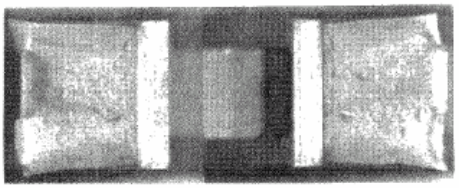

Specimen No. QQ022 test temp. 400° F

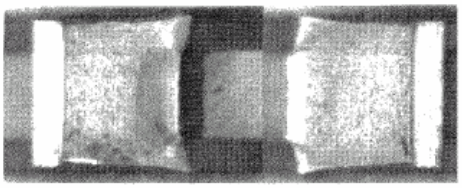

Specimen No. JJ011 test temp. 400° F

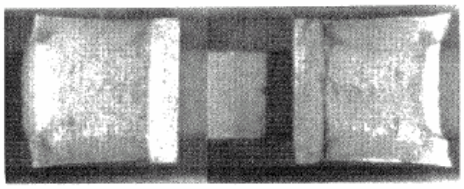

Specimen No. QQ023 test temp. 400° F

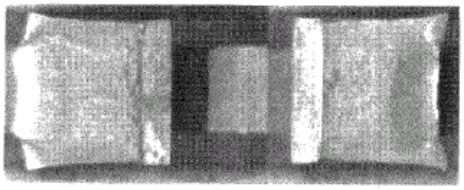

Specimen No. PP026 test temp. 400° F

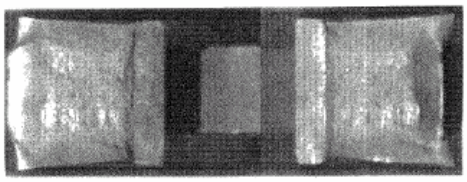

Specimen No. QQ024 test temp. 400° F

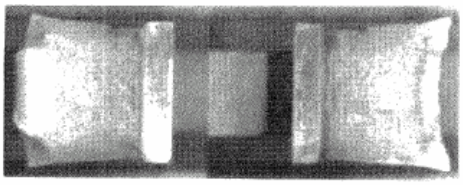

Specimen No. PP025 test temp. 400° F

Figure 4-2. J-Δa Curve (550°F) for Weld Metal SA-1526 (Wire Heat 299L44 / Flux Lot 8596) Irradiated to 1.585×10^{19} n/cm^2 (E > 1 MeV) in the TMI2-LG2 Capsule[23]

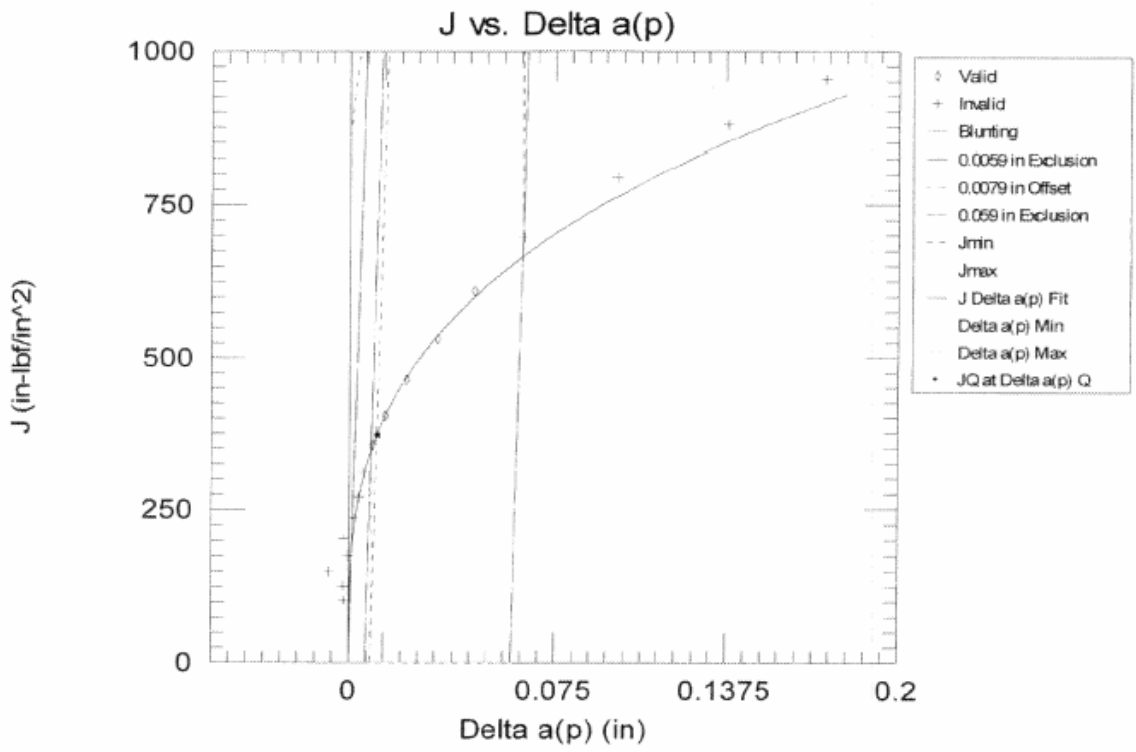

Figure 4-3. J-Δa Curve (550°F) for Weld Metal WF-25(6) (Wire Heat 299L44 / Flux Lot 8650) Irradiated to 1. 585 x 10^{19} n/cm^2 (E > 1 MeV) in the TMI2-LG2 Capsule[23]

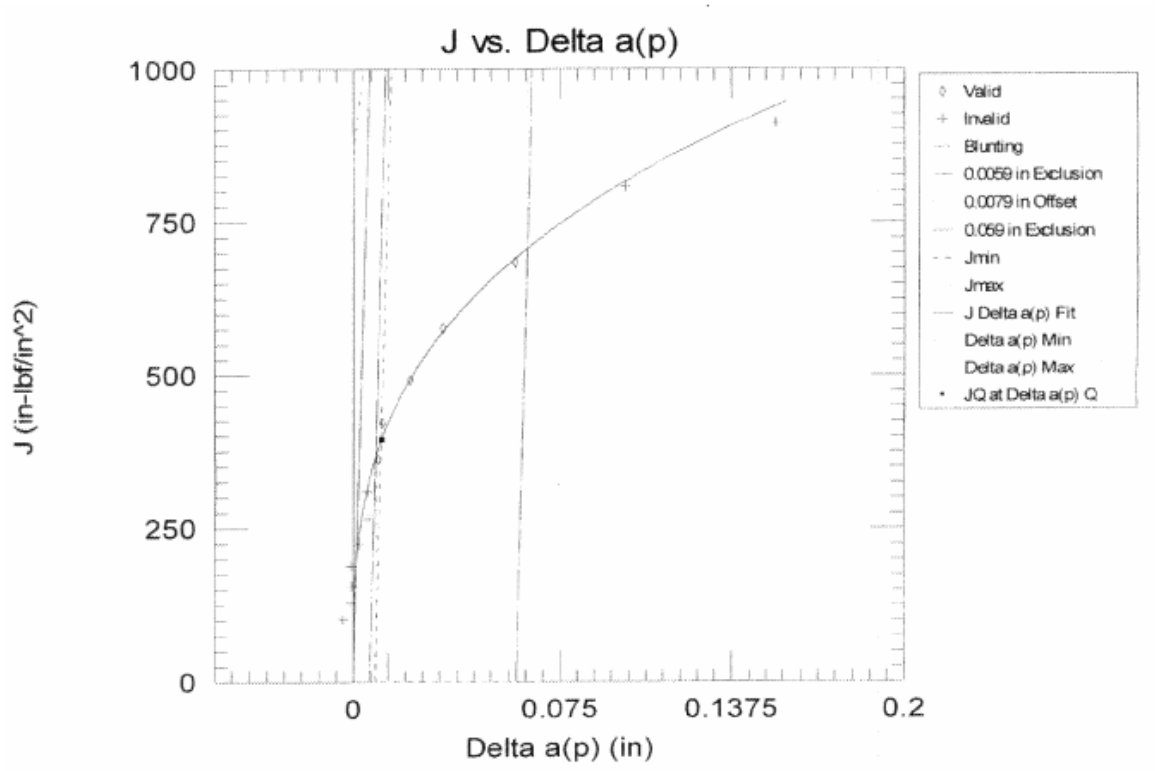

Figure 4-4. J-Δa Curve (550°F) for Weld Metal WF-25(9) (Wire Heat 299L44 / Flux Lot 8650) Irradiated to 1. 585 x 10^{19} n/cm^2 (E > 1 MeV) in the TMI2-LG2 Capsule[23]

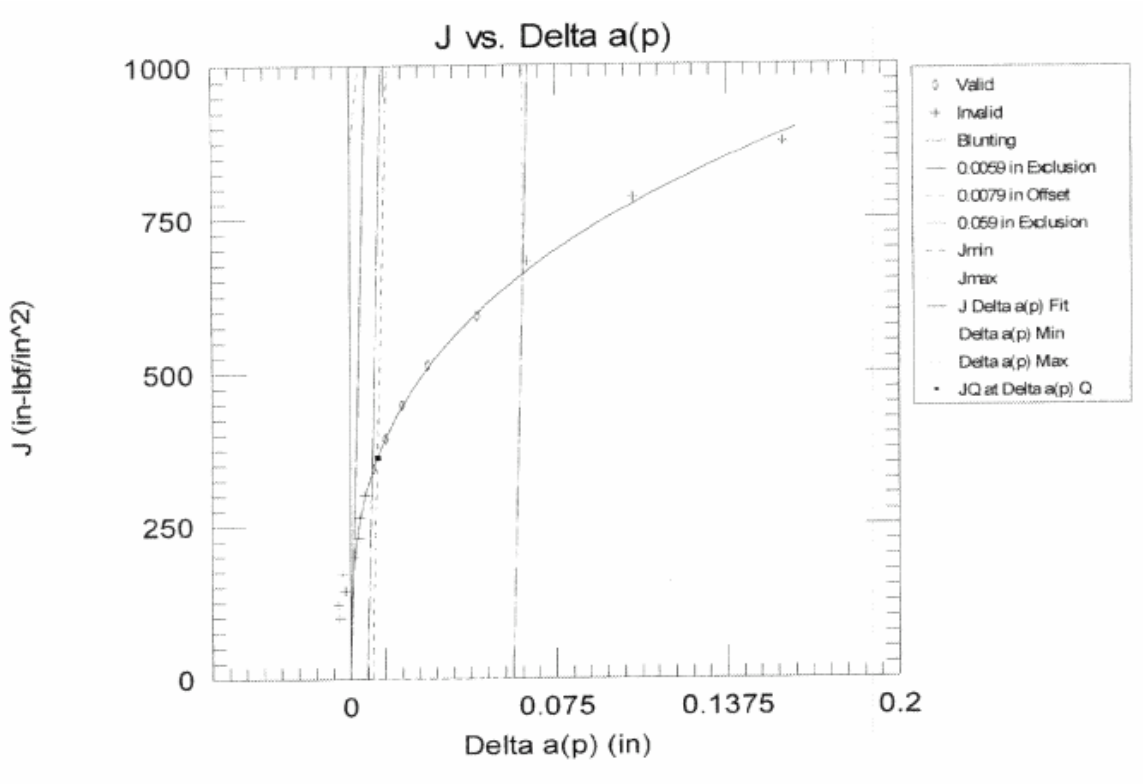

5. Tests of Unirradiated Material

Unirradiated material was evaluated for two purposes: (1) to establish baseline data to which irradiated properties can be compared, and (2) to obtain values of material properties required for compliance with 10CFR50, Appendices G and H.

5.1 Tension Test Results

Baseline data for the three sources of weld metal contained in the TMI2-LG2 capsule were produced through the SUPCAP and HSST Task 2 and 3 programs.[16, 19] Additional baseline testing was conducted on WF-25(6).[34] The baseline tensile data is summarized in Table 5-1.

5.2. Upper-Shelf Charpy V-Notch Impact Test Result

The upper-shelf and transition temperature baseline Charpy V-notch impact test data for the three weld metal sources contained in the TMI2-LG2 capsule were tested as part of the SUPCAP and HSST Task 2 and 3 programs.[16, 19] The baseline Charpy impact properties are summarized in BAW-2325, Supplement 1.[32]

5.3. Upper-Shelf Fracture Toughness Test Results

The upper-shelf baseline fracture toughness data for the three weld metal sources contained in the TMI2-LG2 capsule were tested as part of the SUPCAP and HSST Task 2 and 3 programs.[16, 19]

5.4. Transition Temperature Fracture Toughness Test Results

Transition temperature fracture toughness test results for the three weld metal sources contained in the TMI2-LG2 capsule were tested as part of the B&WOG Reactor Vessel Integrity Program (RVIP). Two of the three weld materials (SA-1526 and WF-25(9)) have been previously reported.[33] Baseline transition temperature fracture toughness testing of WF-25(6) had not been previously conducted, therefore, testing was conducted under the 2002 B&WOG RVIP. The results of the baseline testing of the WF-25(6) weld are included in Table 5-2.[34]

The WF-25(6) baseline specimens used to measure the transition temperature fracture toughness were extra specimens fabricated for the SUPCAP program. The extra specimens that were tested contained two Charpy V-notch, two 0.394 TC(T), two 0.500 TC(T), and two 0.936 DC(T) specimens. The notch geometry of the Charpy V-notch specimens was modified and tested as described in Section 4.5.1. The testing of the fracture toughness specimens was performed at the BWXT LTC and none of the specimens were side-grooved. The typical stress intensity-loading rate for the fracture toughness tests was 0.9 to 1.3 ksi√in/second. A load versus COD plot for each toughness test is shown in Appendix B. The single temperature method (ASTM E1921-97) of calculating the reference temperate was used to calculate an unirradiated WF-25(6) reference temperature of T_0 = -58°C (-60°F).[31] All validity criteria were met as specified in ASTM E1921-97. No crack growth was observed on any of the fracture toughness test specimens. The optical crack length measurements were consistent with those determined from the compliance method. Appendix D contains the optical crack length averages and specimen dimension measurements.

The stress intensity factor rate (Krate) has a significant effect on fracture toughness and thus the reference temperature, for ferritic steel specimens tested in the transition region.[35, 36, and 37] The SA-1526 and WF-25(9) baseline specimens tested previously were conducted at significantly different loading rates than the tests conducted on the irradiated specimens removed from the TMI2-LG2 capsule and the baseline WF-25(6) specimens. Due to the observed loading rate effect in ferritic steels, it is imperative that the T_0 values be normalized to the same loading rate.

It has been determined from a large data set of ferritic reactor pressure vessel steels that the effect on T_0 of loading rate is conservatively represented (nearly bounding) by the following equation[35]:

$$\Delta T_0 = 5.34\ \Delta \ln(\text{Krate})$$

where: Krate is in units of $Mpa\sqrt{m}/\text{sec}$ and T_0 is in units of C.

All the 299L44 T_0 data was adjusted to 1 $Mpa\sqrt{m}/\text{sec}$ (0.9 ksi√in/sec) so that all the data could be directly compared. The following equation is used for this adjustment:

$$\text{Rate adjusted } T_0 = \text{Test } T_0 + 5.34 \ln(\text{Krate}_{\text{adjusted}}/\text{Krate}_{\text{test}})$$

For this adjustment, $\text{Krate}_{\text{adjusted}}$ was set equal to 1 $Mpa\sqrt{m}/\text{sec}$.
Table 5-3 contains the 299L44 baseline data with the loading rate adjustments.

Table 5-1. Baseline Tensile Data for Weld Wire Heat 299L44[16, 19, 34]

Specimen No.	Test Temp.	Strength		Elongation	Reduction
	(°F)	Yield (ksi)	Ultimate (ksi)	Total (%)	in Area (%)
SA-1526 (CR-3 nozzle drop-out)	70	62.2	81.0	33	65
	580	54.3	78.0	21	58
WF-25(6) (TMI-2 nozzle drop-out)	79(a)	69.9	87.1	21	68
	70(b)	62.5	85.9	24	70
	550(a)	59.4	76.9	17	64
	580(b)	56.6	80.3	17	55
WF-25(9) (OC-3 nozzle drop-out)	75	64.9	80.2	26	67
	580	60.3	75.3	16	59

(a) Average of multiple samples.
(b) BWXT retest.[34]

Table 5-2. Fracture Toughness Data for Unirradiated Weld Metal WF-25(6) (TMI-2 nozzle drop-out) (Wire Heat 299L44 / Flux Lot 8650)[34]

Specimen Identification	Specimen Geometry	Test Temperature (°F)	J_c (in-lb/in^2)	K_{Jc}[31] (ksi$\sqrt{in}$)	Violations
QQ025	PCS(a)	-100	536	126.7	
QQ026	PCS	-100	196	76.7	
QQ005	0.936 DC(T) (b)	-70	233	83.4	
QQ006	0.936 DC(T)	-70	195	76.3	
QQ004	0.5 TC(T) (c)	-70	443	115.0	
QQ010	0.5 TC(T)	-70	255	87.2	
QQ005	0.394 TC(T)	-70	352	102.5	
QQ006	0.394 TC(T)	-70	507	123.0	

(a) Precracked Charpy-size single edge notch bend, SE(B), specimen. Excluded from the single temperature T_0 calculation.
(b) Disk shaped compact fracture specimen.
(c) Compact fracture specimen.

Table 5-3. Transition Temperature Data for Weld Wire Heat 299L44 with Loading Rate Adjustment[31]

	Data Set	Test Temperature (°F)	Number of Specimens	T_0 (°F)	Loading Rate (ksi√in/sec)	Loading Rate Adjusted T_0 (°F)
SA-1526 (CR-3 nozzle drop-out)	0.5 TC(T)[(a)]	-70	6	-96	2.1	-105
WF-25(6) (TMI-2 nozzle drop-out)	Various C(T)s	-70	6	-58	1.2	-60
WF-25(9) (OC-3 nozzle drop-out)	0.5 TC(T)	-70	6	-99	2.0	-106
	PCS	-145	7	-126	0.2	-112

(a) Compact Fracture specimen.

6. Neutron Fluence

6.1. Introduction

The B&WOG has conducted the Reactor Vessel Integrity Program for more than ten years with the objective of assuring the continued licensability of the participants' reactor vessels. Reactor Vessel Surveillance Program requirements are defined in 10 CFR 50, Appendix H[4], and BAW-1543[1, 2] "Integrated Reactor Vessel Material Surveillance Program," which addresses the method of compliance with Appendix H. In addition to 10 CFR 50, Appendix H, the NRC's Safety Evaluation Report for BAW-1543 specifies the need for an integrated surveillance program and requires that each reactor in the integrated program have the capability to monitor reactor vessel neutron fluence. Capsule dosimetry measurements are used in a well-defined process to determine the best estimate fluence in the reactor vessel. While the fluence is also determined analytically, the measurements play a crucial role in establishing that the calculations are within the acceptance criteria and in determining the uncertainty in the fluence calculations.

Fluence analysis as part of the B&WOG reactor surveillance program has three objectives:

- Determine the maximum fluence at the reactor vessel as a function of reactor operation
- Predict the reactor vessel fluence in the future, and
- Determine the dosimeter activities within the surveillance capsule or cavity.

Over the last fifteen years, Framatome ANP has developed a calculational based fluence analysis methodology,[38] that can be used to accurately predict the fast neutron fluence in the reactor vessel using surveillance capsule dosimetry or cavity dosimetry (or both) to verify the fluence predictions. This methodology was developed through a full-scale benchmark experiment that was performed at the Davis-Besse Unit 1 reactor.[38] The methodology is described in detail in Appendix C. The results of the benchmark experiment demonstrated that the accuracy of a fluence analysis that employs the Framatome ANP methodology would be unbiased and have a precision well within the NRC-suggested limit of 20%.[38,39]

The Framatome ANP methodology was used to calculate the neutron fluence exposure to the TMI-LG2 capsule, which was irradiated in the TMI-2 and Crystal River Unit 3 nuclear reactors.

The fast neutron fluence (E> 1.0 MeV) at the capsule location was calculated as described in detail in the Framatome ANP fluence topical report, BAW-2241P-A[38], and as required in U.S. NRC Regulatory Guide 1.190.[39]

The energy-dependent flux in the reactor was used to determine the calculated activity of each dosimeter. Neutron transport calculations in two-dimensional geometry were used to obtain energy dependent flux distributions throughout the core. Reactor conditions were representative of average conditions over the irradiation period. Geometric detail was selected to explicitly represent the surveillance capsules and the reactor vessel. A more detailed discussion of the calculational procedure is given in Appendix C. The calculated activities were adjusted for known biases (photofission, short-half-life, and non-saturation), and compared to measured activities directly. It is noted that these measurements are not used in any way to determine the magnitude of the flux or the fluence. The measurements are used only to show that the calculational results are reasonable, and to show that the results of the TMI2-LG2 capsule are consistent with the Framatome ANP benchmark database of uncertainties.

6.2. Fluence Results

The surveillance specimen holder tube in which the TMI2-LG2 capsule was irradiated is attached to the thermal shield of the reactor, 10.0° off of the major axis. The dosimetry of the capsule received a total irradiation time of 3619.86 EFPD's. The rated thermal power for the four cycle groups was 2568 MWt.

The layout of the reactor vessel and dosimetry is shown in Figure 6-1 based on a quarter-core layout.

The locations of the Charpy and 0.936T fracture specimens and dosimeters within the capsule holders are shown in Figures 6-2 and 6-3, taken from the schematic capsule diagrams. Figure 6-4 shows the layout of the 0.394T inch and 0.5T inch fracture specimens, and Figure 6-5 shows the layout of the tensile specimens.

Axially averaged flux estimates were made at each location within the Charpy specimen blocks and at the center of the temperature monitor compartments. These estimates are of particular importance in determining the effect of neutron fluence on the properties of the specimens.

The three-dimensionally synthesized fluxes, including bias removal correction factors for each energy group, are given in Table 6-1 for each TMI2-LG2 capsule Charpy position, and Table 6-2 shows the tensile and fracture specimen fluxes for the TMI2-LG2 capsule. Fluence values for

each position are also shown, and were determined by multiplying the synthesized flux by the total irradiation time of 3522.56 EFPD's. This time is the period of irradiation within the Crystal River Unit 3 reactor, and was determined to be adequate for evaluating the dosimetry of the capsule.

6.3. Dosimetry Activity

The ratio of the specified activities to the measured specific activities (C/M) is presented in Table 6-3 for the TMI2-LG2 capsule. In this table, the target averaged C/M represents the average of all the individual target dosimeters and the overall average is the average C/M for the entire capsule.

Table 6-1. TMI2-LG2 Capsule 3D Synthesized Fluxes (E> 1.0 MeV)

Location	Flux (n/cm^2/s)	Fluence (n/cm^2)
1	6.47706E+10	1.97129E+19
2	6.59503E+10	2.00719E+19
3	6.61027E+10	2.01183E+19
4	6.49308E+10	1.97616E+19
5	5.64522E+10	1.71812E+19
6	5.64522E+10	1.71812E+19
7	5.67755E+10	1.72796E+19
8	5.66355E+10	1.72370E+19
9	5.57067E+10	1.69543E+19
10	4.82723E+10	1.46916E+19
11	4.82723E+10	1.46916E+19
12	4.82671E+10	1.46901E+19
13	4.72589E+10	1.43832E+19
14	4.57683E+10	1.39295E+19
15	4.03810E+10	1.22899E+19
16	4.01188E+10	1.22101E+19
17	3.94873E+10	1.20179E+19
18	3.85255E+10	1.17252E+19

Table 6-2. TMI2-LG2 Tensile and Fracture Specimen Fluxes (E> 1.0 MeV)

Compartment	Flux (n/cm^2/s)	Fluence (n/cm^2)
Tensile Specimen C	5.19030E+10	1.57966E+19
Tensile Specimen 1	5.54894E+10	1.68882E+19
Tensile Specimen 2	4.26708E+10	1.29868E+19
Tensile Specimen 3	6.51974E+10	1.98428E+19
Tensile Specimen 4	3.39356E+10	1.03283E+19
Tensile Specimen 5	5.69654E+10	1.73374E+19
Tensile Specimen 6	4.11675E+10	1.25293E+19
.936T Fracture Specimens	5.20858E+10	1.58523E+19
.394T Fracture Specimen F	5.87174E+10	1.78706E+19
.394T Fracture Specimen R	4.13236E+10	1.25768E+19
.5T Fracture Specimen 1	5.13660E+10	1.56332E+19
.5T Fracture Specimen 2	5.15087E+10	1.56766E+19
.5T Fracture Specimen 3	5.13459E+10	1.56271E+19
.5T Fracture Specimen 4	5.03686E+10	1.53296E+19

Table 6-3. TMI2-LG2 Capsule C/M Ratios

Dosimeter	Calculated (μCi/g)	Measured (μCi/g)	C/M	Capsule Average
LD7 U238	1.16568E+01	1.339E+01	0.8706	0.9349
LD7 Ni	8.56784E+02	9.591E+02	0.8933	
LD7 Cu	5.32840E+00	5.068E+00	1.0514	
LD7 Fe	8.19207E+02	7.241E+02	1.1313	
LD8 U238	1.19214E+01	1.460E+01	0.8165	
LD8 Ni	8.68669E+02	1.035E+03	0.8393	
LD8 Cu	5.44315E+00	5.615E+00	0.9694	
LD8 Fe	8.33346E+02	8.180E+02	1.0188	
LD9 U238	2.21461E+01	2.887E+01	0.7671	
LD9 Ni	1.71386E+03	2.003E+03	0.8556	
LD9 Cu	1.06600E+01	9.978E+00	1.0683	
LD9 Fe	1.64881E+03	1.540E+03	1.0707	
LD10 U238	2.16526E+01	2.903E+01	0.7459	
LD10 Ni	1.66589E+03	2.004E+03	0.8313	
LD10 Cu	1.03817E+01	1.010E+01	1.0279	
LD10 Fe	1.60218E+03	1.550E+03	1.0337	
LD11 U238	1.16046E+01	1.614E+01	0.7190	
LD11 Ni	8.78752E+02	1.101E+03	0.7981	
LD11 Cu	5.51680E+00	5.265E+00	1.0478	
LD11 Fe	8.41336E+02	7.480E+02	1.1248	
LD12 U238	1.13378E+01	1.549E+01	0.7319	
LD12 Ni	8.89876E+02	1.112E+03	0.8002	
LD12 Cu	5.77745E+00	5.328E+00	1.0844	
LD12 Fe	8.56495E+02	7.250E+02	1.1814	
SD2 U238	1.62978E+01	1.960E+01	0.8315	
SD2 Fe	1.17337E+03	1.187E+03	0.9885	

Figure 6-1. Crystal River Unit 3 Core and Capsule Overview

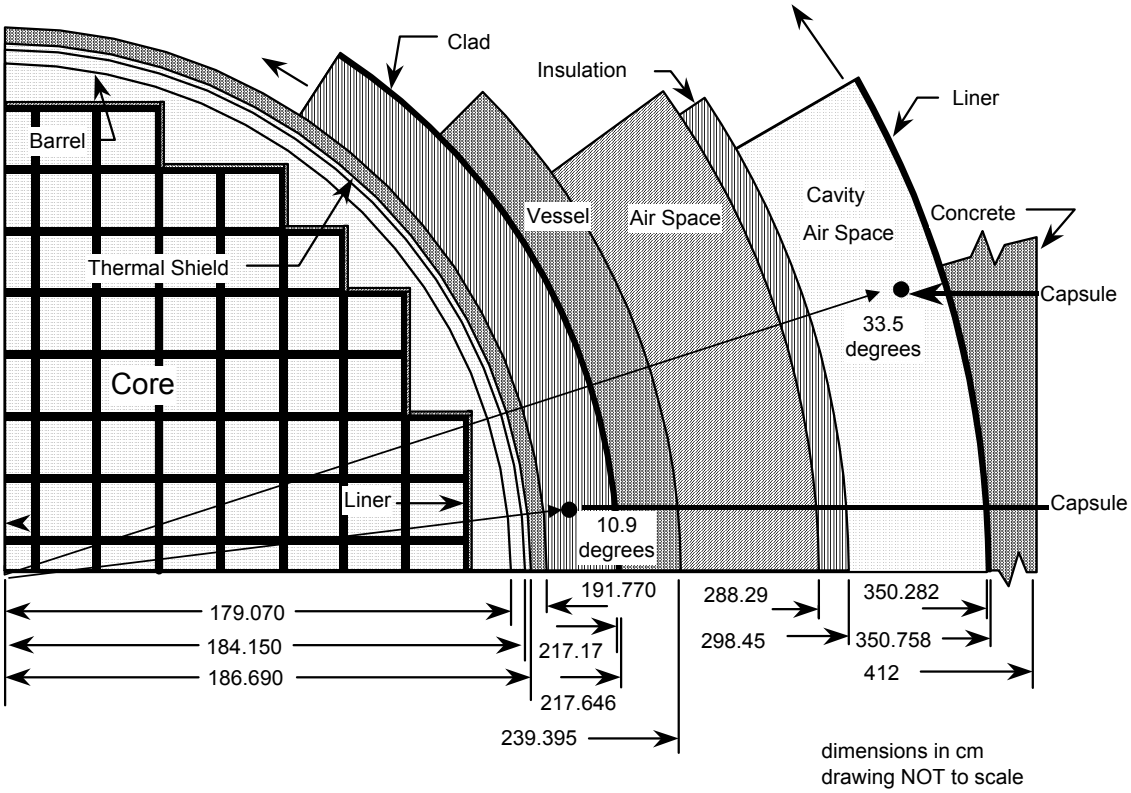

Figure 6-2. TMI2-LG2 Capsule Charpy Specimen and Dosimetry Layout

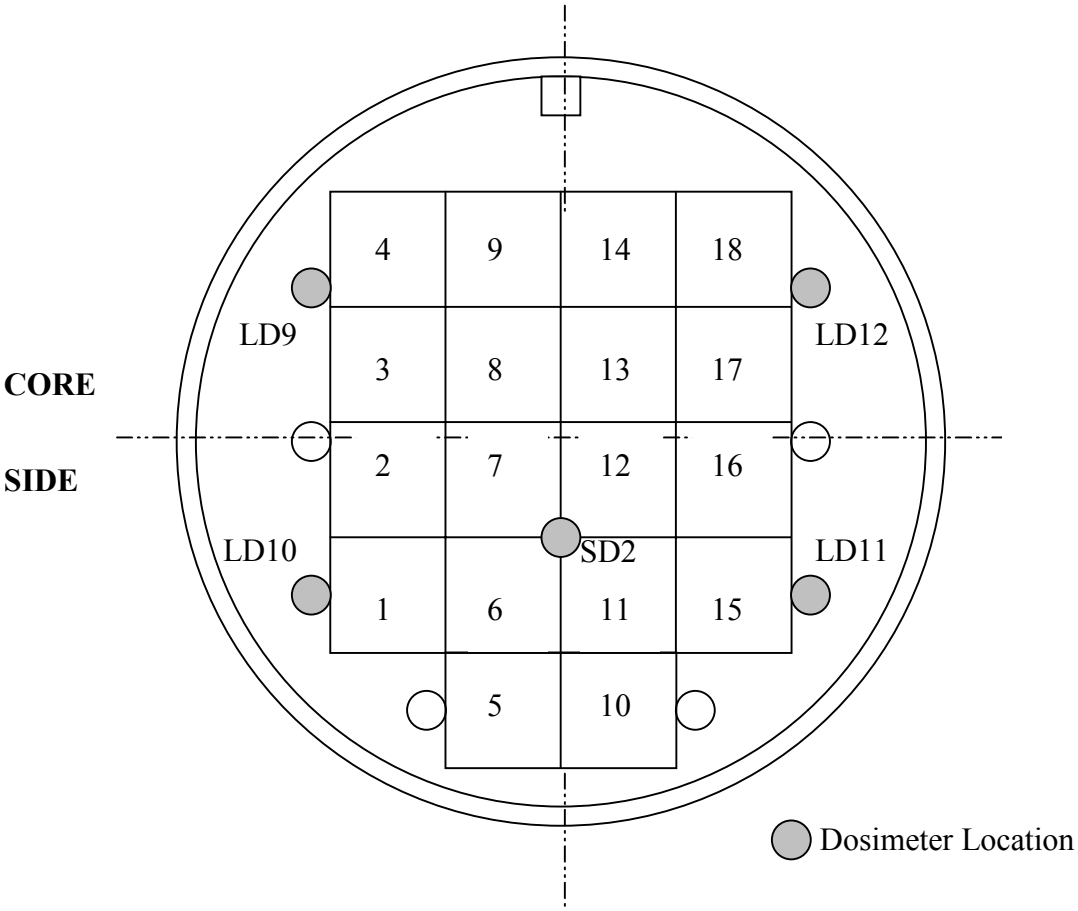

Figure 6-3. TMI2-LG2 Capsule Temperature Monitor Dosimetry Layout

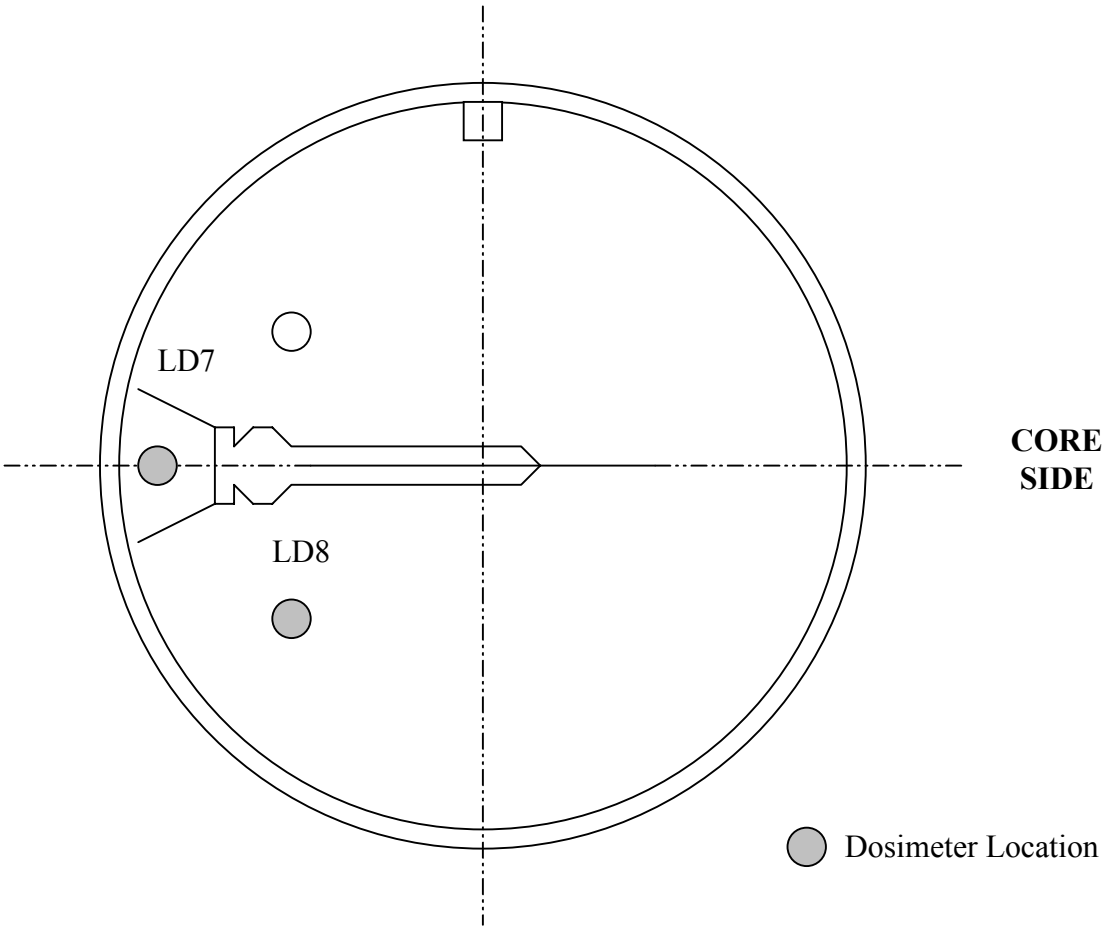

Figure 6-4. TMI2-LG2 Small Fracture Specimen Layout

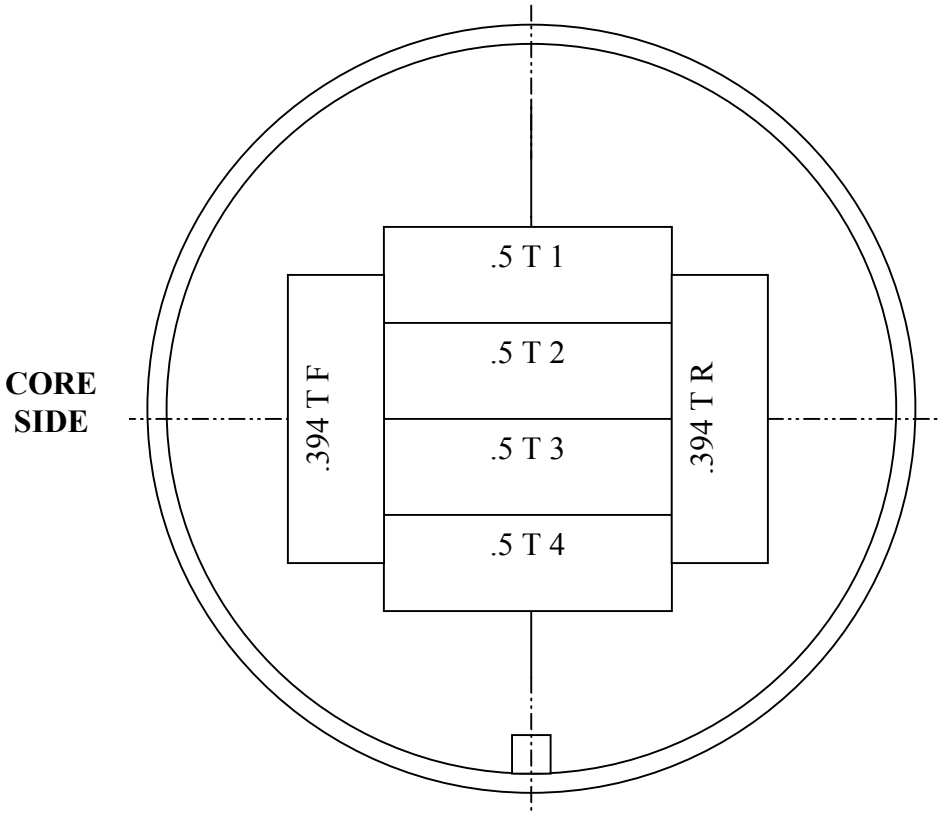

Figure not drawn to scale.

Figure 6-5. TMI2-LG2 Tensile Specimen Layout

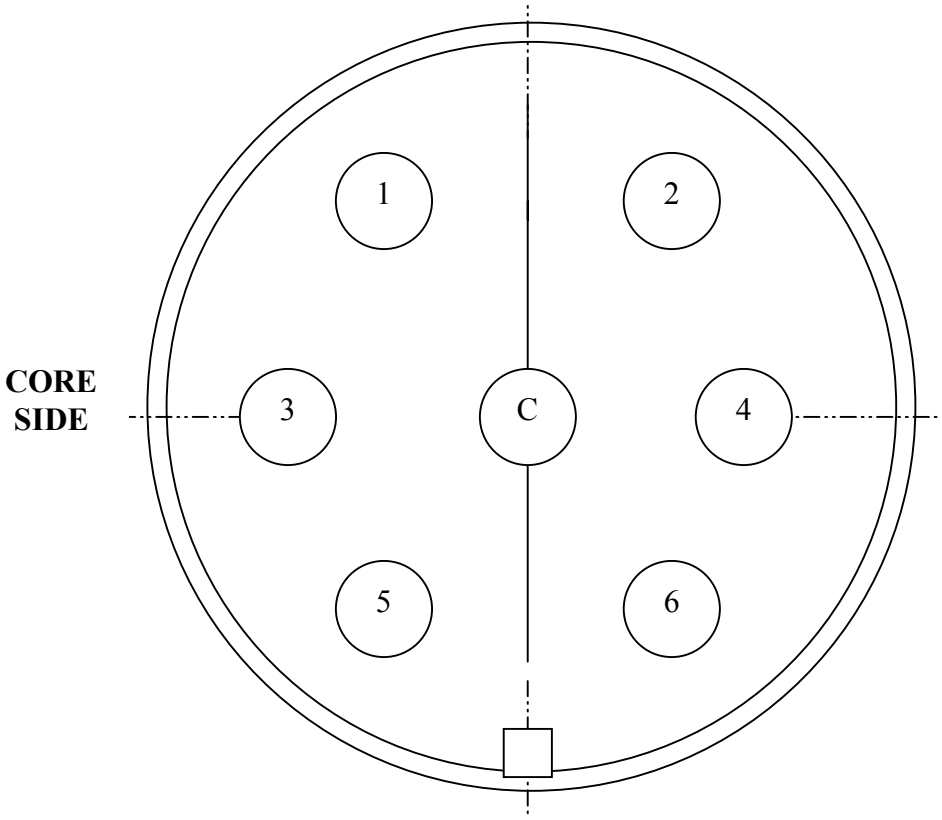

Figure not drawn to scale.

7. Discussion of Capsule Results

In addition to the TMI2-LG2 capsule mechanical test data, surveillance data for weld wire heat 299L44 is available from the Surry-1 and TMI-1 plant specific reactor vessel surveillance program (RVSP) capsule programs as well as other B&WOG MIRVSP capsules: CR3-LG1, TMI2-LG1, and W1.[16,19 and 40] The description of the testing and evaluation for these capsules are contained in their respective capsule reports.

7.1. Tensile Properties

The general behavior of tensile properties as a function of neutron irradiation is an increase in both ultimate and yield strength and a decrease in ductility as measured by total elongation and reduction in area.

Tables 7-1 and 7-2 and Figures 7-1 and 7-2 show the effect of irradiation on the tensile properties of all available weld wire heat 299L44 data at room temperature and near operating temperature, respectively. Review of the surveillance tensile test data indicates that the ultimate strength and yield strength changes in the wire heat 299L44 as a result of irradiation and the corresponding changes in ductility are within the typical range observed for similar irradiated materials.[41] Typical behavior of the Linde 80 welds show a reduced effect of irradiation on tensile properties beyond 1 x 10^{19} n/cm^2 (E>1 MeV).

The WF-25(6) data show an increase in ductility as measured by total elongation with irradiation, which is atypical. The baseline data was tested at ORNL. Additional baseline specimens were tested at BWXT to clear up this discrepancy. The new data shows that there is data scatter and the elongation trend does not change significantly with irradiation for WF-25(6) with both the room temperature and 580°F tests. Since the yield stress, ultimate stress, and reduction of area all behave as expected and similar to the other 299L44 welds and since there is normal scatter in the data, the atypical behavior of the elongation measurement is within the normal distribution of the data.

7.2. Upper-Shelf Charpy V-Notch Impact Test Results

The general behavior of the upper-shelf Charpy V-notch impact properties as a function of neutron irradiation is a decrease in upper-shelf energy (C_vUSE).

The C_vUSE values for the wire heat 299L44 welds irradiated in capsule TMI2-LG2 are presented in Table 7-3 along with 299L44 specimens irradiated other capsules. The changes in C_vUSE are compared to the predicted changes in accordance with Regulatory Guide 1.99, Revision 2[42] in Table 7-3.

The measured upper-shelf energy for the three wire heat 299L44 welds removed from the TMI2-LG2 capsule are in good agreement with the value predicted using Regulatory Guide 1.99, Revision 2 and with data from other capsules. All three weld C_vUSE values fall below the required 50 ft-lb limit as expected.[3]

7.3. Upper-Shelf Fracture Toughness Test Results

The upper-shelf fracture toughness data for the welds contained in the TMI2-LG2 capsule are part of the RVIP to justify continued operation for the RVWG reactor vessels that contain welds with C_VUSE values below 50 ft-lbs. Figure 7-3 shows prior data tested under the RVIP and the B&WOG J-integral resistance (J_d) model used for previous analyses[11]. The new data, which is PTS limiting in several reactor vessels and has a relatively high copper content, lies well above the model median line. Figure 7-4 compares the J-R curves developed from the three tested 299L44 specimens to the B&WOG J_d model median and lower bound curves. The median J_d model curve represents the specimen J-R curves fairly well, while the lower bound curve conservatively represents the test data. This data supports the claim that the current model is conservative.

7.4. Reference Temperature

The master curve reference temperature is a fracture mechanics based measurement that can be used to evaluate the shift in transition temperature as a function of neutron irradiation. The master curve reference temperature can also be used to directly evaluate the fracture toughness of the reactor vessel beltline region.

Table 7-4 compares the measured reference temperature changes in the irradiated weld metals fabricated with weld wire heat 299L44 with the predicted changes of 30 ft-lb Charpy impact test in accordance with Regulatory Guide 1.99, Revision 2, Position 1[42]. All but one of the measured reference temperature shifts are significantly less than the prediction using Regulatory Guide 1.99, Revision 2, Position 1. The WF-25(6) CT specimen shift exceeds the Regulatory Guide 1.99, Revision 2, Position 1 prediction, but is still within one standard deviation.

Figures 7-5, 7-6, and 7-7 show a plot of the measured and predicted shift values with respect to the calculated fluence for master curve reference temperature and Charpy 30 ft-lb shift values. For all the material sources for which there are 30 ft-lb CVN and T_0 data, the T_0 data showed a lower shift. In addition, the T_0 shift was almost always less than that predicted by Regulatory Guide, Revision 2, Position 1. Whereas, the CVN 30 ft-lb transition temperature shift was generally higher than the Regulatory Guide 1.99, Revision 2, Position 1 prediction.

Figure 7-8 shows a plot of the measured 30 ft-lb CVN and T_0 shifts normalized to a chemistry factor of 215.2 and an irradiation temperature of 556°F relative to the fluence factor. A one degree decrease in shift was used for each degree the irradiation temperature was lower than 556°F. The normalization and fluence factor calculation followed the Regulatory Guide 1.99, Revision 2 procedure. The calculation of the best-fit line through the normalized data results in the calculation of the chemistry factor used when surveillance data is available (provided the data is credible). The resulting fit for the 30 ft-lb CVN (224) is significantly higher than for the T_0 data (192). Neither shift measurement would be judged credible per Regulatory Guide 1.99, Revision 2, Position 2. Except for one point, the T_0 has an acceptable amount of scatter about the best-fit line, while the 30 ft-lb CVN data has an unacceptable amount of scatter to use the Regulatory Guide 1.99, Revision 2, Position 2 approach.

Figure 7-9 shows the fracture toughness data for the irradiated weld wire heat 299L44 plotted with the master curve and the 5%/95% tolerance bounds. As expected, about 90% of the data falls within the 5%/95% tolerance bounds. This data conforms to the behavior expected with the master curve concept.

Tregoning and Joyce suggested that on average the precracked Charpy size (PCS) bend specimens resulted in T_0 measurements that are about 18°F lower than those measured using compact fracture specimens.[43] This is known as the PCS bias. The PCS bias for the Linde 80 baseline specimens also averaged about 18°F.[33] It has been suggested that the bias for irradiated specimens is lower than the bias for the baseline specimens due to the irradiation hardening. The bias for the three 299L44 welds irradiated in the TMI2-LG2 capsule was evaluated by adjusting for the differences in fluence between the PCS and C(T) specimens using 192•(difference in fluence factor). The three bias measurements average 31°F with a standard deviation of 22°F. Due to the large variation in the bias measurements, the evidence is not strong enough to say that the baseline and irradiated Linde 80 biases are different.

Table 7-1. Summary of Weld Wire Heat 299L44
Room Temperature Tensile Test Results

Source	Capsule	Fluence, 10^{19} n/cm^2 (E>1 MeV)	Test Temp., F	Strength, ksi				Ductility, %			
				Yield	%[a]	Ultimate	%[a]	Total Elong.	%[a]	Reduction of Area	%[a]
WF-25	Unirradiated	0.000	RT	69.2[b]	---	86.2[b]	---	26.7[b]	---	62.8[b]	---
TMI-1 RVSP	E	0.107	RT	82.6	19.3	97.2	12.8	24.8	-7.2	55.8	-11.3
	C	0.882[c]	67	97.7	41.1	105.7	22.6	23.0	-13.8	55.0	-12.5
SA-1526	Unirradiated	0.000	RT	69.7[b]	---	83.2[b]	---	26.5[b]	---	66.7[b]	---
Surry-1 RVSP	T	0.292[c]	88	89.9	29.0	105.5	26.8	21.6	-18.5	56.0	-16.0
	X	1.599	70	97.9	40.5	111.3	33.8	21.7	-18.1	51.3	-23.1
SA-1526	Unirradiated	0.000	70	62.2	---	81.0	---	33.0	---	65.0	---
CR-3 ND	TMI2-LG1	0.873	70	85.9	38.1	101.0	24.7	---	---	---	---
	TMI2-LG2	1.984	70	87.0	39.9	102.6	26.7	21.3	-35.5	58.1	-10.6
WF-25(6)	Unirradiated	0.000	70[d]	62.5	---	85.9	---	24.0	---	70.1	---
TMI-2 ND	Unirradiated	0.000	79[e]	69.9[b]	---	87.1[b]	---	20.5[b]	---	67.5[b]	---
	TMI2-LG1	0.992	70	92.3	32.0[f]	107.0	22.8[f]	---	---	47.5	-29.6[f]
	TMI2-LG2	1.580	70	94.0	34.5[f]	108.9	25.0[f]	24.5	19.5[f]	57.6	-14.7[f]
WF-25(9)	Unirradiated	0.000	75	64.9	---	80.2	---	26.0	---	67.0	---
OC-3 ND	CR3-LG1	0.500	75	86.3	33.0	100.0	24.7	22.0	-15.4	57.0	-14.9
	TMI2-LG2	1.299	70	92.8	43.0	106.9	33.3	24.6	-5.4	57.0	-14.9

(a) Change relative to unirradiated material property.
(b) Average of multiple samples.
(c) Updated fluence values.[44,45]
(d) BWXT Retest.[34]
(e) Original ORNL tests.
(f) Change relative to unirradiated ORNL data.

Table 7-2. Summary of Weld Wire Heat 299L44
Operating Temperature Tensile Test Results

Source	Capsule	Fluence, 10^{19} n/cm^2 (E>1 MeV)	Test Temp., F	Strength, ksi				Ductility, %			
				Yield	%[a]	Ultimate	%[a]	Total Elong.	%[a]	Reduction of Area	%[a]
WF-25	Unirradiated	0.000	570	64.3[b]	---	81.7[b]	---	20.5[b]	---	52.3[b]	---
TMI-1 RVSP	E	0.107	570	76.0	18.3	94.8	16.0	19.1	-6.8	38.4	-26.6
	C	0.882[c]	580	80.0	24.4	97.1	18.8	17.0	-16.9	49.0	-6.4
SA-1526	Unirradiated	0.000	600	58.1[b]	---	79.0[b]	---	22.9[b]	---	62.0[b]	---
Surry-1 RVSP	T	0.292[c]	550	77.9	34.1	96.2	21.7	17.0	-25.8	51.2	-17.4
	X	1.599	550	85.1	46.4	101.3	28.3	16.3	-28.8	49.9	-19.5
	V	1.992[c]	550	82.5	41.9	101.9	29.0	17.1	-25.3	51.0	-17.7
SA-1526	Unirradiated	0.000	580	54.3	---	78.0	---	21.0	---	58.0	---
CR-3 ND	TMI2-LG1	0.873	580	76.5	40.9	94.2	20.8	16.9	-19.5	40.0	-31.0
	TMI2-LG2	1.734	580	79.4	46.2	96.7	24.0	15.8	-24.8	40.2	-30.7
WF-25(6)	Unirradiated	0.000	580[d]	56.6	---	80.3	---	17.1	---	54.6	---
TMI-2 ND	Unirradiated	0.000	550[e]	59.4[b]	---	76.9[b]	---	16.5[b]	---	63.5[b]	---
	TMI2-LG1	0.992	580	80.1	35.0[f]	98.0	27.4[f]	18.4	11.5[f]	42.0	-33.9[f]
	TMI2-LG2	1.689	580	82.4	38.8[f]	100.0	30.0[f]	17.4	5.5[f]	49.4	-22.2[f]
WF-25(9)	Unirradiated	0.000	580	60.3	---	75.3	---	16.0	---	59.0	---
OC-3 ND	CR3-LG1	0.500	580	76.7	27.2	90.3	19.9	14.0	-12.5	46.0	-22.0
	TMI2-LG2	1.253	580	80.8	34.0	97.7	29.7	15.8	-1.3	39.1	-33.7

(a) Change relative to unirradiated material property.
(b) Average of multiple samples.
(c) Updated fluence values.[44,45]
(d) BWXT Retest.[34]
(e) Original ORNL tests.
(f) Change relative to unirradiated ORNL data.

Table 7-3. Measured vs. Predicted Upper-Shelf Energy Decreases for Weld Wire Heat 299L44

Weld	Capsule	Fluence 10^{19} n/cm^2 (E>1 MeV)	Measured Upper-Shelf		% Decrease Predicted In Accordance With Regulatory Guide 1.99, Rev. 2, Figure 2[(a)]
			Energy, ft-lbs	% Decrease	
WF-25 TMI-1 RVSP	Unirradiated	0.000	81.0	---	---
	E	0.107	61.5	24.1	27.7
	C	0.882[(b)]	48.0	40.7	41.6
SA-1526 Surry-1 RVSP	Unirradiated	0.000	69.0	---	---
	T	0.292[(b)]	52.0	24.6	27.6
	V	1.992[(b)]	47.0	31.9	43.6
	X	1.599	39.0	43.5	41.3
SA-1526 (CR-3 nozzle drop-out)	Unirradiated	0.000	78.5	---	---
	W1	0.669	42.0	46.5	39.9
	TMI2-LG1	0.830	47.0	40.1	41.2
	TMI2-LG2	1.998	42.5	45.9	47.0
WF-25(6) (TMI-2 nozzle drop-out)	Unirradiated	0.000	65.5	---	---
	TMI2-LG1	0.968	43.0	34.4	42.2
	TMI2-LG2	1.716	38.7	40.9	46.0
WF-25(9) (OC-3 nozzle drop-out)	Unirradiated	0.000	78.0	---	---
	CR3-LG1	0.779	47.5	39.1	40.8
	TMI2-LG2	1.433	41.7	46.5	44.7

(a) Based on mean copper content as shown in BAW-2325, Revision 1.[22]
(b) Updated fluence values.[44,45]

Table 7-4. Measured Shift in Reference Temperature for Wire Heat 299L44

Weld	Capsule	Fluence x 10^{19} n/cm^2 (E > 1 MeV)	Specimen Type	T_0 (°F)[33]	T_0 Shift (°F)	30 ft-lb CVN Predicted[(a)] Shift, F
SA-1526 Surry 1 RVSP	X	1.599	PCS	87[(d)]	192[(c)]	199
SA-1526 (CR-3 nozzle drop-out)	Unirradiated	0.000	C(T)	-105[(d)]	---	---
	TMI2-LG2	1.628	C(T)	116	221	265
	TMI2-LG2	1.812	PCS	111	216[(c)]	272
WF-25(6) (TMI-2 nozzle drop-out)	Unirradiated	0.000	C(T)	-58	---	---
	TMI2-LG2	1.545	C(T)	203[(b)]	261	241
	TMI2-LG2	1.595	PCS	151	209	243
WF-25(9) (OC-3 nozzle drop-out)	Unirradiated	0.000	PCS	-112[(d)]	---	---
	CR3-LG1	0.78	PCS	76[(d)]	188	214
	TMI2-LG2	1.235	PCS	97[(b)]	209	244
	Unirradiated	0.000	C(T)	-106[(d)]	---	---
	TMI2-LG2	1.463	C(T)	135	241	255

(a) In Accordance with Regulatory Guide 1.99, Rev. 2, Position 1; Based on mean copper and nickel content as shown in BAW-2325, Rev. 1.

(b) Insufficient data available for calculation of a valid reference temperature.[31]

(c) Calculated relative to the unirradiated SA-1526 CR-3 nozzle drop-out CT(T) specimens.

(d) Rate adjusted to 1 MPa√m/s as reported in BAW-2308.[33]

Figure 7-1. Weld Wire Heat 299L44
Room Temperature Tensile Test Results

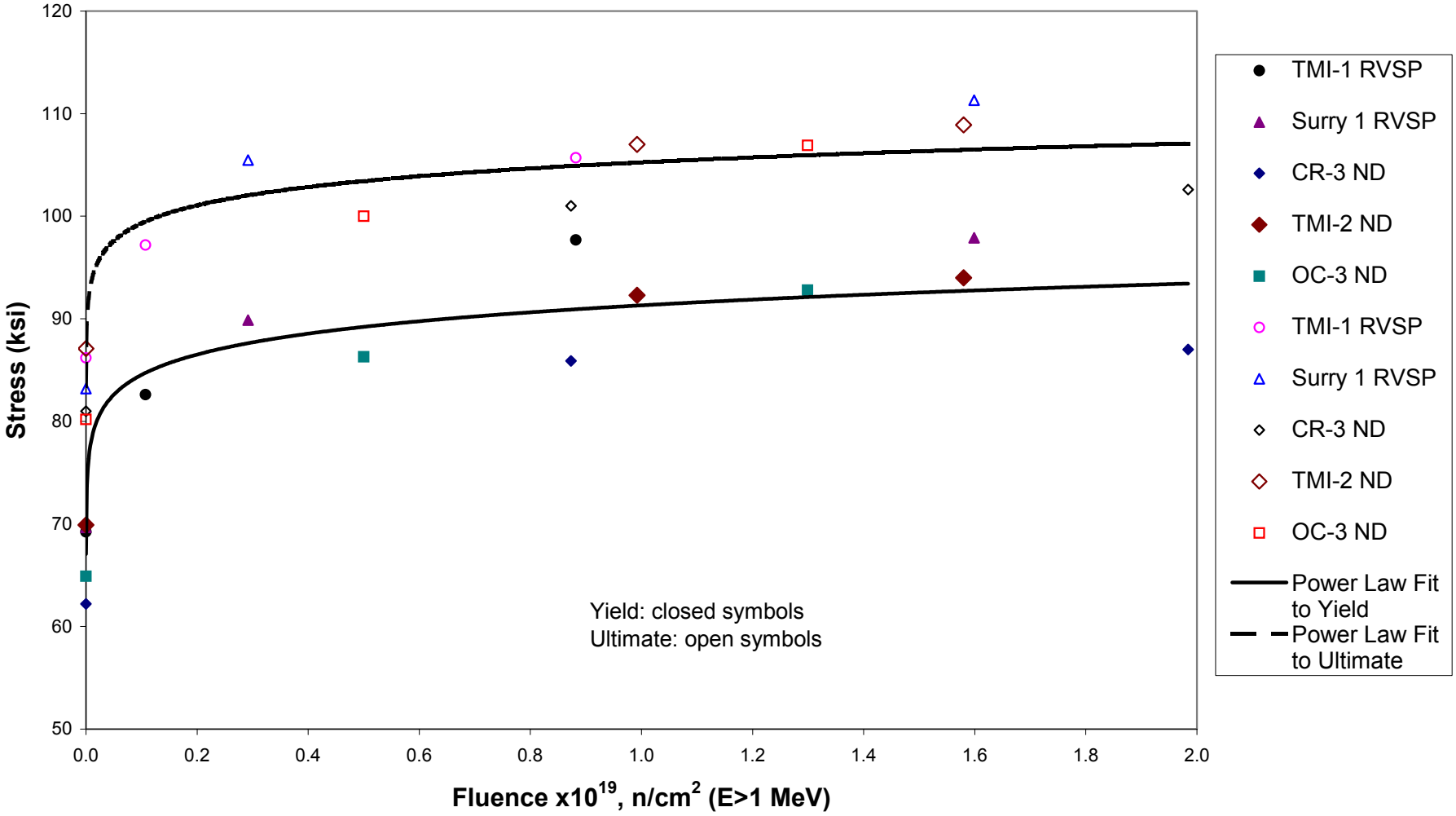

Figure 7-2. Weld Wire Heat 299L44
Operating Temperature Tensile Test Results

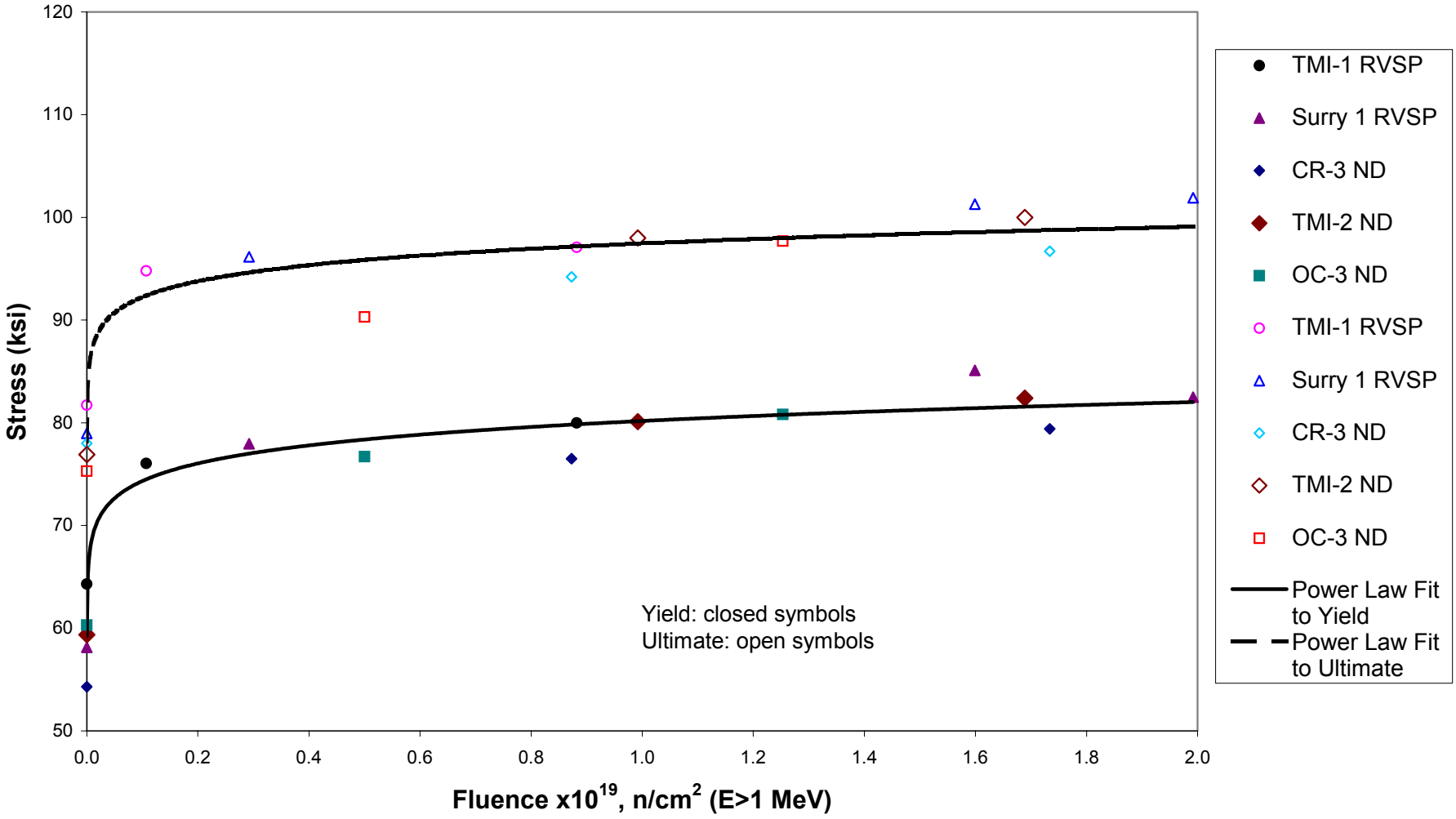

Figure 7-3. Upper-Shelf Fracture Toughness Data as Compared to B&WOG Linde 80 J_d Model

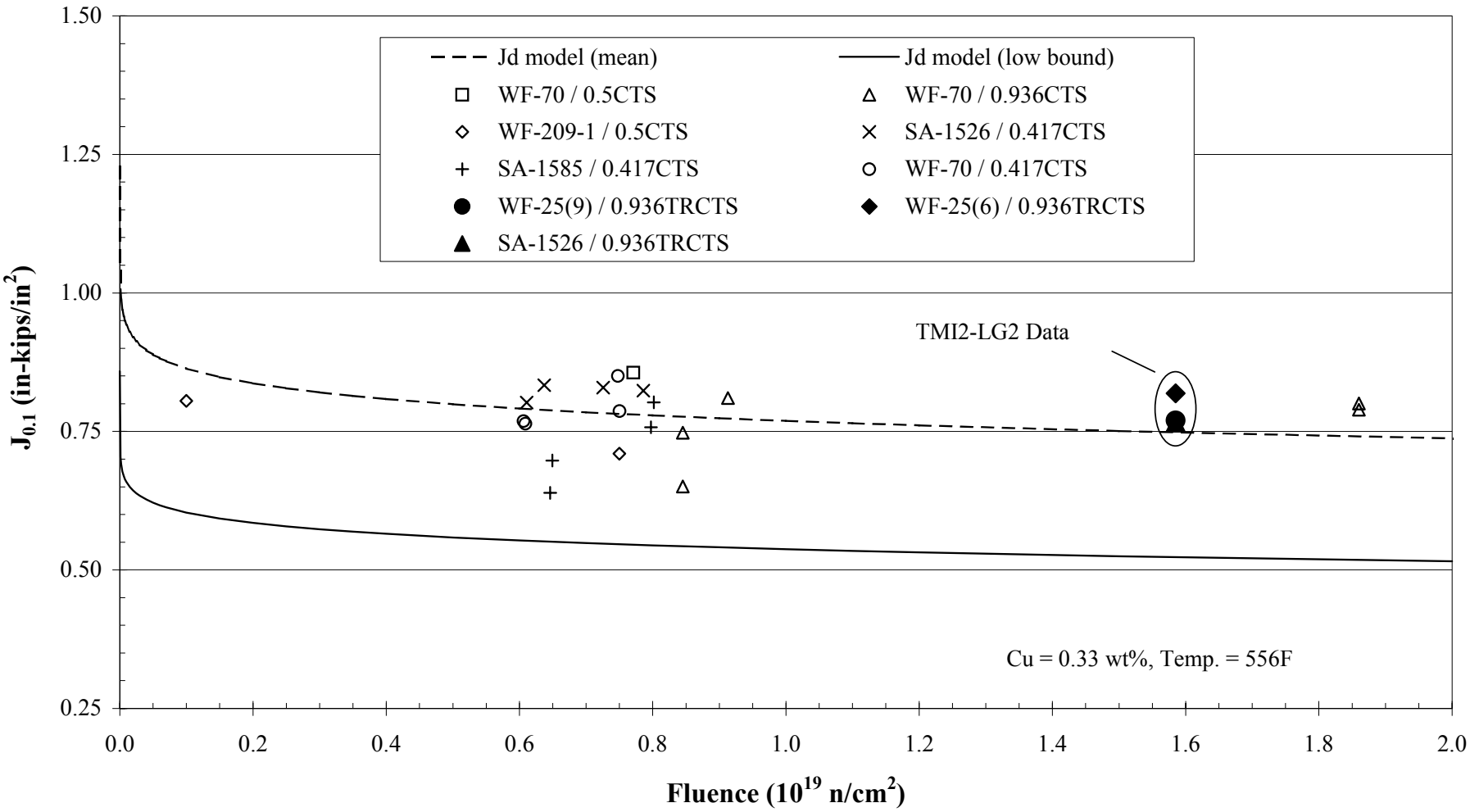

Figure 7-4. Upper-Shelf Fracture Toughness J-R Curves Compared to B&WOG Linde 80 J_d Model

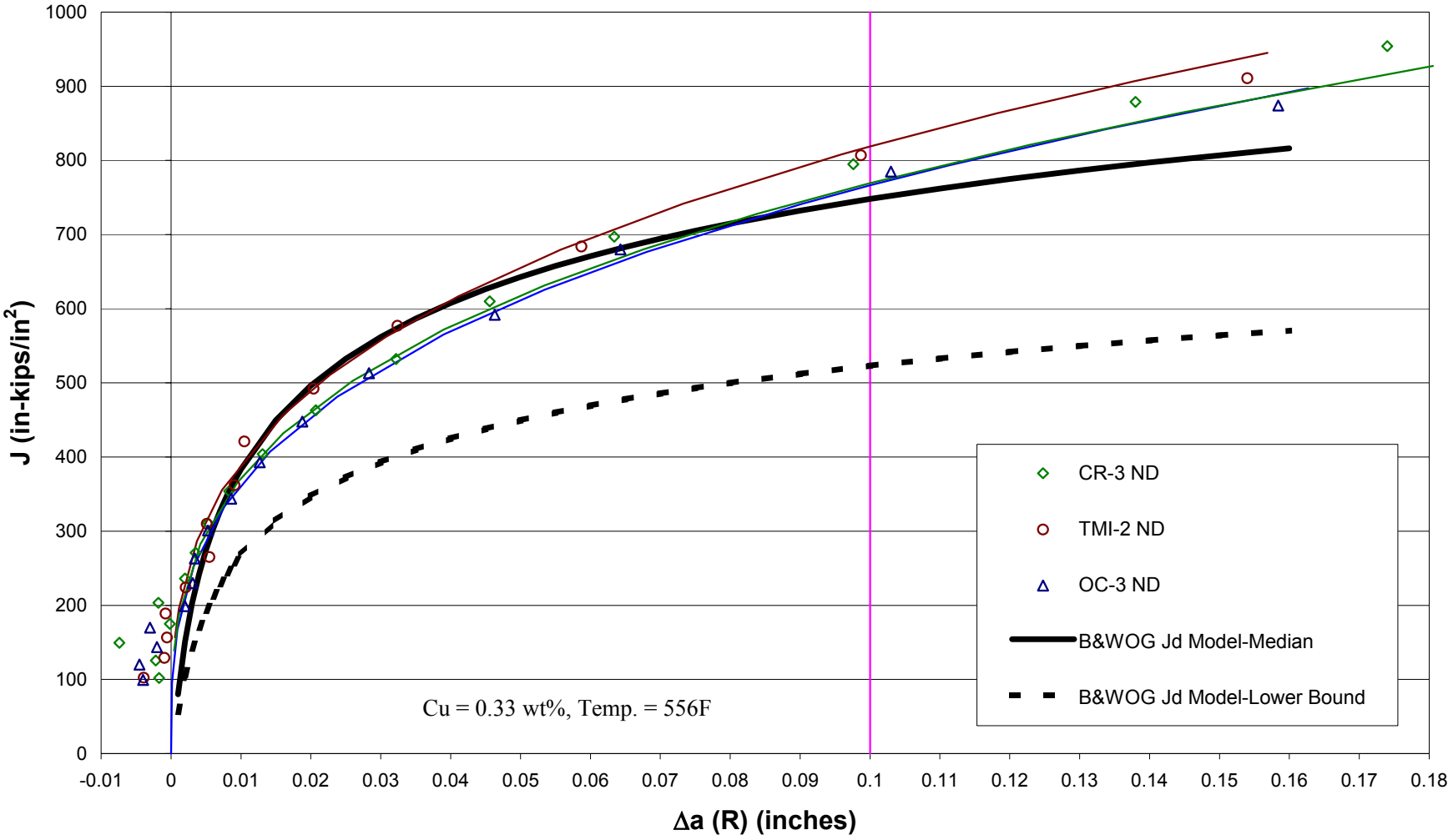

Figure 7-5. Measured Shift in Reference Temperature and 30 ft-lb CVN Shift as compared to the Regulatory Guide 1.99, Rev. 2, Position 1, 30 ft-lb CVN Shift Prediction for Surry 1 RVSP Weld

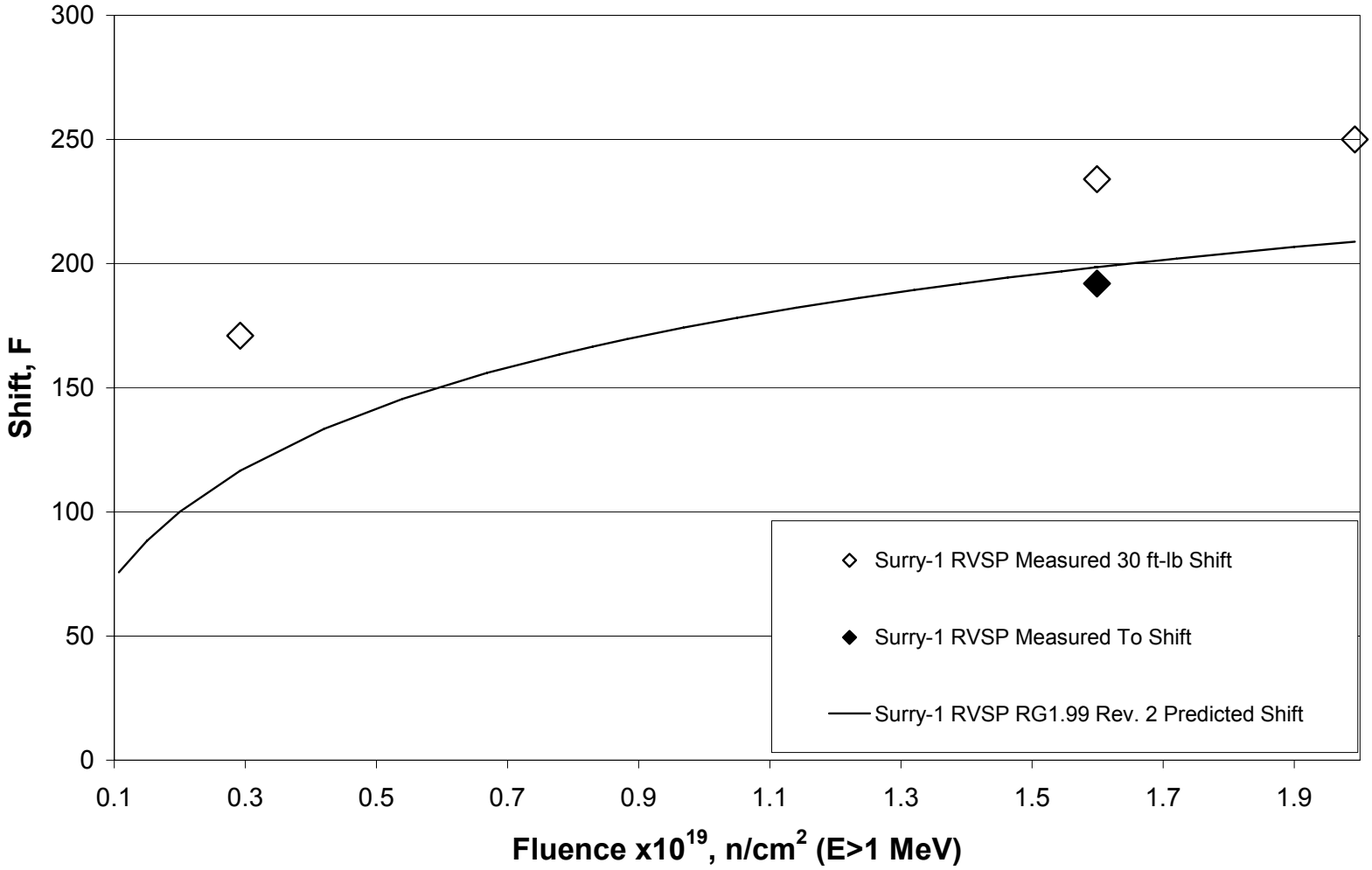

Figure 7-6. Measured Shift in Reference Temperature and 30 ft-lb CVN Shift as compared to the Regulatory Guide 1.99, Rev. 2, Position 1, 30 ft-lb CVN Shift Prediction for CR-3 and OC-3 Nozzle Dropout Welds

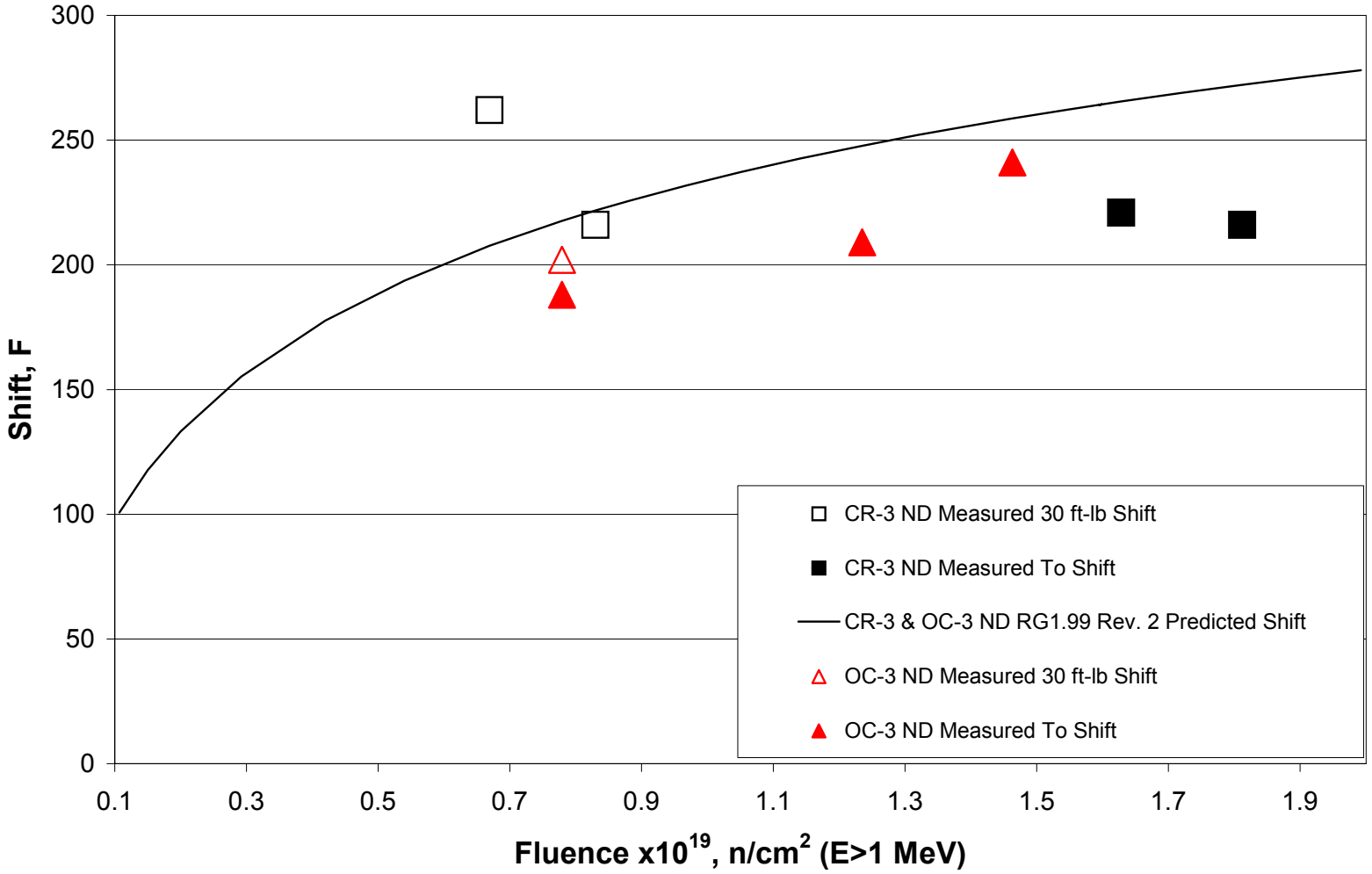

Figure 7-7. Measured Shift in Reference Temperature and 30 ft-lb CVN Shift as compared to the Regulatory Guide 1.99, Rev. 2, Position 1, 30 ft-lb CVN Shift Prediction for TMI-1 RVSP and TMI-2 Nozzle Dropout Welds

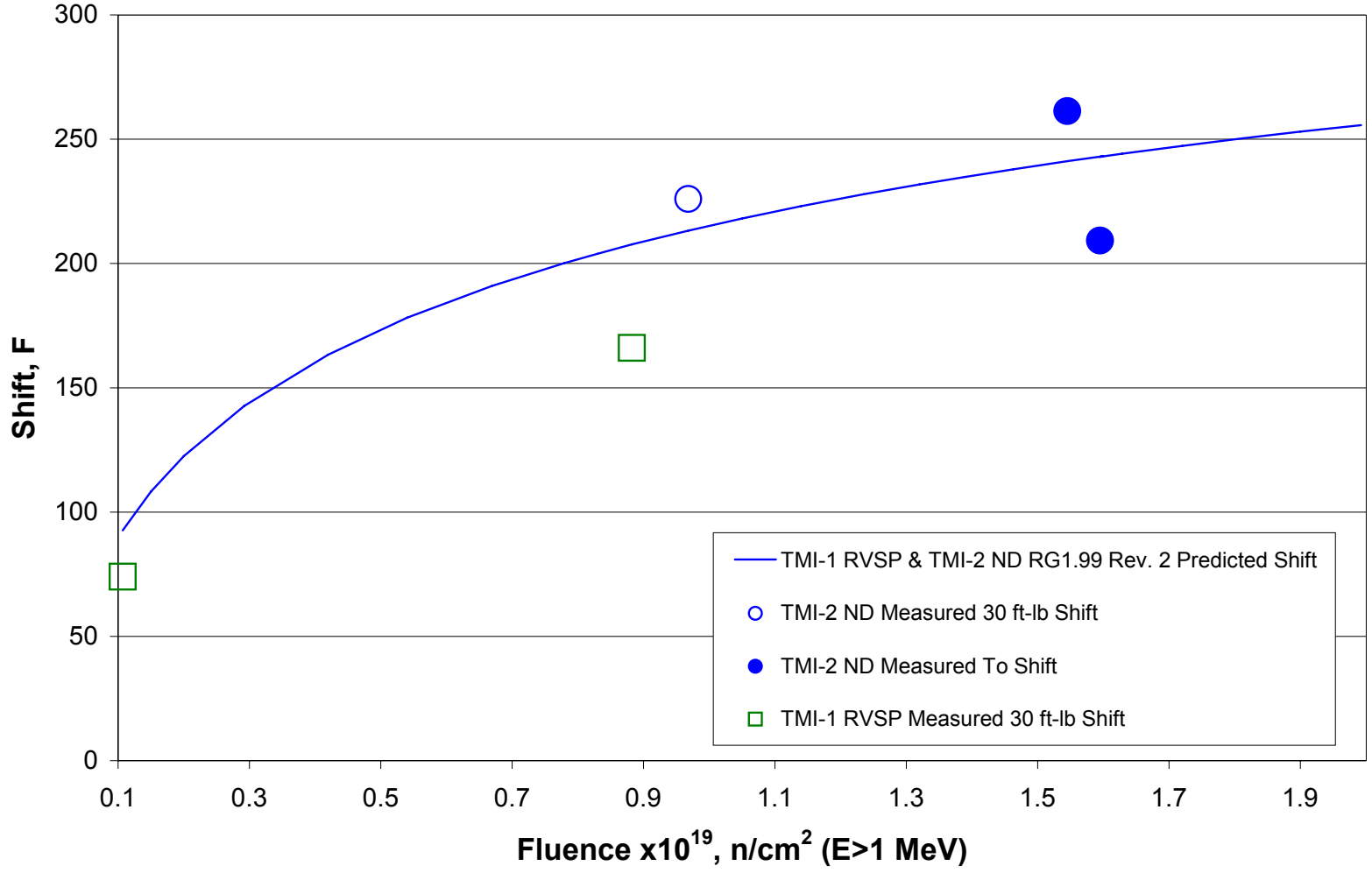

Figure 7-8. Normalized Shift in Reference Temperature and 30 ft-lb CVN Shift Relative to the Regulatory Guide 1.99, Rev. 2 Fluence Factor for Weld Wire Heat 299L44

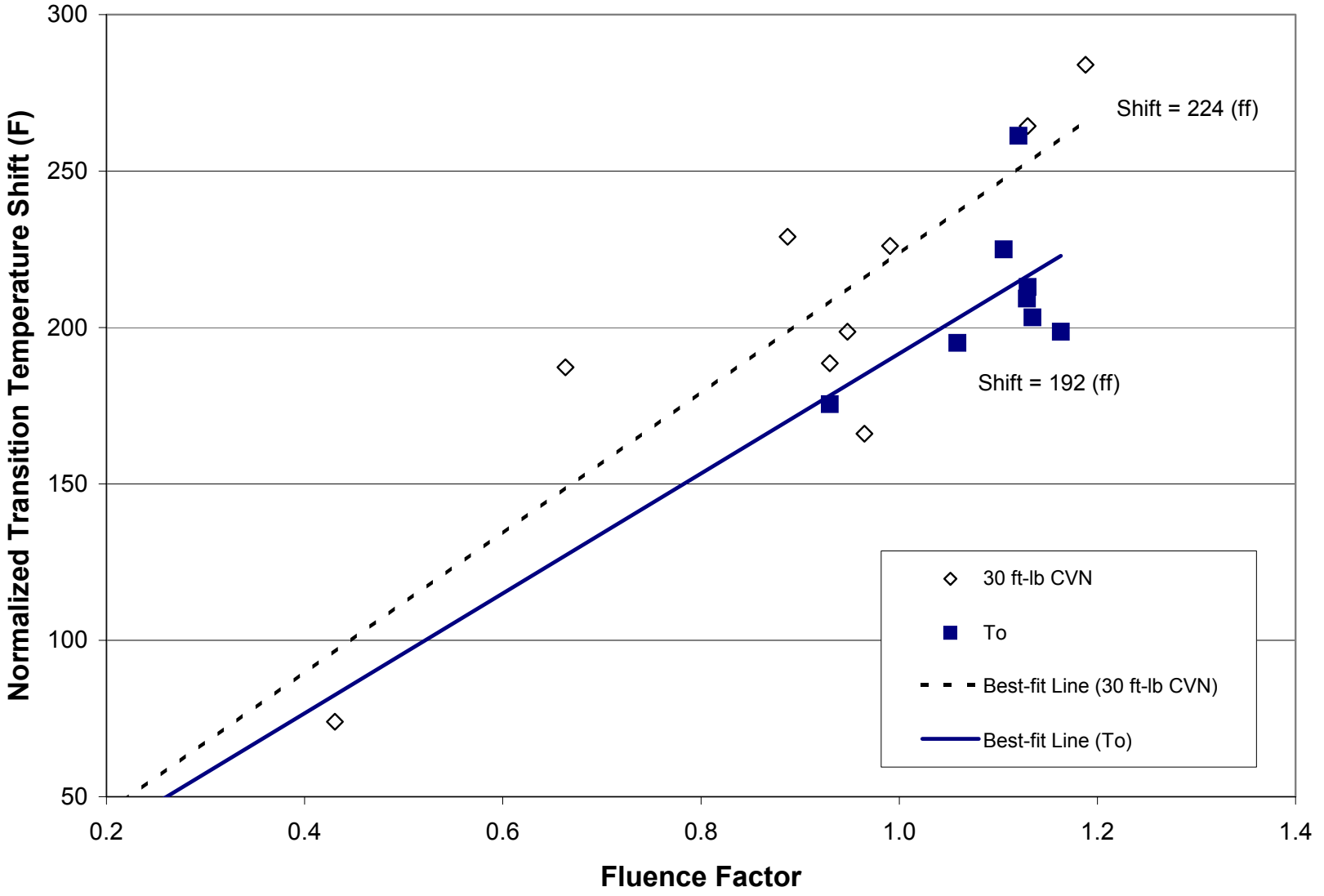

Figure 7-9. Fracture Toughness Data Plotted with the Master Curve and the 5%/95% Tolerance Bounds for Weld Wire Heat 299L44 (Irradiated in TMI2-LG2)

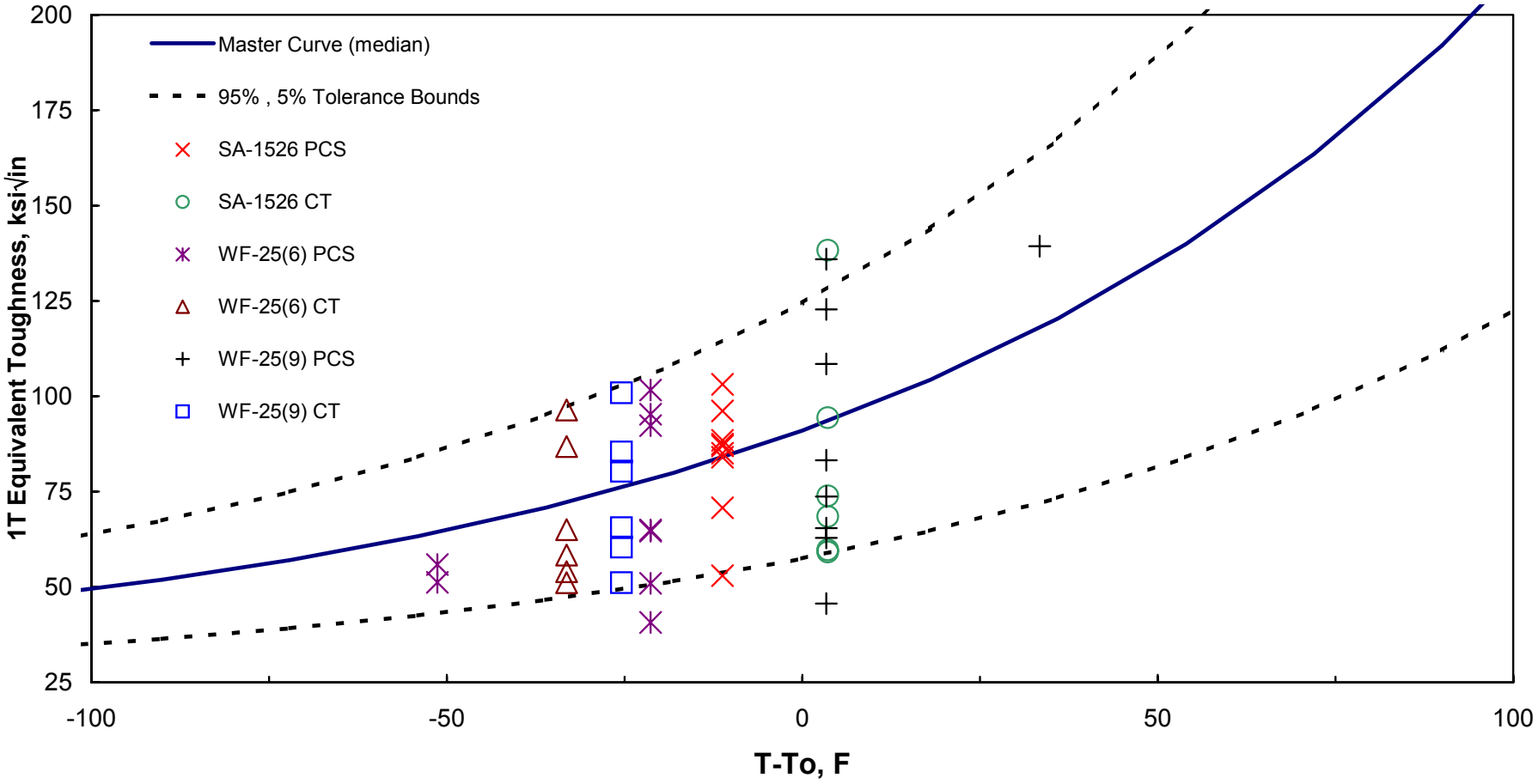

8. Summary of Results

The analysis of the reactor vessel material contained in the B&W Owners Group Master Integrated Reactor Vessel Surveillance Program TMI2-LG2 Capsule are summarized as follows:

1. The specimens within the TMI2-LG2 capsule received an average fast neutron fluence of 1.17 to 2.01 x 10^{19} n/cm^2 (E > 1.0 MeV) after exposure in the Crystal River Unit 3 reactor vessel for 6 cycles and in Three Mile Island Unit 2 from start-up until shut-down on March 29, 1979.

2. The maximum temperature reached by the capsule during irradiation in Crystal River Unit 3 could not be determined from the thermal monitors. The thermal monitors melted in Three Mile Island Unit 2 during the incident on March 29, 1979. The typical surveillance capsule irradiation temperature for the B&W designed 177 fuel assembly plants is 556°F.

3. The change in tensile yield, ultimate strength and ductility of the three wire heat 299L44 welds irradiated in the TMI2-LG2 capsule are within the typical range observed for similar irradiated materials.

4. The measured Charpy V-notch upper-shelf energy (38.7 to 42.5 ft-lbs) for the three 299L44 welds tested are less than the required 50 ft-lbs limit with irradiation to 1.43 to 2.00 x 10^{19} n/cm^2 (E > 1.0 MeV) as expected.

5. The upper-shelf fracture toughness tests conducted on the three 299L44 welds at 550°F demonstrate that the current model in use conservatively represents this data in justifying continued operation with the Linde 80 low upper shelf welds.

6. On average, the shift in the fracture toughness based reference temperature (T_0) for the 299L44 welds measured to date are less than the predicted 30 ft-lb transition temperature shift based on Regulatory Guide 1.99, Revision 2, Position 1.

7. On average, the shift in the fracture toughness based reference temperature for all 299L44 welds measured to date are less than the measured 30 ft-lb Charpy impact transition temperature shift.

8. The scatter in the measured shift of the fracture toughness based reference temperature is less than the measured 30 ft-lb Charpy impact transition temperature shift.

9. Certification

The specimens obtained from the B&W Owners Group Master Integrated Reactor Vessel Surveillance Program TMI2-LG2 capsule were tested and evaluated using accepted techniques and established standard methods and procedures.

J. B. Hall (Material Analysis) — 5-28-03
Materials & Structural Analysis Unit

J. W. Newman, Jr. (Fluence Analysis) — 5/28/03
Radiological Analysis Unit

This report has been reviewed for technical content and accuracy.

R. R. Grambau (Material Analysis) — 5/28/03
Materials & Structural Analysis Unit

M. A. Rutherford (Fluence Analysis) — 5/28/03
Radiological Analysis Unit

Verification of independent review.

A. D. McKim, Manager — 5/28/03
Materials & Structural Analysis Unit

This report is approved for release.

W. R. Gray — 5/28/03
Program Manager

10. References

1. L. S. Harbison, "*Master Integrated Reactor Vessel Surveillance Program*," BAW-1543, Revision 4, B&W Nuclear Technologies, Inc., Lynchburg, Virginia, February 1993.*

2. J. B. Hall, "*Supplement to the Master Integrated Reactor Vessel Surveillance Program,"* BAW-1543A, Revision 4, Supplement 4, Framatome ANP, Lynchburg, Virginia, May 2002.*

3. Code of Federal Regulation, Title 10, Part 50, *"Domestic Licensing of Production and Utilization Facilities,"* Appendix G, Fracture Toughness Requirements.

4. Code of Federal Regulation, Title 10, Part 50, *"Domestic Licensing of Production and Utilization Facilities,"* Appendix H, Reactor Vessel Material Surveillance Program Requirements.

5. S. Fyfitch and W. A. McInteer, "*Requalification of the TMI-2 Reactor Vessel Surveillance Program Capsules*," BAW-2042, Babcock & Wilcox's Nuclear Power Generation Division, Lynchburg, Virginia, August 1988.*

6. American Society of Mechanical Engineers (ASME) Boiler and Pressure Vessel Code, Section III, *"Nuclear Power Plant Components,"* Appendix G, Protection Against Nonductile Failure, 1989 Edition.

7. American Society of Mechanical Engineers (ASME) Boiler and Pressure Vessel Code, Section XI, *"Rules for Inservice Inspection of Nuclear Power Plant Components,"* Appendix G, Fracture Toughness Criteria for Protection Against Failure, 1989 Edition.

8. ASTM Standard E 208-81, *"Method for Conducting Drop-Weight Test to Determine Nil-Ductility Transition Temperature of Ferritic Steels,"* American Society for Testing and Materials, Philadelphia, Pennsylvania.

9. K. K. Yoon, "*Low Upper-Shelf Toughness Fracture Analysis of Reactor Vessels of B&W Owners Group Reactor Vessel Working Group for Load Level A & B Conditions*," BAW-2192PA, B&W Nuclear Technologies, Inc., Lynchburg, Virginia, April 1994.*

10. K. K. Yoon, "*Low Upper-Shelf Toughness Fracture Mechanics Analysis of Reactor Vessels of B&W Owners Group Reactor Vessel Working Group for Load Level C & D Service Loads*," BAW-2178PA, B&W Nuclear Technologies, Inc., Lynchburg, Virginia, April 1994.*

* - Available from Framatome ANP, Lynchburg, Virginia.

11. T. M. Wiger and D. E. Killian, "*Low Upper-Shelf Toughness Fracture Mechanics Analysis of B&W Designed Reactor Vessels for 48 EFPY*," BAW-2275A, Framatome Technologies, Inc., Lynchburg, Virginia, August 1999.*

12. U.S. Nuclear Regulatory Commission, "*Safety Evaluation by the Office of Nuclear Reactor Regulation Regarding Amendment of the Kewaunee Nuclear Power Plant License to include the Use of a Master Curve-Based Methodology for Reactor Pressure Vessel integrity Assessment, Docket No. 50-305*," May 2001.

13. ASTM Standard E 1921-97, *"Standard Test Method for Determination of Reference Temperature, T_0, for Ferritic Steels in the Transition Region,"* American Society for Testing and Materials, Philadelphia, Pennsylvania.

14. American Society for Mechanical Engineers, "*Use of Fracture Toughness Test Data to Establish Reference Temperature for Pressure Retaining Materials, Section XI, Division 1*," Code Case N-629, approved May 4, 1999.

15. A. L. Lowe, Jr., et al., "*Evaluation of Surveillance Capsule Temperatures*," BAW-2040, Babcock & Wilcox's Nuclear Power Generation Division, Lynchburg, Virginia, March 1989.*

16. A. L. Lowe, Jr., et al., *"Analysis of Capsule CR3-LG1 Babcock & Wilcox Owners Group Integrated Reactor Vessel Materials Surveillance Program,"* BAW-1910P, Babcock & Wilcox Nuclear Power Division, Lynchburg, Virginia, August 1986.*

17. M. J. DeVan, et al., *"Test Results of Capsule CR3-LG2 B&W Owners Group Master Integrated Reactor Vessel Surveillance Program,"* BAW-2254P, B&W Nuclear Technologies, Inc., Lynchburg, Virginia, October 1995.*

18. A. L. Lowe, Jr., et al., *"Analysis of Capsule DB1-LG1 Babcock & Wilcox Owners Group Integrated Reactor Vessel Materials Surveillance Program,"* BAW-1920P, Babcock & Wilcox's Nuclear Power Division, Lynchburg, Virginia, October 1986.*

19. M. J. DeVan, et al., *"Test Results of Capsule TMI2-LG1 B&W Owners Group Master Integrated Reactor Vessel Surveillance Program,"* BAW-2253P, B&W Nuclear Technologies, Inc., Lynchburg, Virginia, October 1995.*

20. ASTM Standard E 419-73, "*Standard Guide for Selection of Neutron Activation Detector Materials*," American Society for Testing and Materials, Philadelphia, Pennsylvania.

21. ASTM Standard E 482-82, "*Standard Recommended Practice for Neutron Dosimetry for Reactor Pressure Vessel Surveillance*," American Society for Testing and Materials, Philadelphia, Pennsylvania.

* - Available from Framatome ANP, Lynchburg, Virginia.

22. M. J. DeVan, "Response to Request for Additional Information (RAI) Regarding Reactor Pressure Vessel Integrity B&W Owners Group – Reactor Vessel Working Group," BAW-2325, Revision 1, Framatome Technologies, Inc., Lynchburg, Virginia, January 1999.*

23. K. Y. Hour, *"Evaluation of B&W Owners Group TMI2-LG2 MIRVSP Capsule,"* 1150-022-01-24:00 (Framatome ANP Document No. 31-1182412-00), BWX Technologies, Inc., Lynchburg, Virginia, December 2002.*

24. ASTM Standard E 8-94, *"Standard Test Methods for Tension Testing of Metallic Materials,"* American Society for Testing and Materials, Philadelphia, Pennsylvania.

25. ASTM Standard E 21-92, *"Standard Test Methods for Elevated Temperature Tension Tests of Metallic Materials,"* American Society for Testing and Materials, Philadelphia, Pennsylvania.

26. ASTM Standard E 23-94a, *"Standard Test Methods for Notched Bar Impact Testing of Metallic Materials,"* American Society for Testing and Materials, Philadelphia, Pennsylvania.

27. ASTM Standard E 185-82, *"Standard Practice for Conducting Surveillance Tests for Light-Water Cooled Nuclear Power Reactor Vessels, E 706 (IF),"* American Society for Testing and Materials, Philadelphia, Pennsylvania.

28. ASTM Standard E 813-89, *"Standard Test Method for,"* American Society for Testing and Materials, Philadelphia, Pennsylvania.

29. ASTM Standard E 1152-87, *"Standard Test Method for,"* American Society for Testing and Materials, Philadelphia, Pennsylvania.

30. ASTM Standard E 1921-02, *"Standard Test Method for Determination of Reference Temperature, T_0, for Ferritic Steels in the Transition Region,"* American Society for Testing and Materials, Philadelphia, Pennsylvania.

31. J. B. Hall, "*Linde-80 Weld Reference Temperature Calculations*," 32-5006571-03, Framatome ANP, May 2003.*

32. M. J. DeVan, "*Supplement to the Response to Request for Additional Information (RAI) Regarding Reactor Pressure Vessel Integrity B&W Owners Group – Reactor Vessel Working Group*," BAW-2325, Supplement 1, Framatome Technologies, Inc., Lynchburg, Virginia, December 1998.*

33. J. B. Hall, "*Initial RT_{NDT} of Linde 80 Weld Materials,"* BAW-2308, Framatome ANP, Lynchburg, Virginia, July 2002.*

* - Available from Framatome ANP, Lynchburg, Virginia.

34. K. Y. Hour, "*Transition Temperature Fracture Toughness Testing on Linde-80 Weld Metals*," BWXT Services, Inc. Report 1150-023-02-41:00 (Framatome ANP Document 31-5028401-00), May 2003.*

35. K. K. Yoon, W. A. VanDerSluys, and K. Hour, "*Effect of Loading Rate on Fracture Toughness of Pressure Vessel Steels*," Journal of Pressure Vessel Technology, ASME, May 2000, Vol. 122.

36. W. A. VanDerSluys, C. L. Hoffman, K. K. Yoon, D. E. Killian, and J. B. Hall, "*Fracture Toughness Master Curve Development: Fracture Toughness of Ferritic Steels and ASTM Reference Temperature (To)*," Welding Research Council Bulletin 457, New York, NY, December 2000.

37. K. K. Yoon and K. Hour, "*Dynamic Fracture Toughness Test and Master curve Method Analysis of IAEA JRQ Material*," 15th SMIRT Conference, August 1999.

38. J. R. Worsham, et al., *"Fluence and Uncertainty Methodologies,"* BAW-2241P-A, Revision 1, Framatome ANP, Lynchburg, Virginia, April 1999.*

39. U.S. Nuclear Regulatory Commission, *"Calculational and Dosimetry Methods for Determining Pressure Vessel Neutron Fluence,"* Regulatory Guide 1.190, March 2001.

40. M. J. DeVan, E. Giavedoni, and K. K. Yoon, *"Test Results of W1 Capsule Babcock & Wilcox Owners Group Master Integrated Reactor Vessel Surveillance Program,"* BAW-2350P, Framatome Technologies, Inc., Lynchburg, Virginia, April 1999.*

41. M. J. DeVan, "*Evaluation of Tension Test Data for Reactor Vessel Beltline Materials,"* BAW-2240P, B&W Nuclear Technologies, Inc., Lynchburg, Virginia, December 1994.*

42. U.S. Nuclear Regulatory Commission, *"Radiation Embrittlement of Reactor Vessel Materials,"* Regulatory Guide 1.99, Revision 2, May 1988.

43. Tregoning, R. L. and Joyce, J. A., "T_0 *Evaluation in Common Specimen Geometries*," Proceedings of ASME Pressure Vessel and Piping Conference, PVP-Vol. 412, 2000.

44. J. W. Newman, Jr., "*TMI1 Capsule C Fluence Analysis Report*," 86-5021026-01, Framatome ANP, January 2003.*

45. J. W. Newman, Jr., "*Surry 1 Capsule T and V Fluence Analysis Report*," 86-5020802-01, Framatome ANP, January 2003.*

* - Available from Framatome ANP, Lynchburg, Virginia.

APPENDIX A

Stress-Strain Curves

Figure A-1. Tension Test Stress-Strain Curve
for Weld Metal SA-1526 (Wire Heat 299L44 / Flux Lot 8596)
Specimen No. PP004, Tested at 70°F

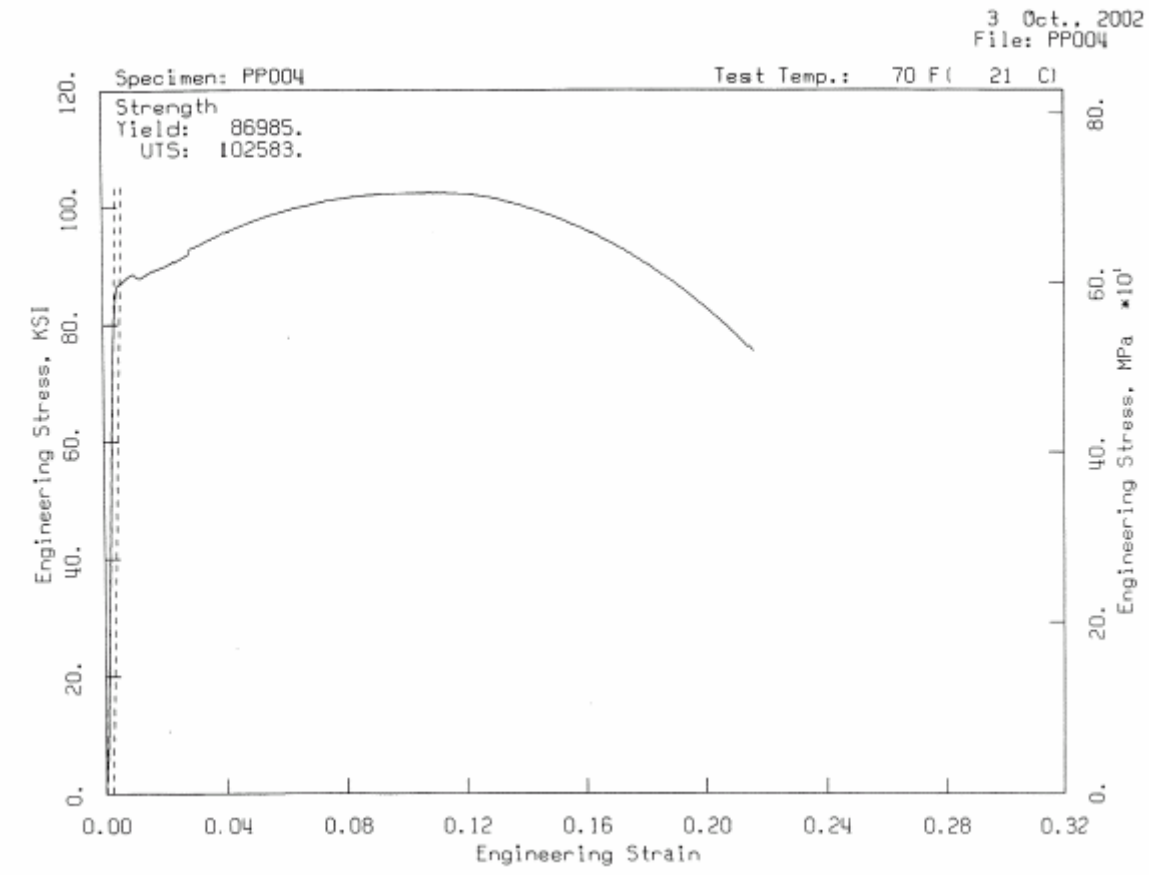

**Figure A-2. Tension Test Stress-Strain Curve
for Weld Metal SA-1526 (Wire Heat 299L44 / Flux Lot 8596)
Specimen No. PP003, Tested at 580°F**

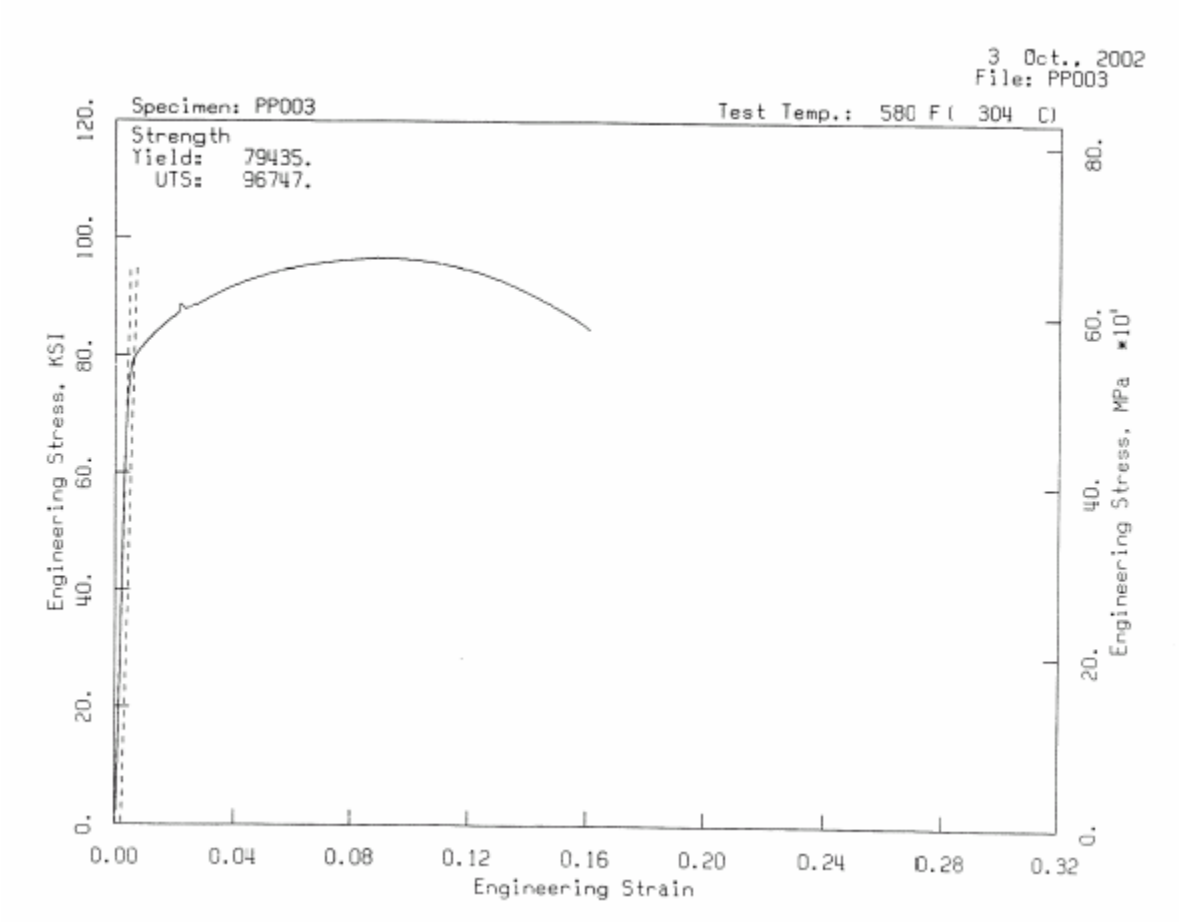

**Figure A-3. Tension Test Stress-Strain Curve
for Weld Metal WF-25(6) (Wire Heat 299L44 / Flux Lot 8650)
Specimen No. QQ004, Tested at 70°F**

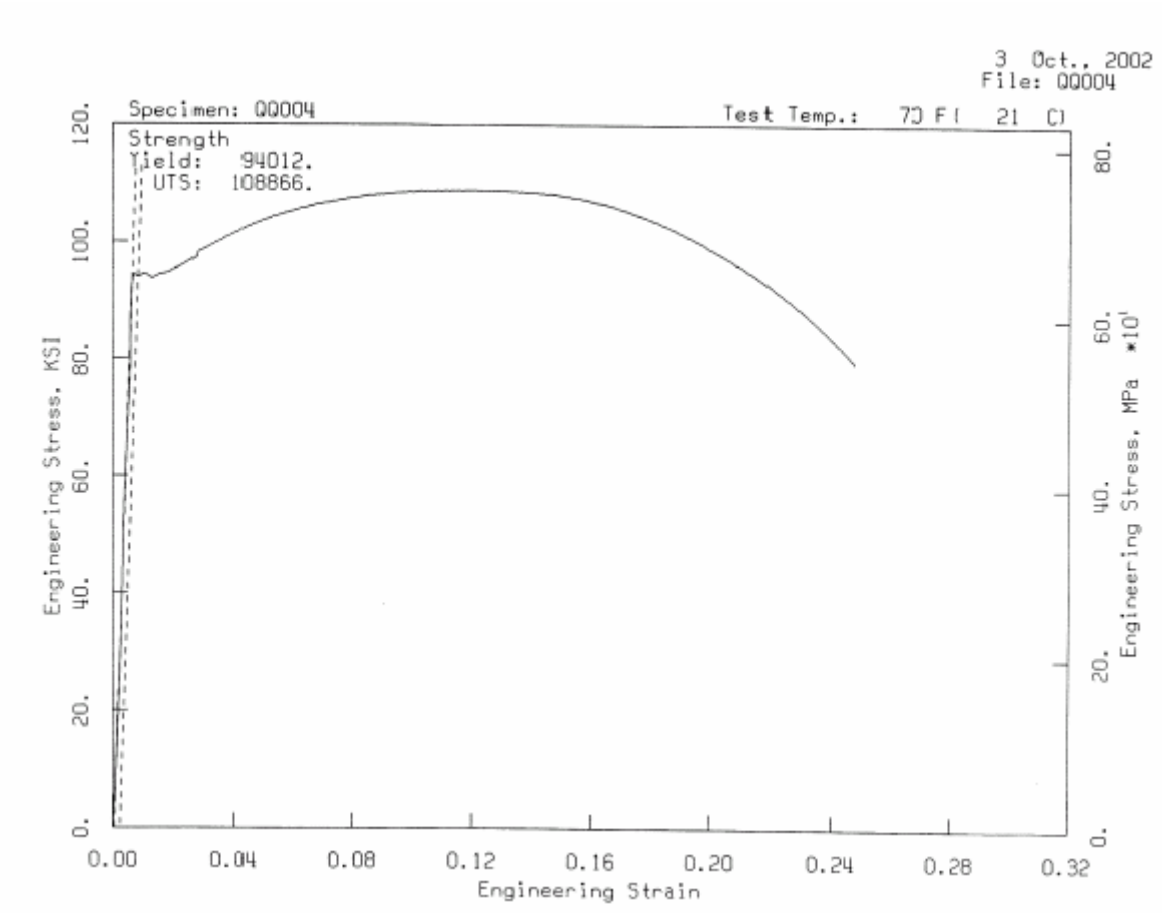

**Figure A-4. Tension Test Stress-Strain Curve
for Weld Metal WF-25(6) (Wire Heat 299L44 / Flux Lot 8650)
Specimen No. QQ003, Tested at 580°F**

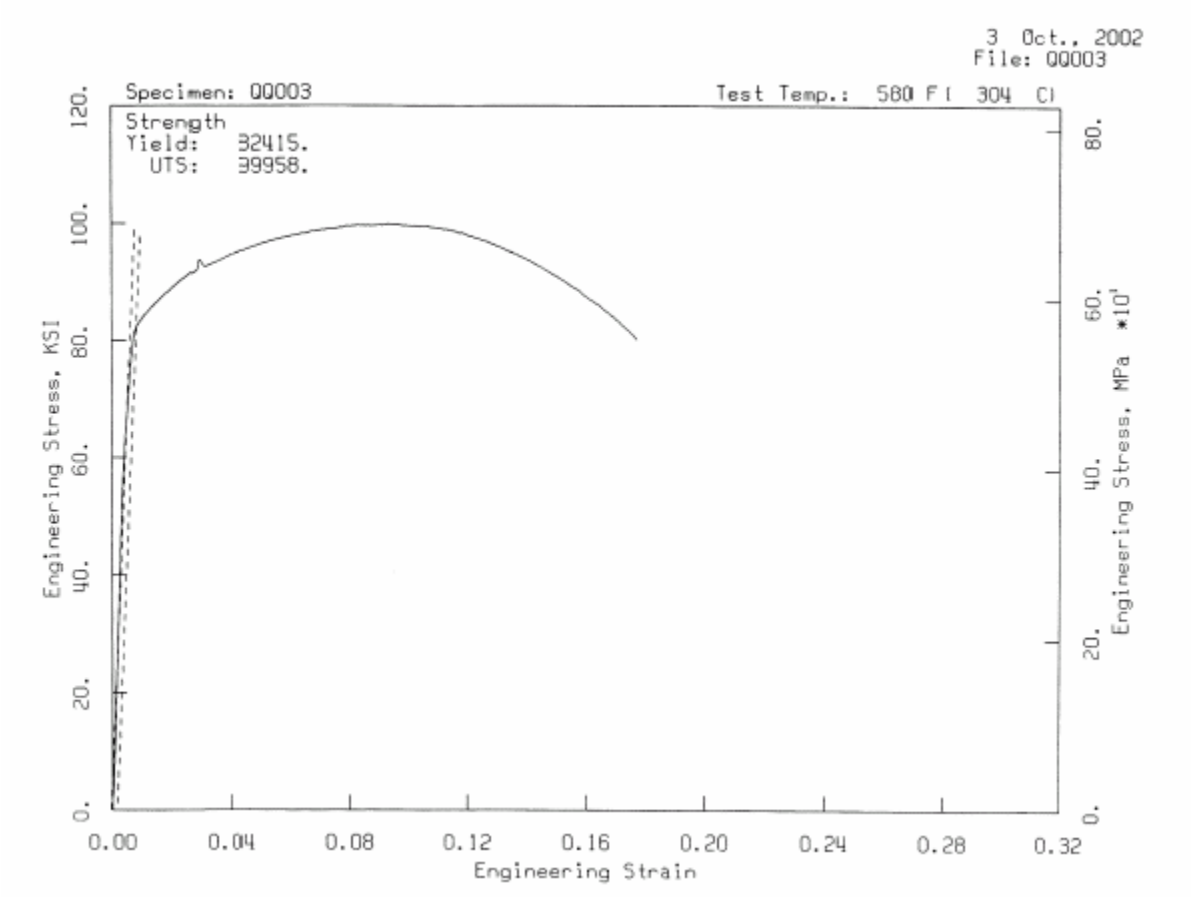

**Figure A-5. Tension Test Stress-Strain Curve
for Weld Metal WF-25(9) (Wire Heat 299L44 / Flux Lot 8650)
Specimen No. JJ011, Tested at 70°F**

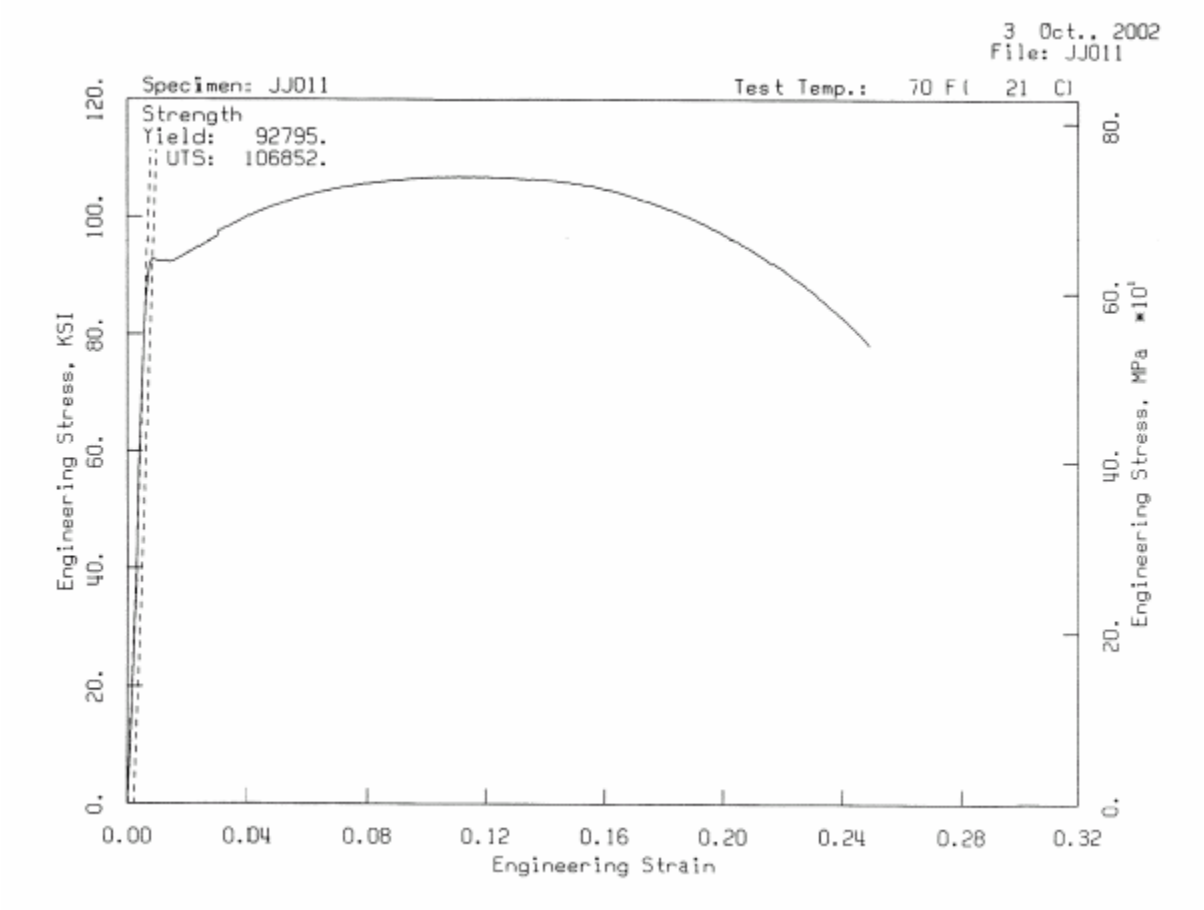

**Figure A-6. Tension Test Stress-Strain Curve
for Weld Metal WF-25(9) (Wire Heat 299L44 / Flux Lot 8650)
Specimen No. JJ010, Tested at 580°F**

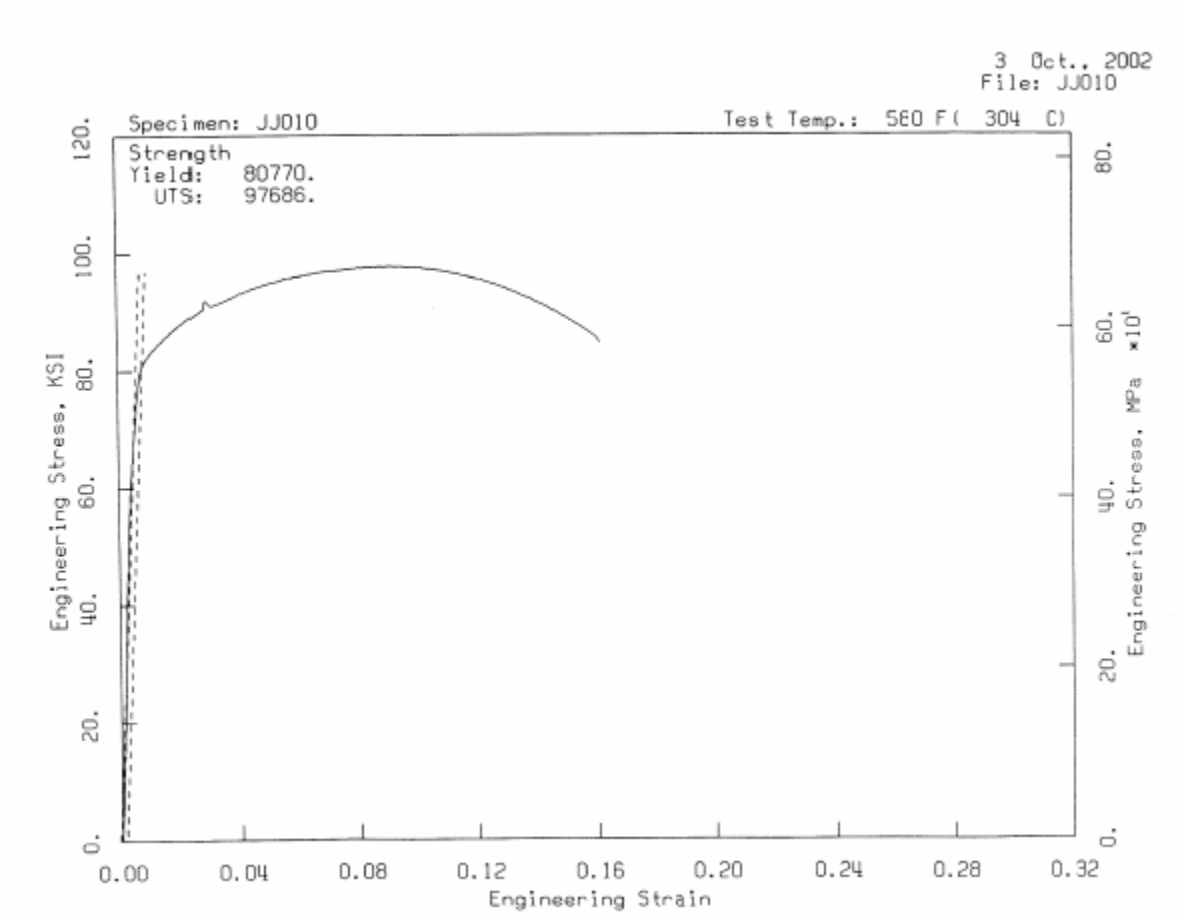

APPENDIX B

Toughness Test Load Versus Crack Opening Displacement Plots

Figure B-1. Load-COD Plot for SA-1526 0.936 TDC(T) Toughness Specimen PP004 (550 °F)

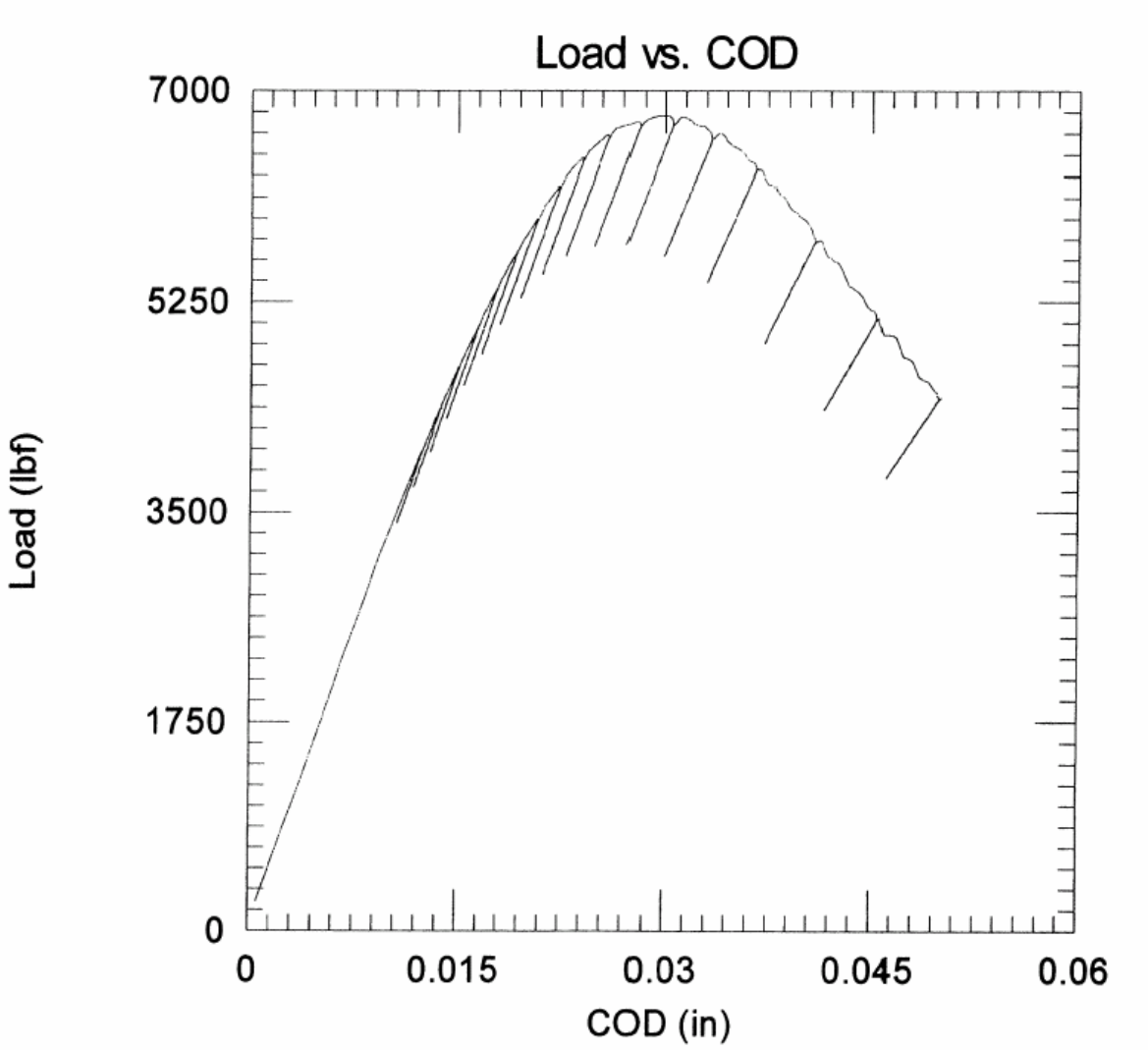

Figure B-2. Load-COD Plot for WF-25(6) 0.936 TDC(T) Toughness Specimen QQ002 (550 °F)

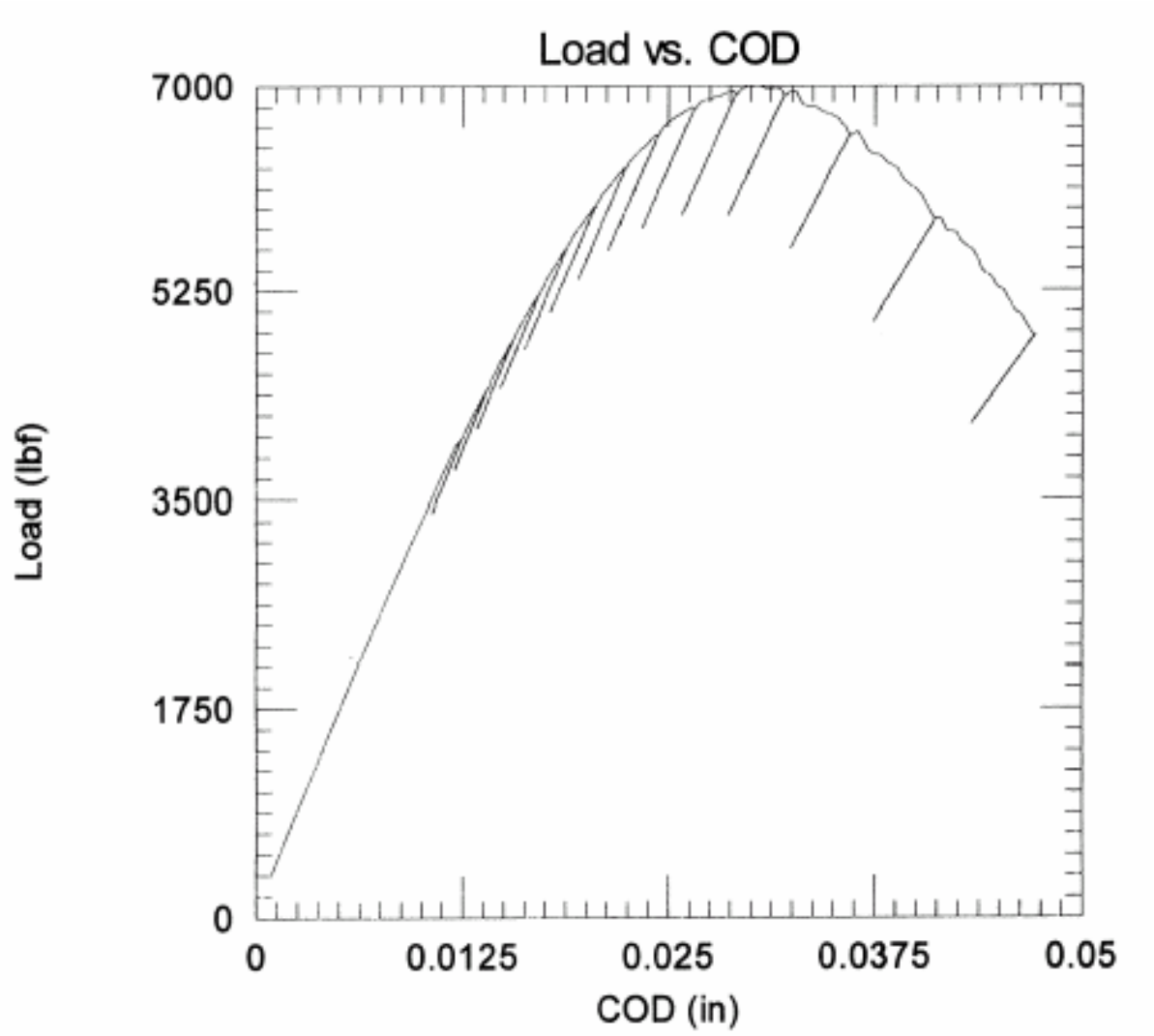

Figure B-3. Load-COD Plot for WF-25(9) 0.936 TDC(T) Toughness Specimen JJ002 (550 °F)

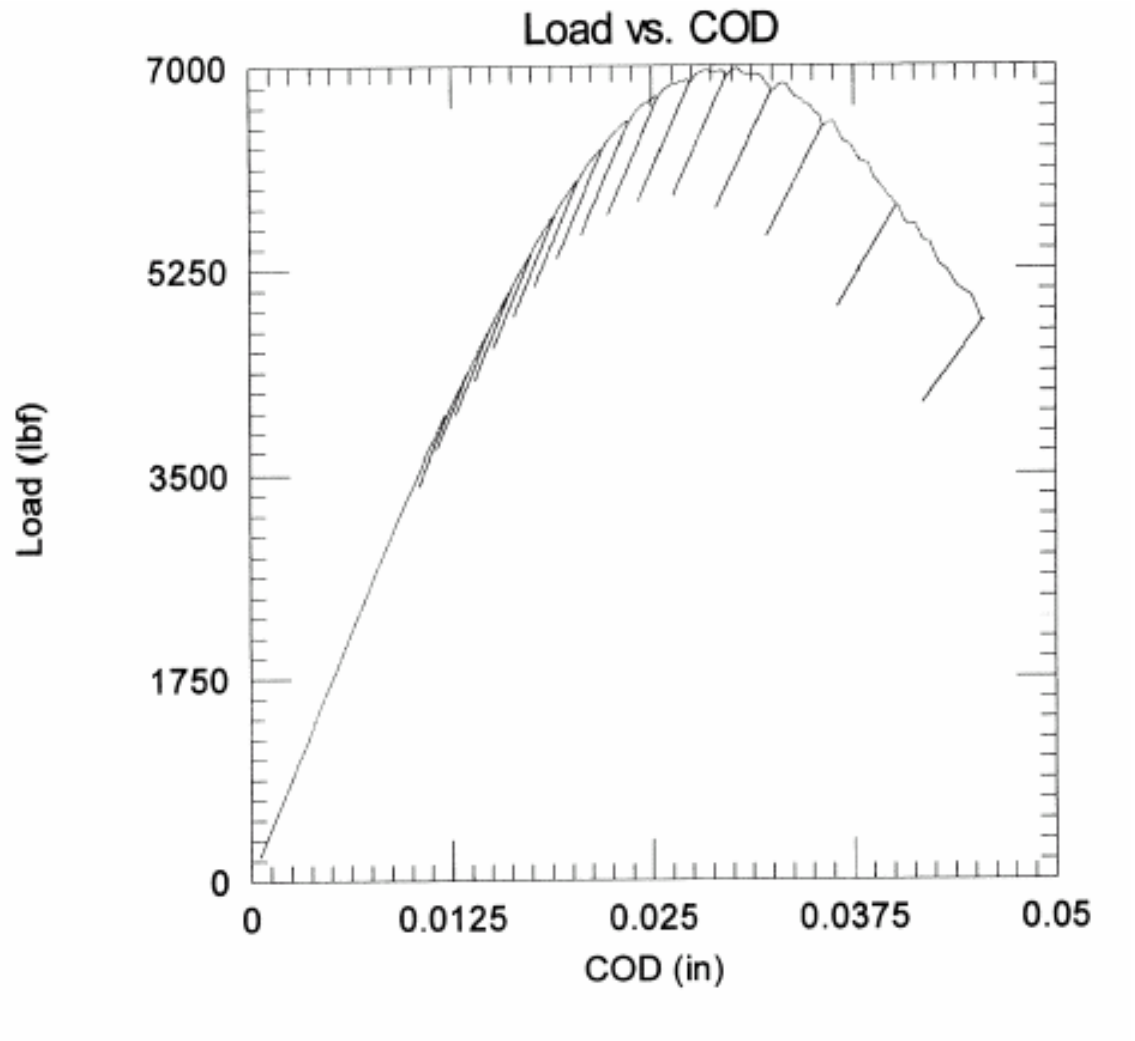

Figure B-4. Load-COD Plot for SA-1526 PCS Toughness Specimen PP014 (100 °F)

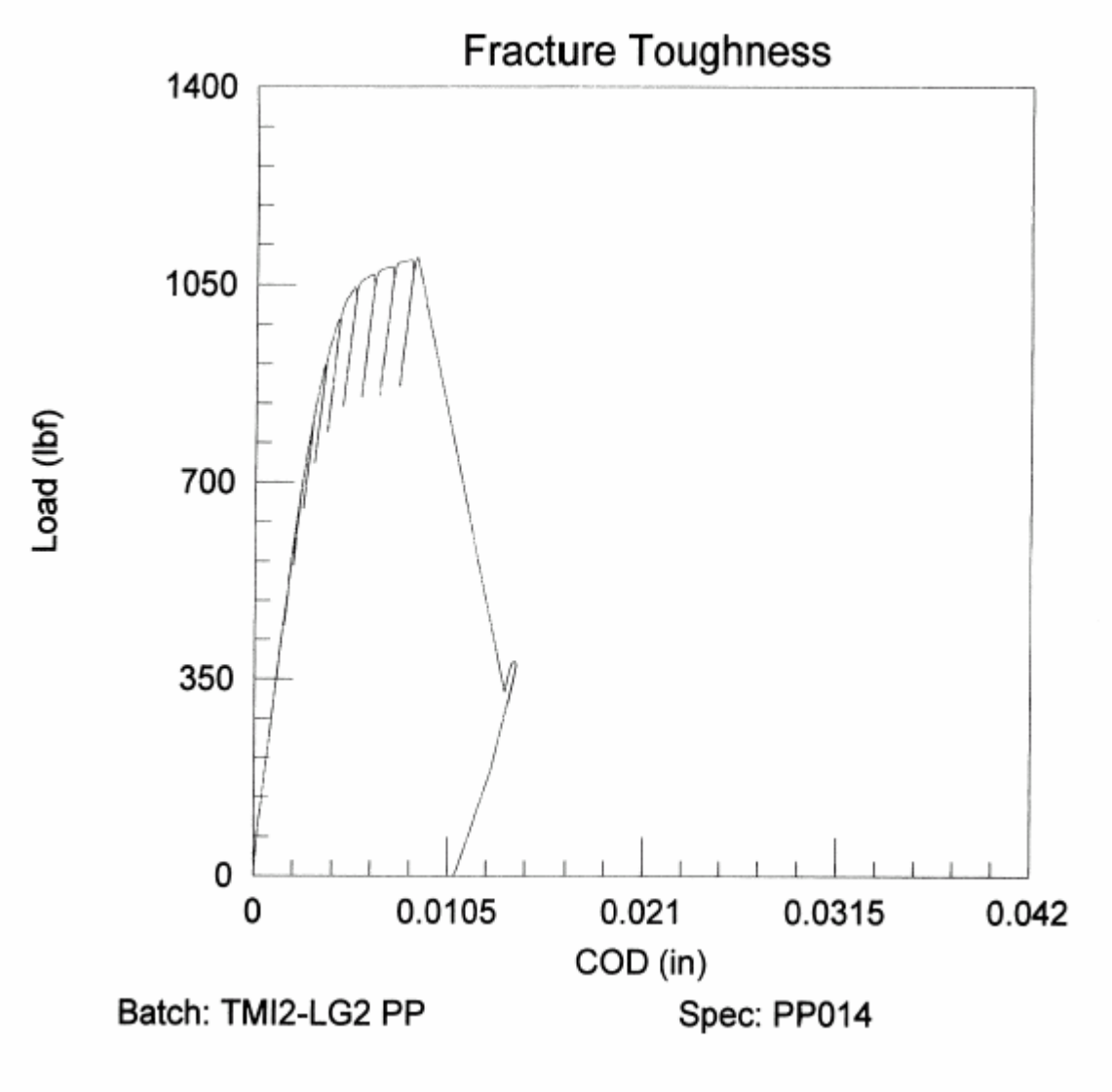

Figure B-5. Load-COD Plot for SA-1526 PCS Toughness Specimen PP015 (100 °F)

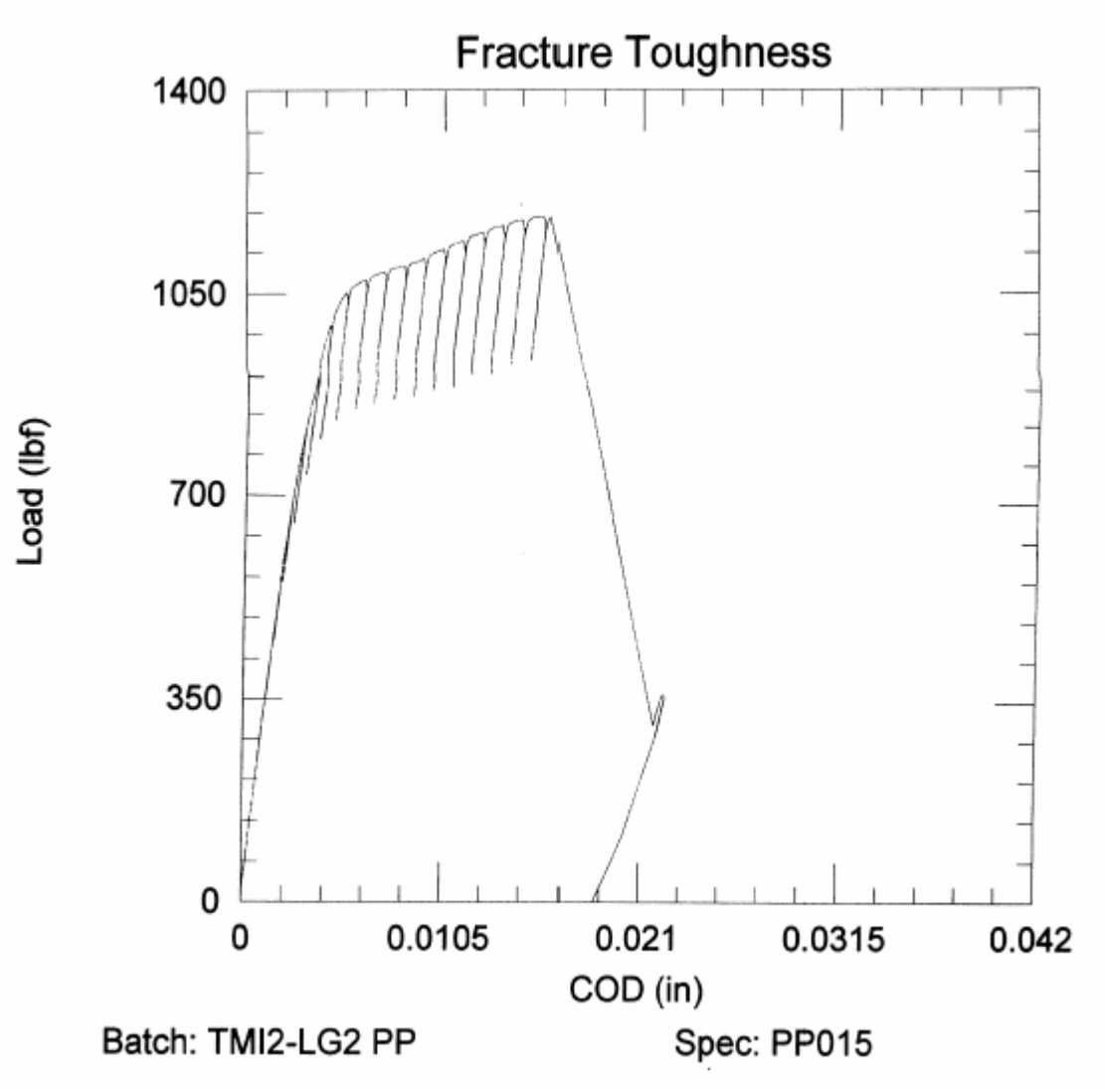

Figure B-6. Load-COD Plot for SA-1526 PCS Toughness Specimen PP016 (100 °F)

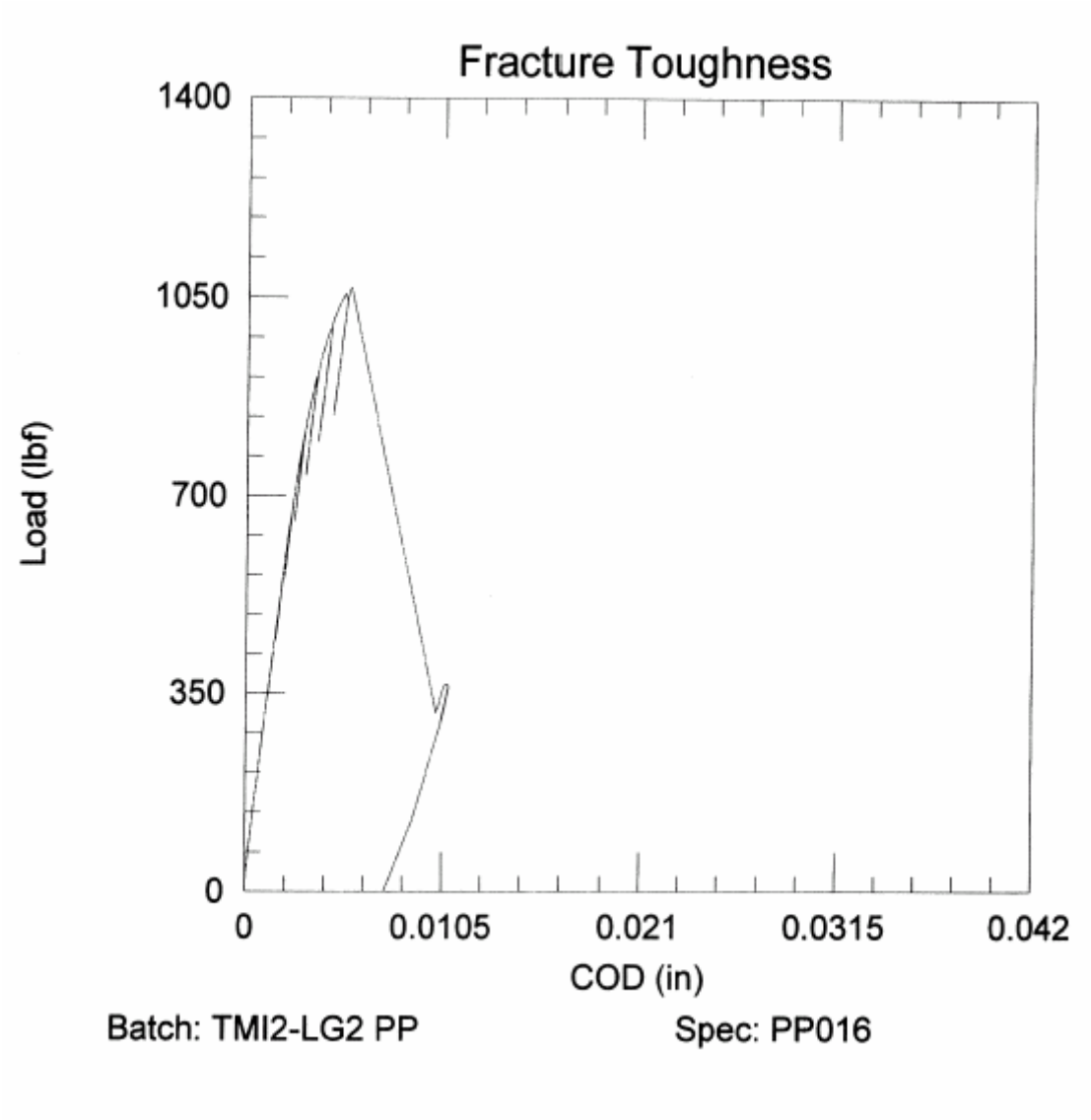

Figure B-7. Load-COD Plot for SA-1526 PCS Toughness Specimen PP017 (100 °F)

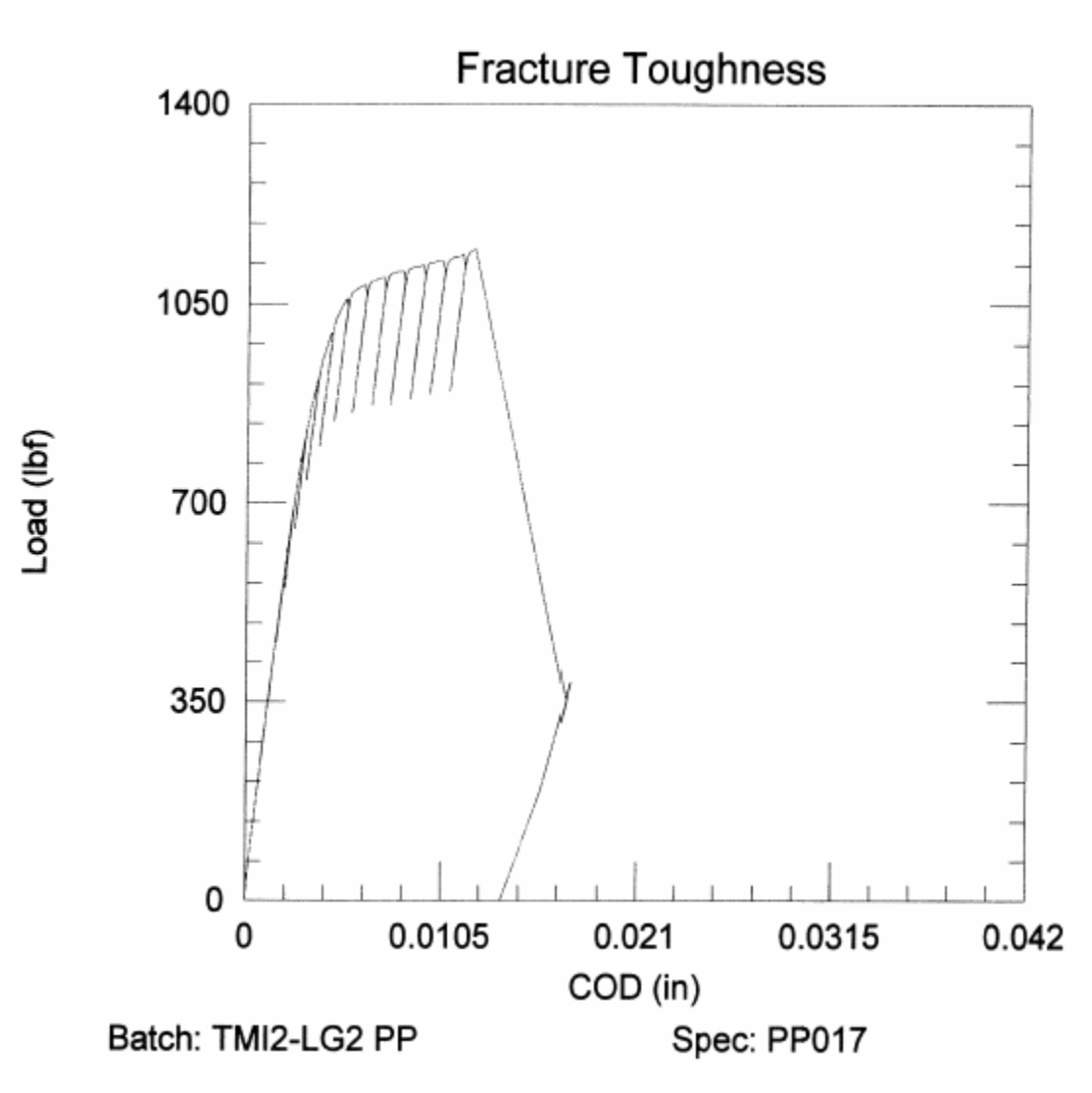

Figure B-8. Load-COD Plot for SA-1526 PCS Toughness Specimen PP018 (100 °F)

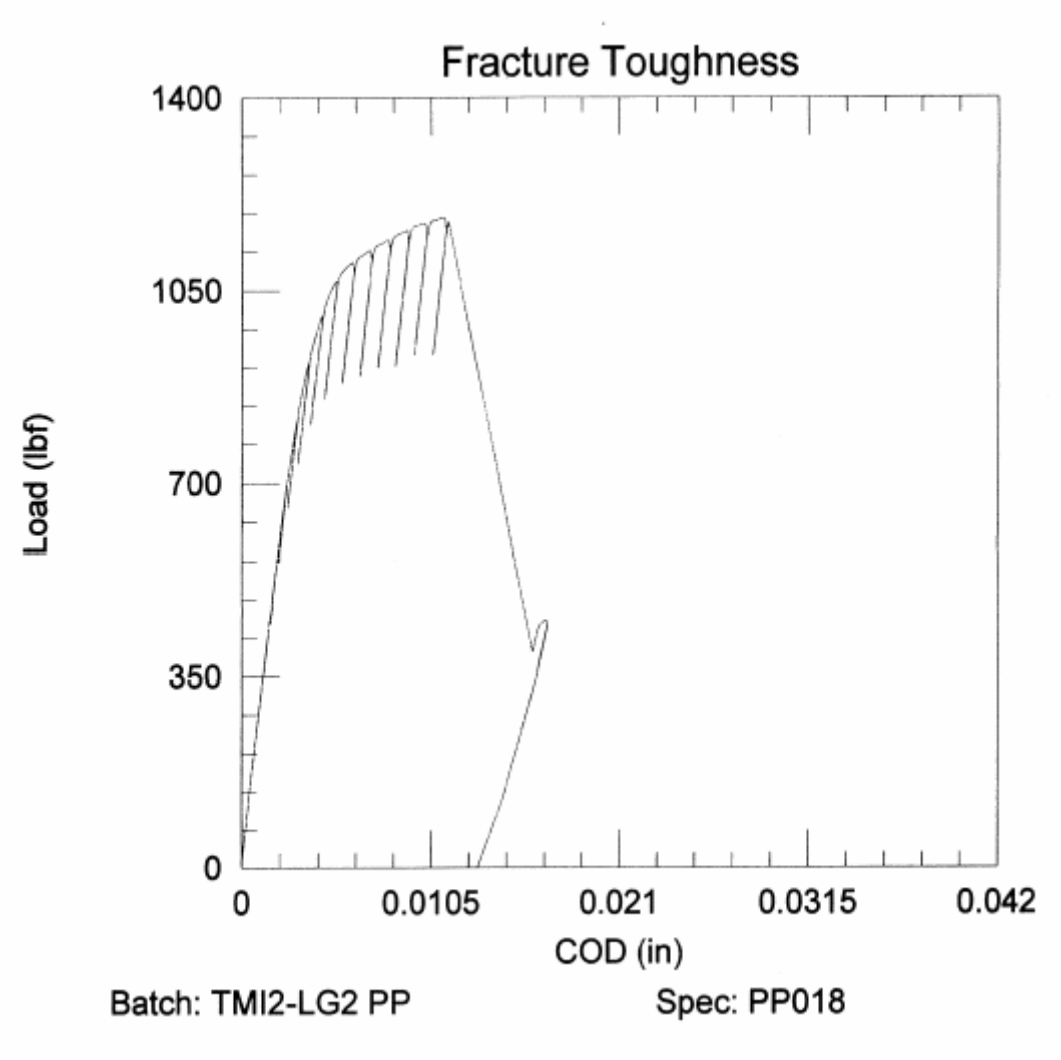

Figure B-9. Load-COD Plot for SA-1526 PCS Toughness Specimen PP019 (100 °F)

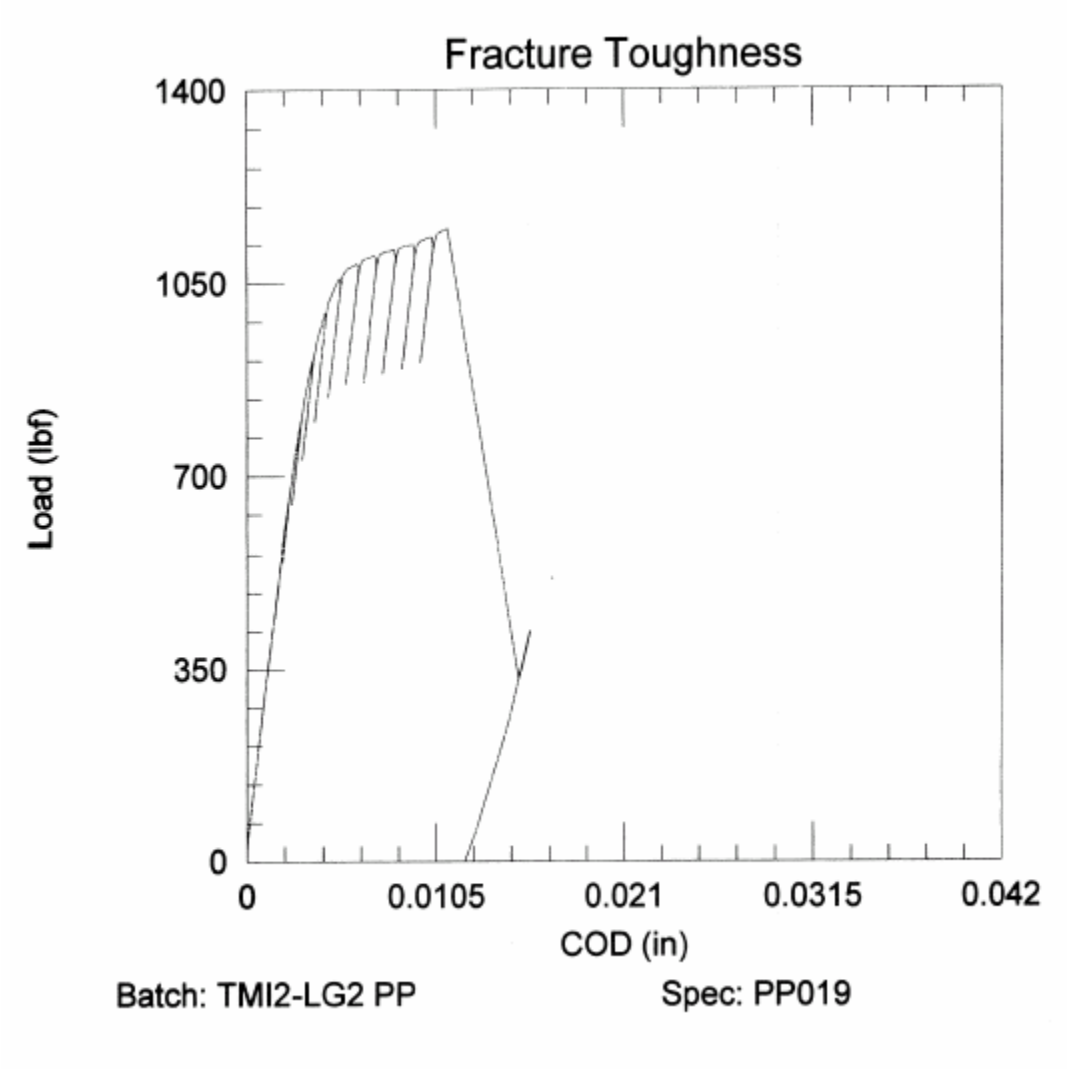

Figure B-10. Load-COD Plot for SA-1526 PCS Toughness Specimen PP020 (100 °F)

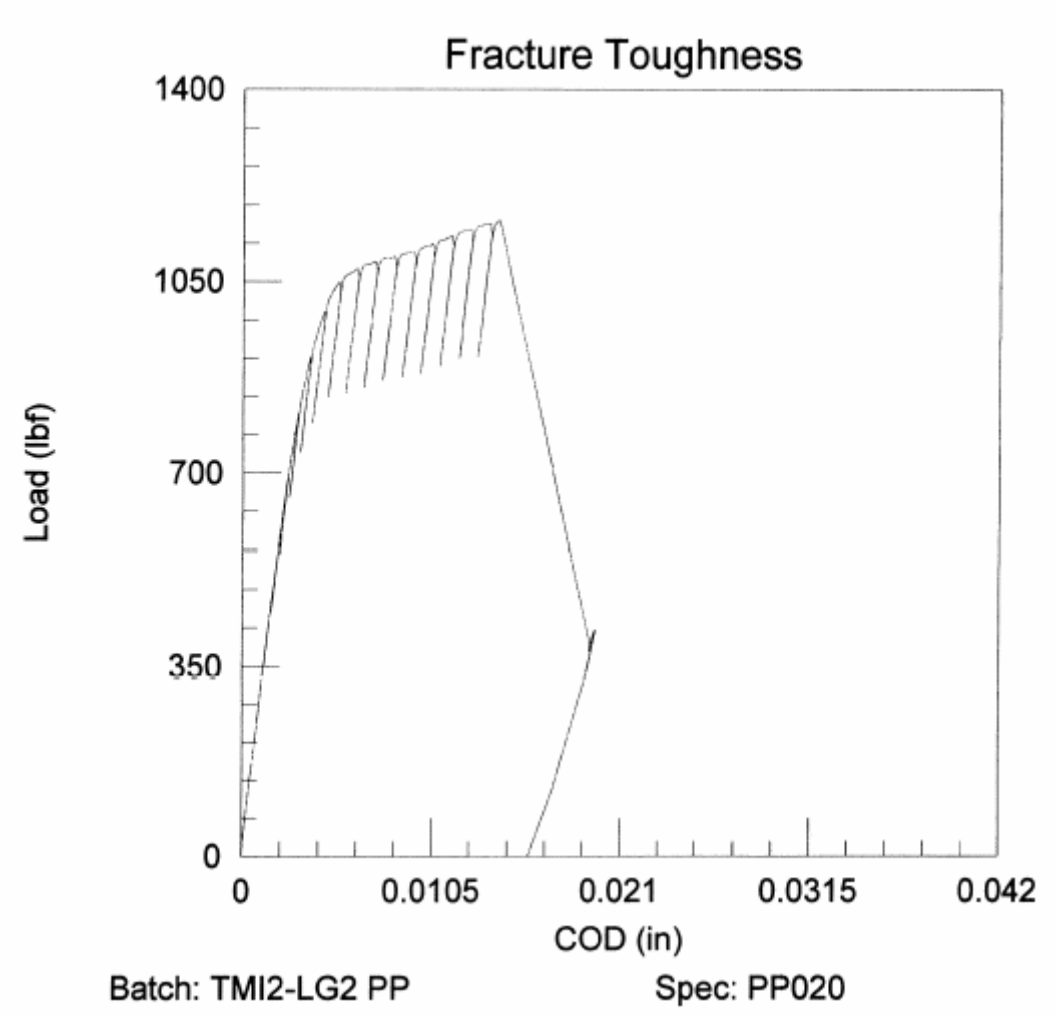

Figure B-11. Load-COD Plot for SA-1526 PCS Toughness Specimen PP021 (100 °F)

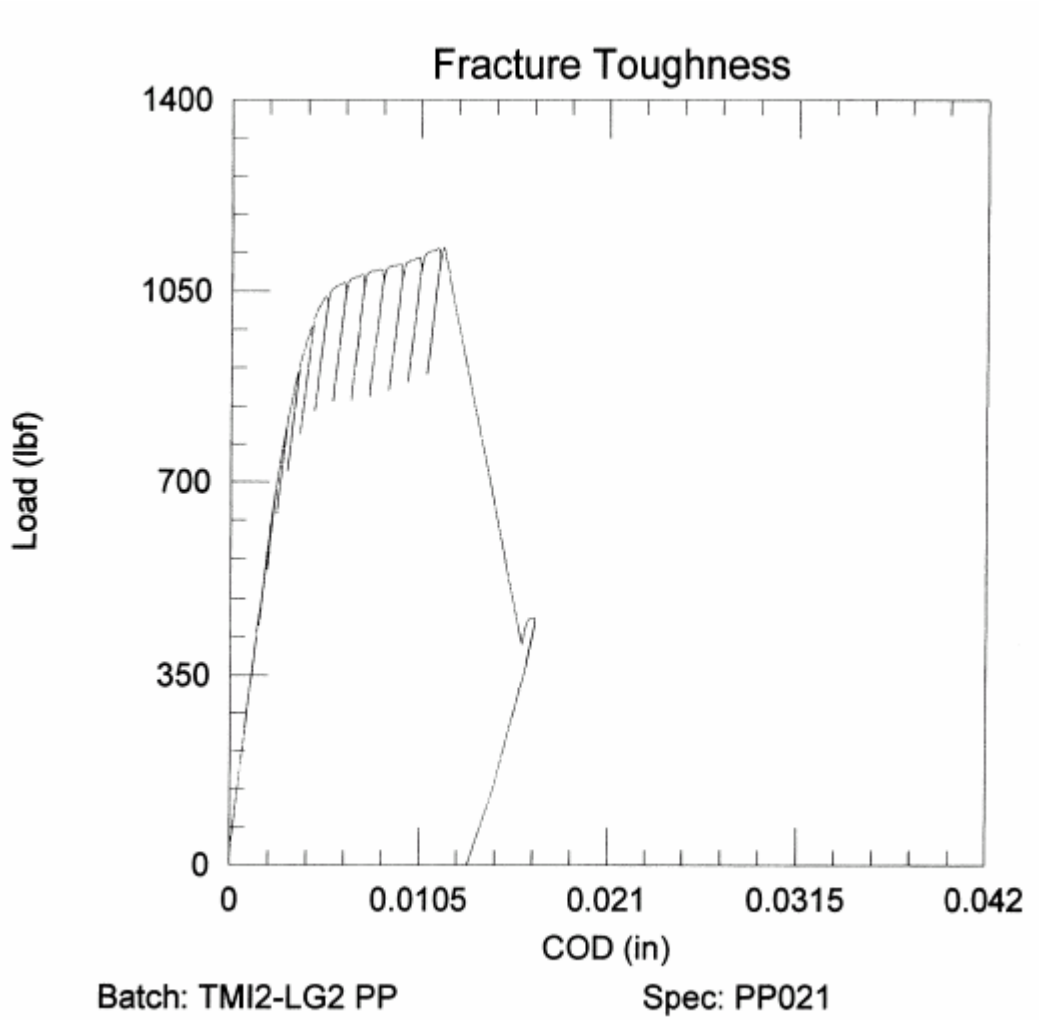

Figure B-12. Load-COD Plot for SA-1526 PCS Toughness Specimen PP022 (100 °F)

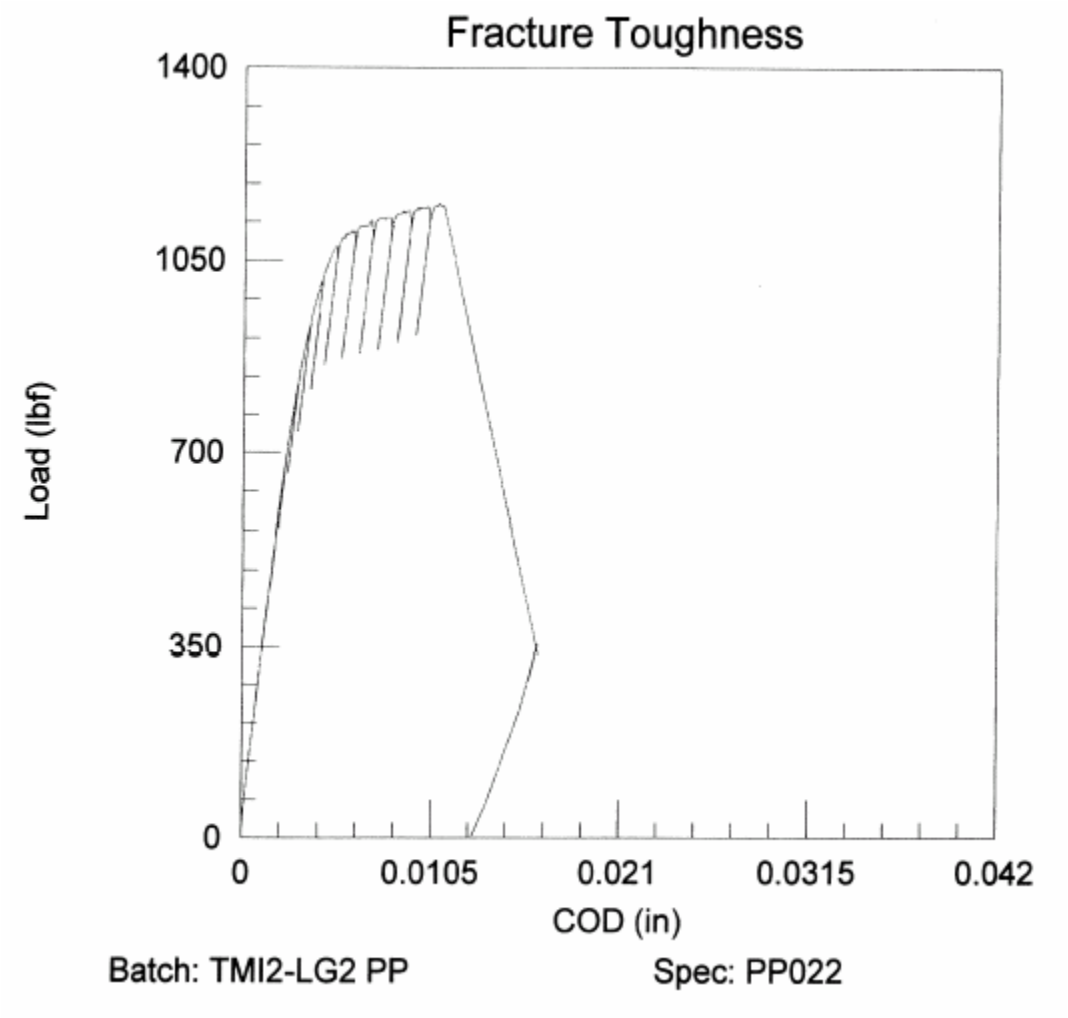

Figure B-13. Load-COD Plot for SA-1526 0.5 TC(T) Toughness Specimen PP006 (120 °F)

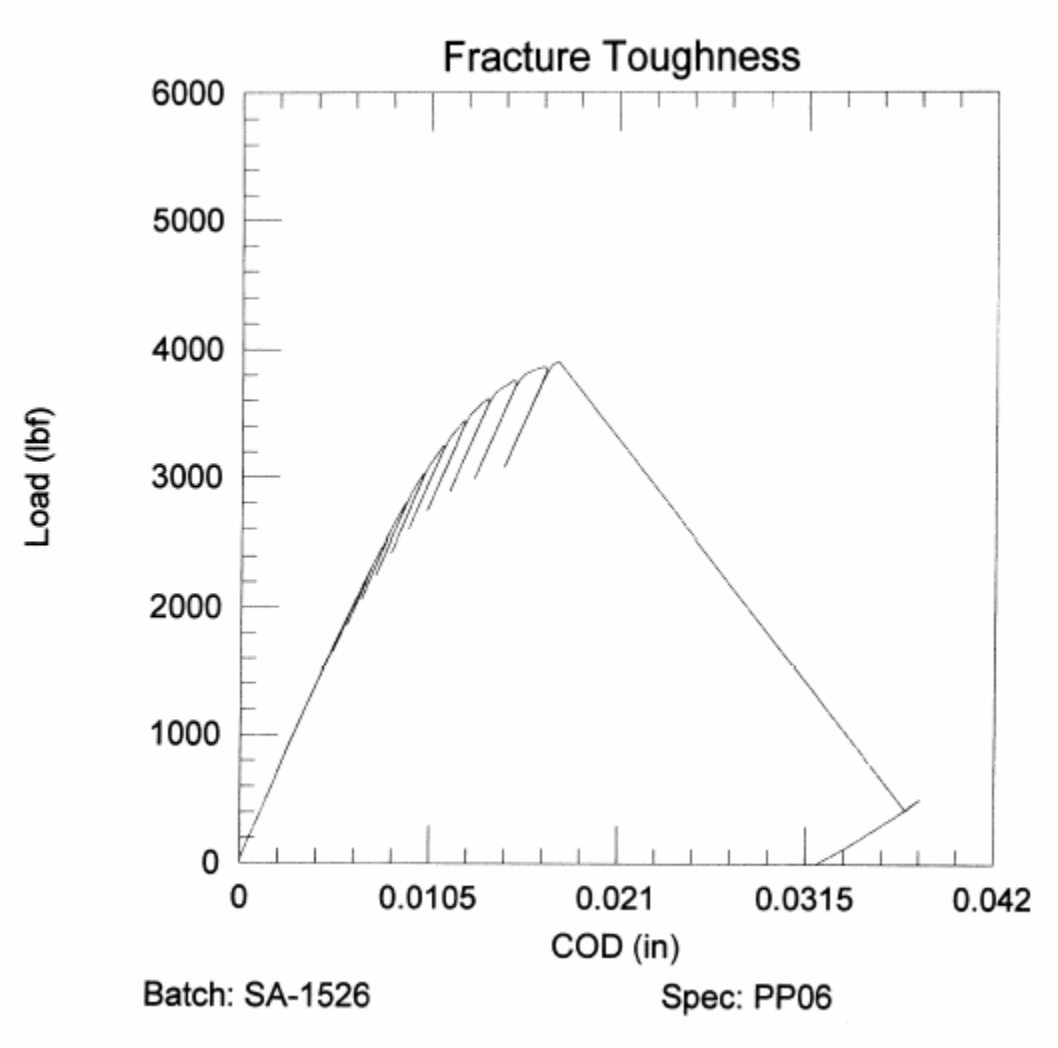

Figure B-14. Load-COD Plot for SA-1526 0.5 TC(T) Toughness Specimen PP009 (120 °F)

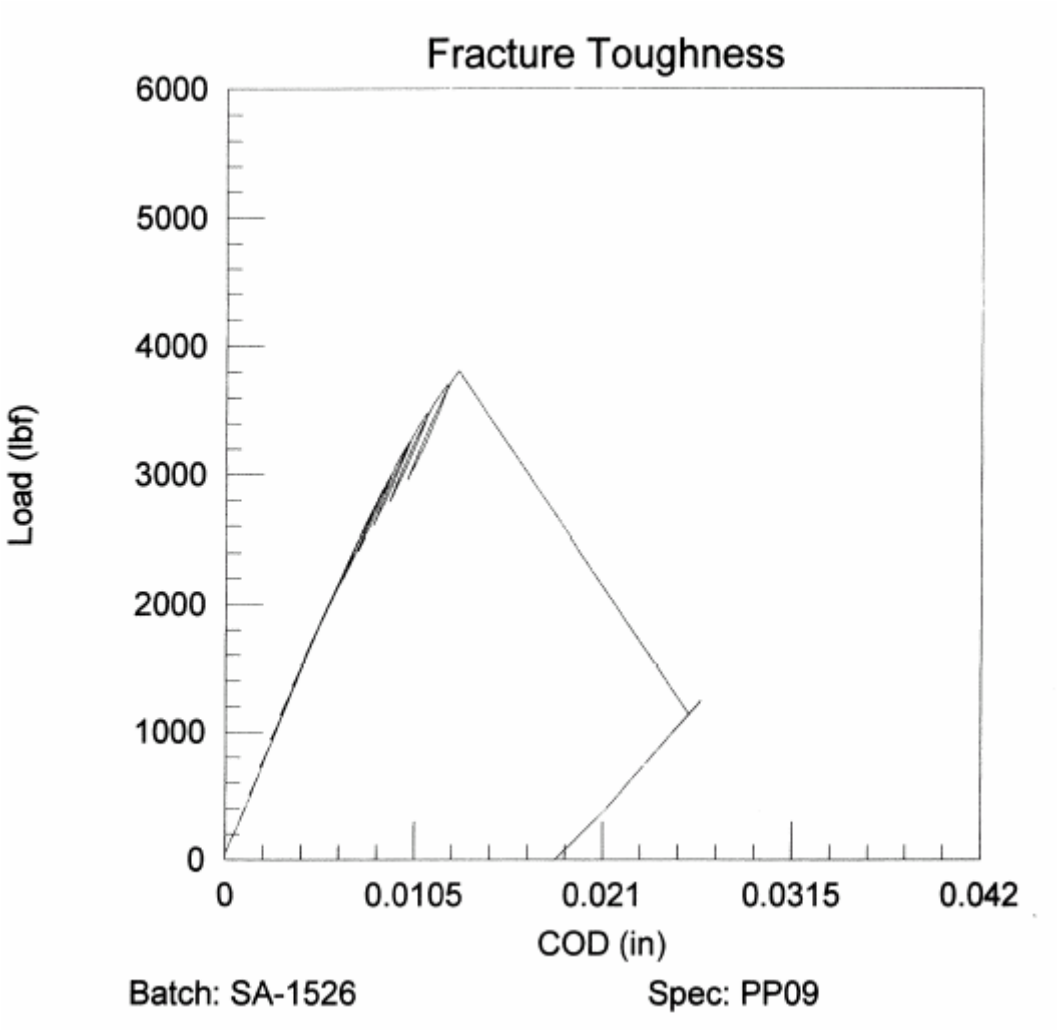

Figure B-15. Load-COD Plot for SA-1526 0.5 TC(T) Toughness Specimen PP013 (120 °F)

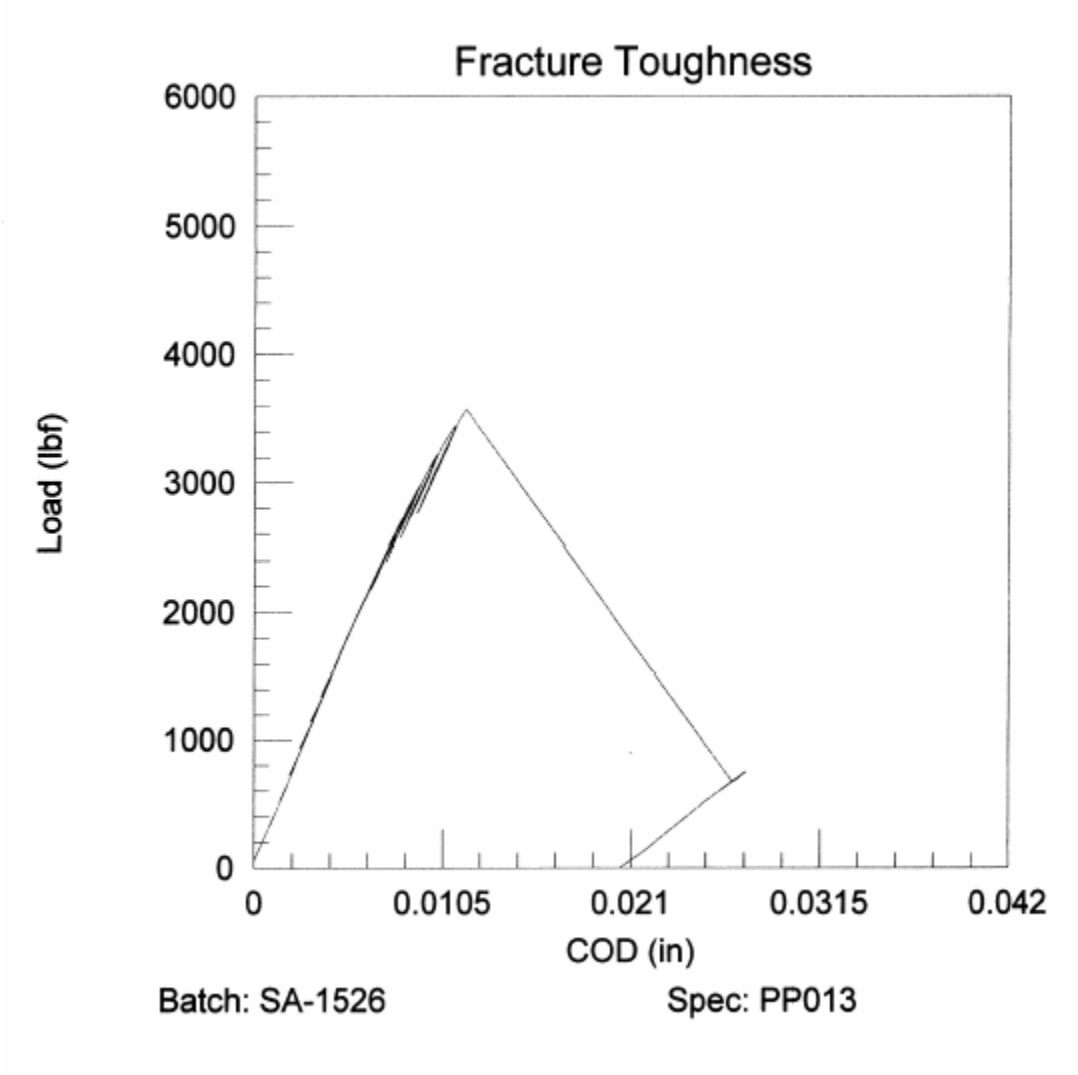

Figure B-16. Load-COD Plot for SA-1526 0.5 TC(T) Toughness Specimen PP015 (120 °F)

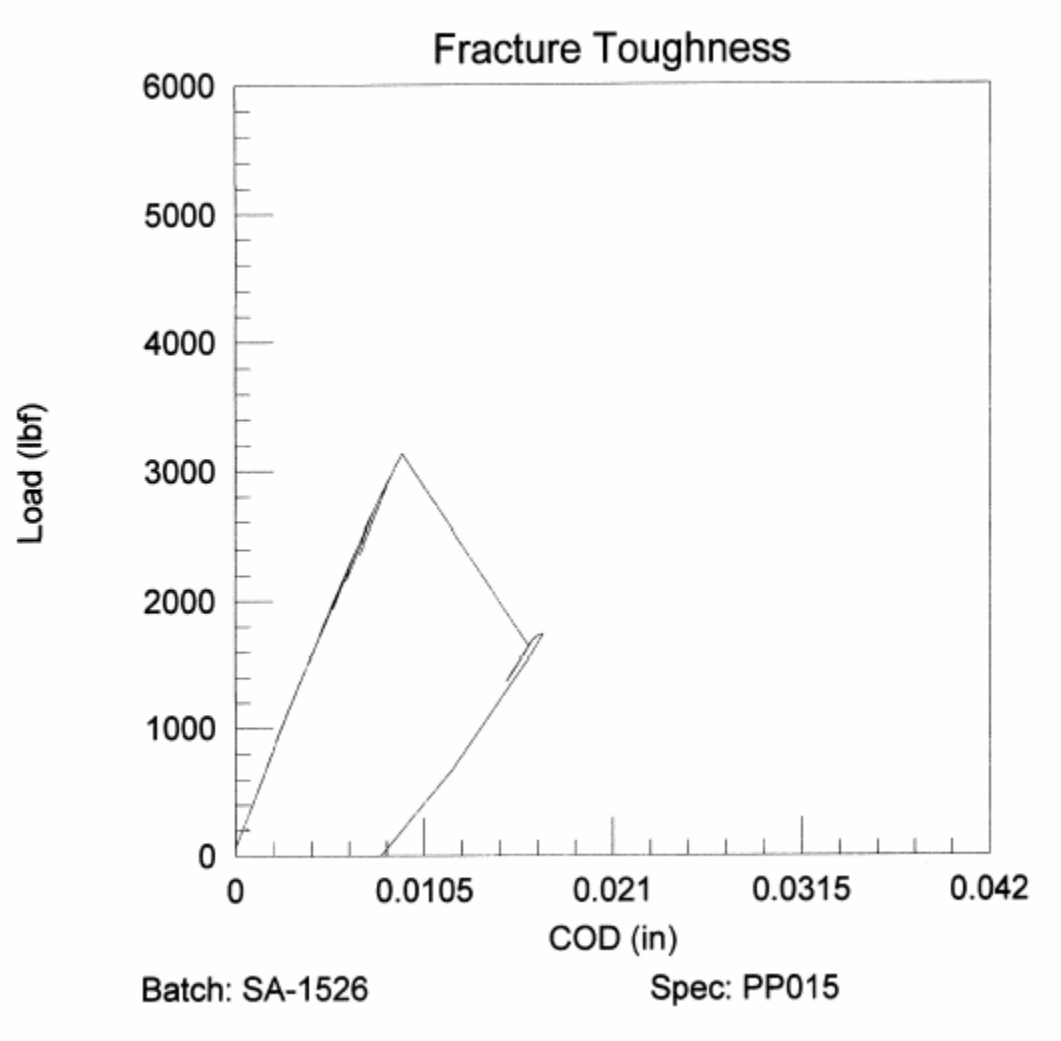

Figure B-17. Load-COD Plot for SA-1526 0.394 TC(T) Toughness Specimen PP007 (120 °F)

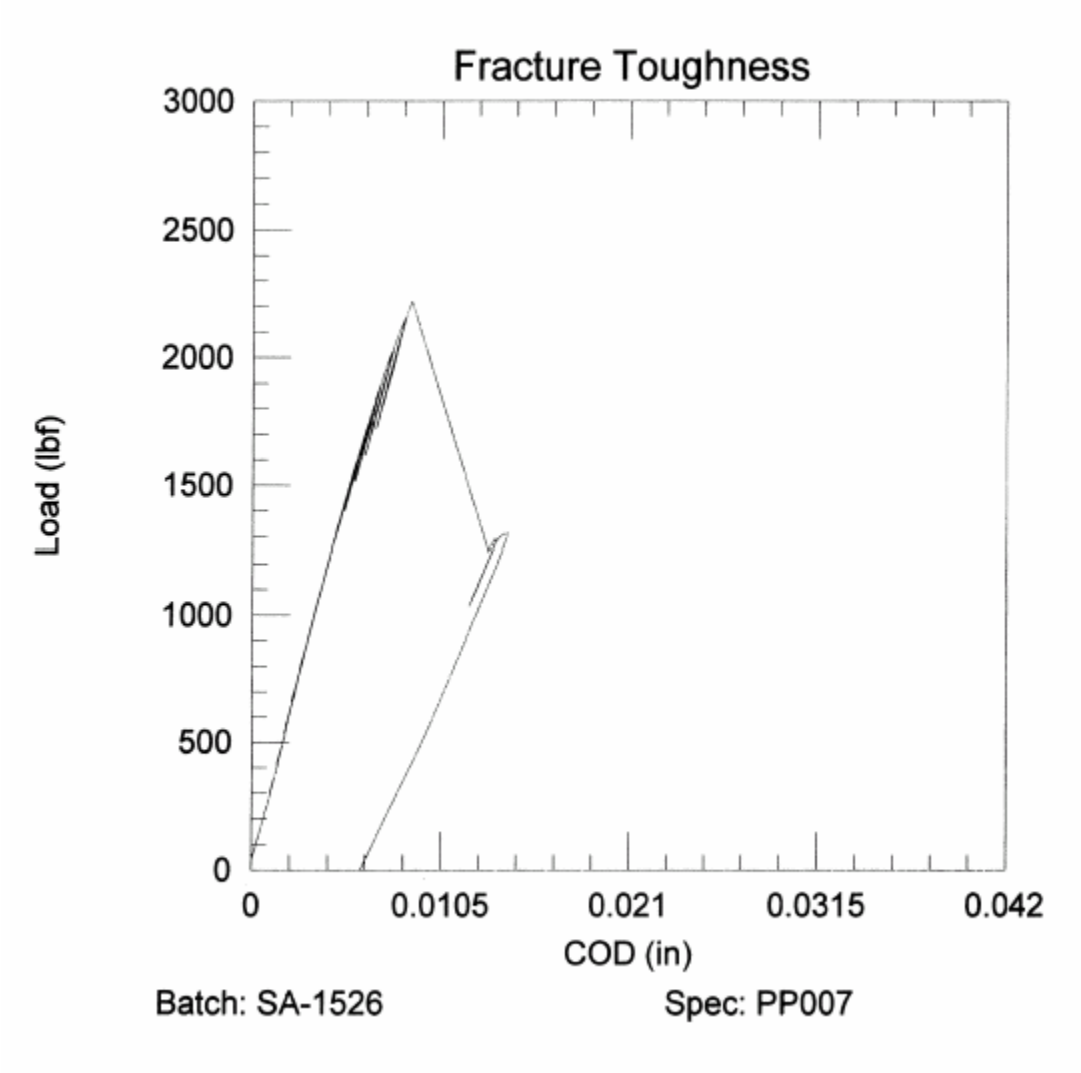

Figure B-18. Load-COD Plot for SA-1526 0.394 TC(T) Toughness Specimen PP010 (120 °F)

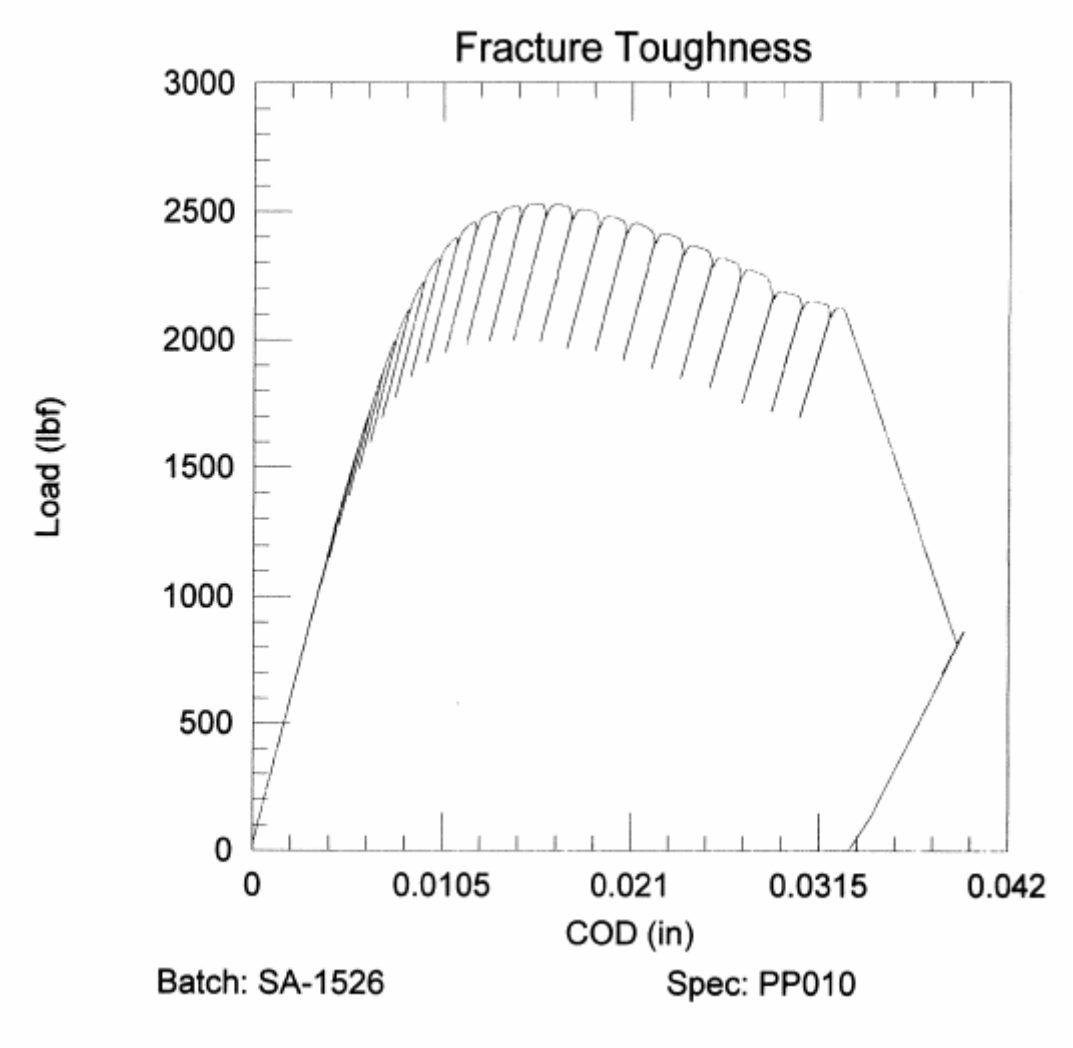

Figure B-19. Load-COD Plot for WF-25(6) PCS Toughness Specimen QQ013 (130 °F)

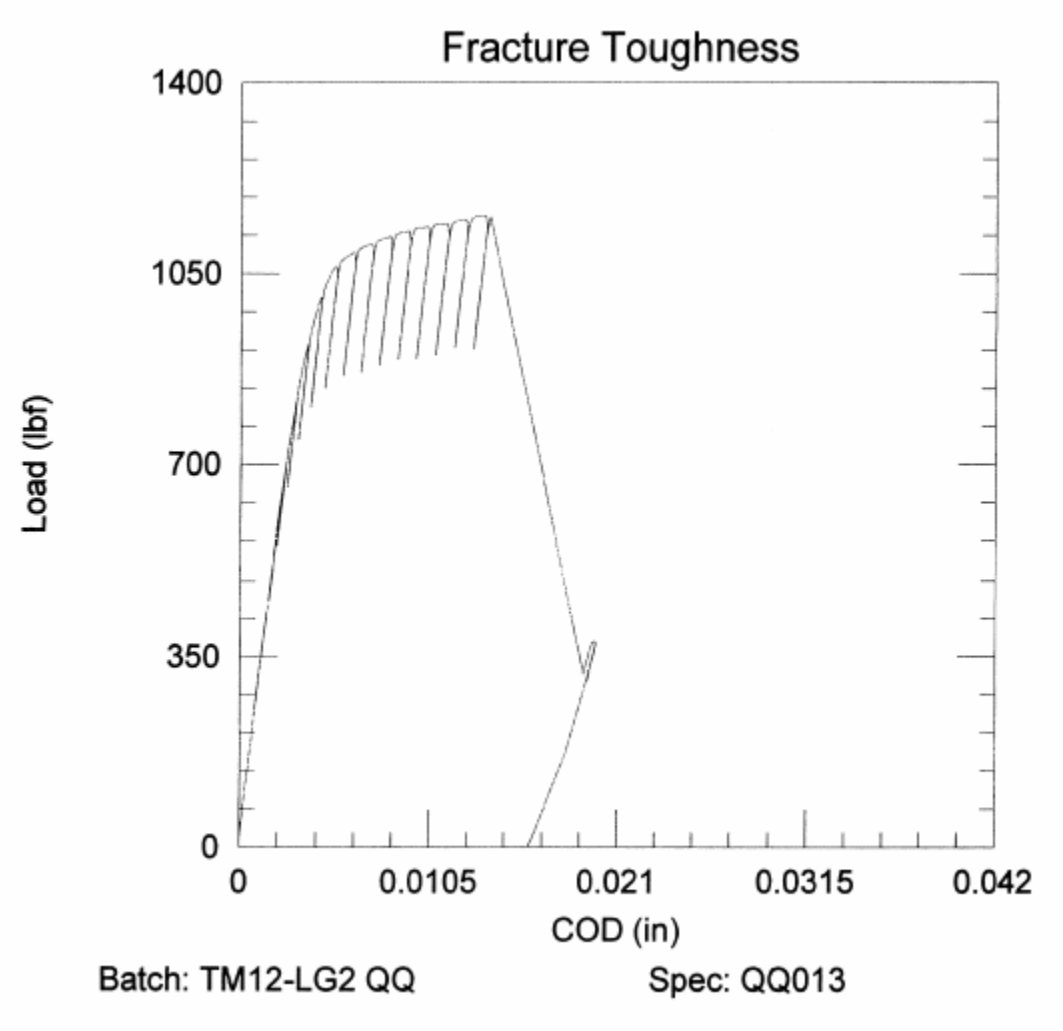

Figure B-20. Load-COD Plot for WF-25(6) PCS Toughness Specimen QQ014 (130 °F)

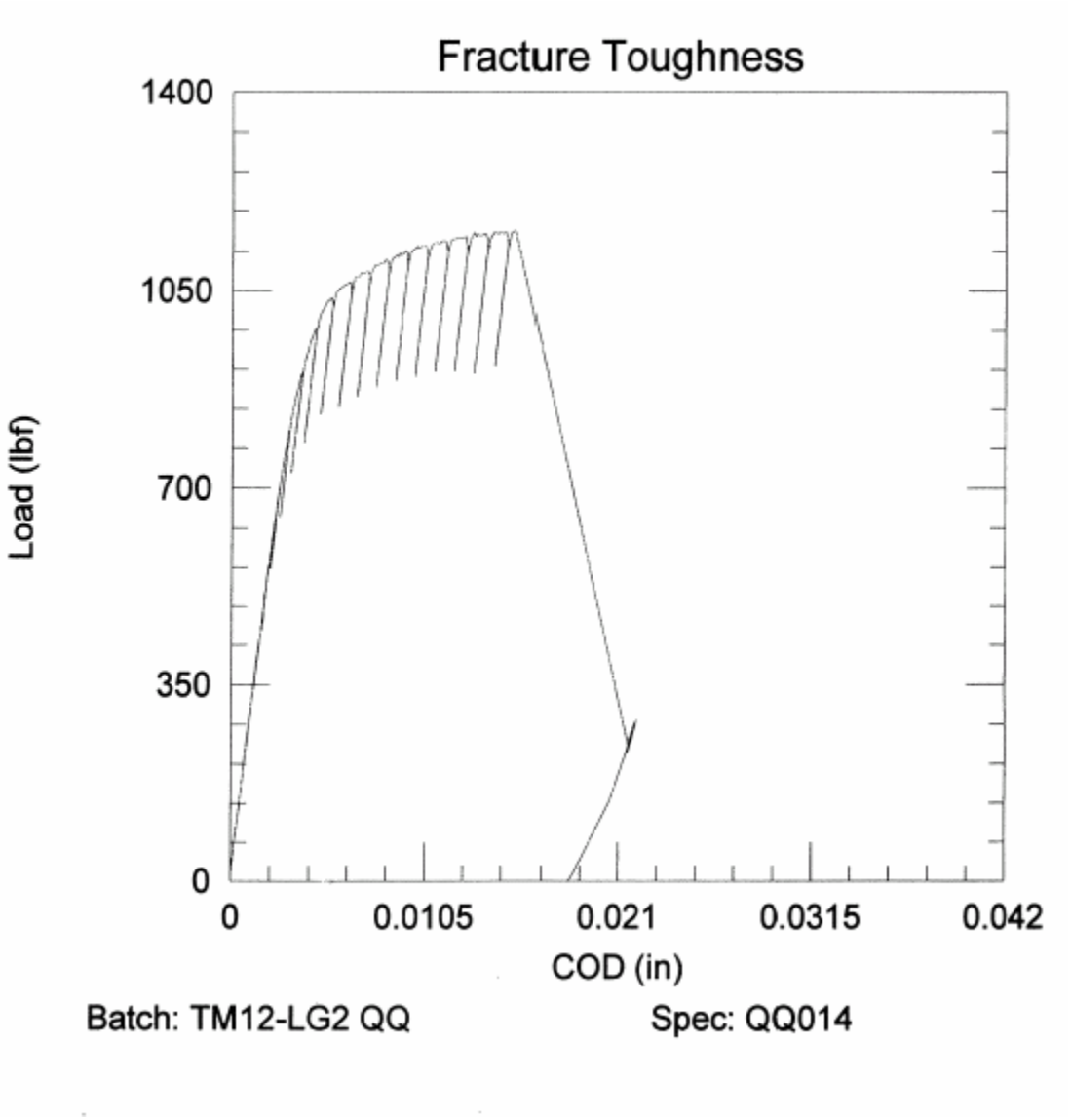

Figure B-21. Load-COD Plot for WF-25(6) PCS Toughness Specimen QQ015 (130 °F)

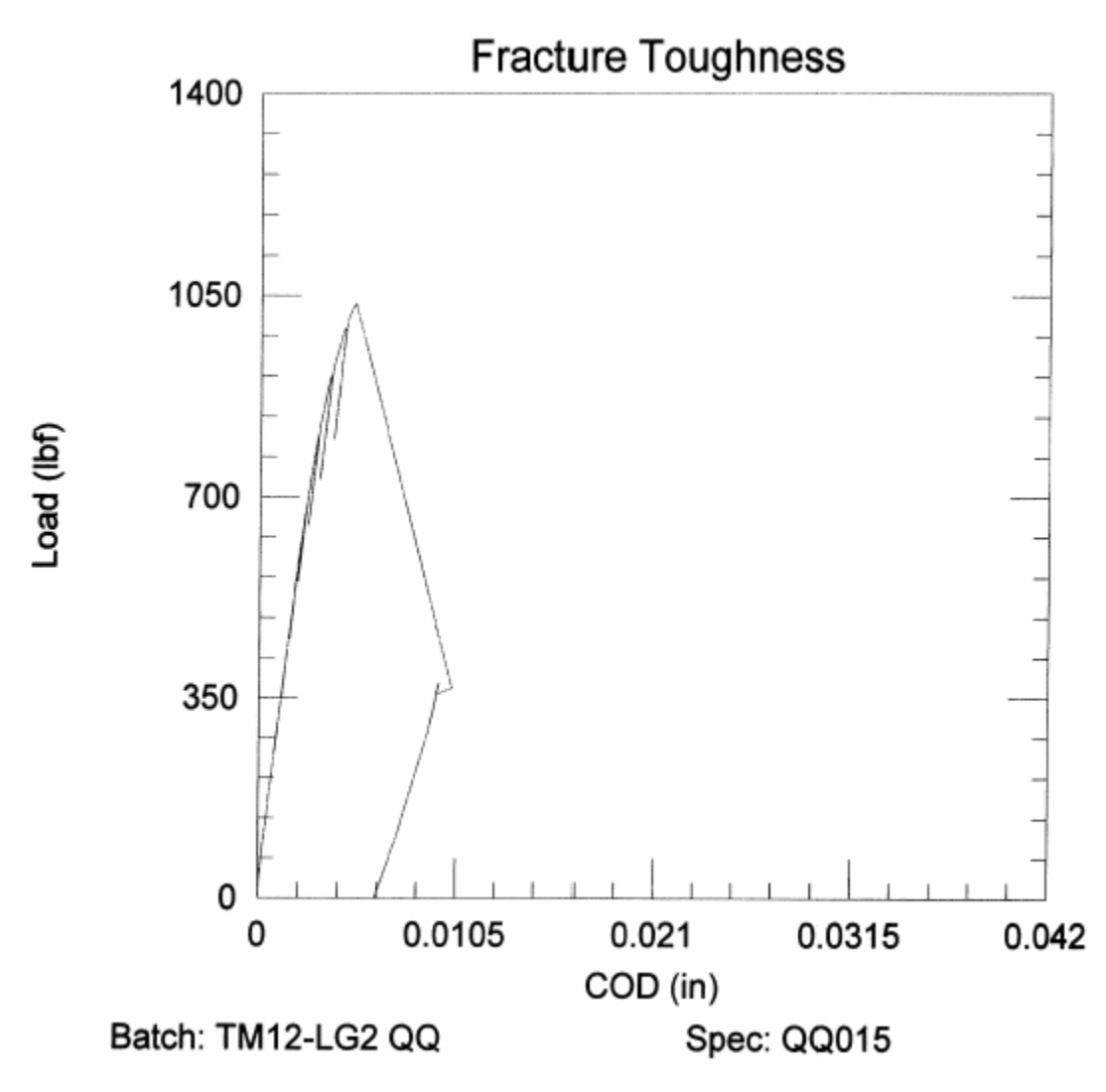

Figure B-22. Load-COD Plot for WF-25(6) PCS Toughness Specimen QQ016 (130 °F)

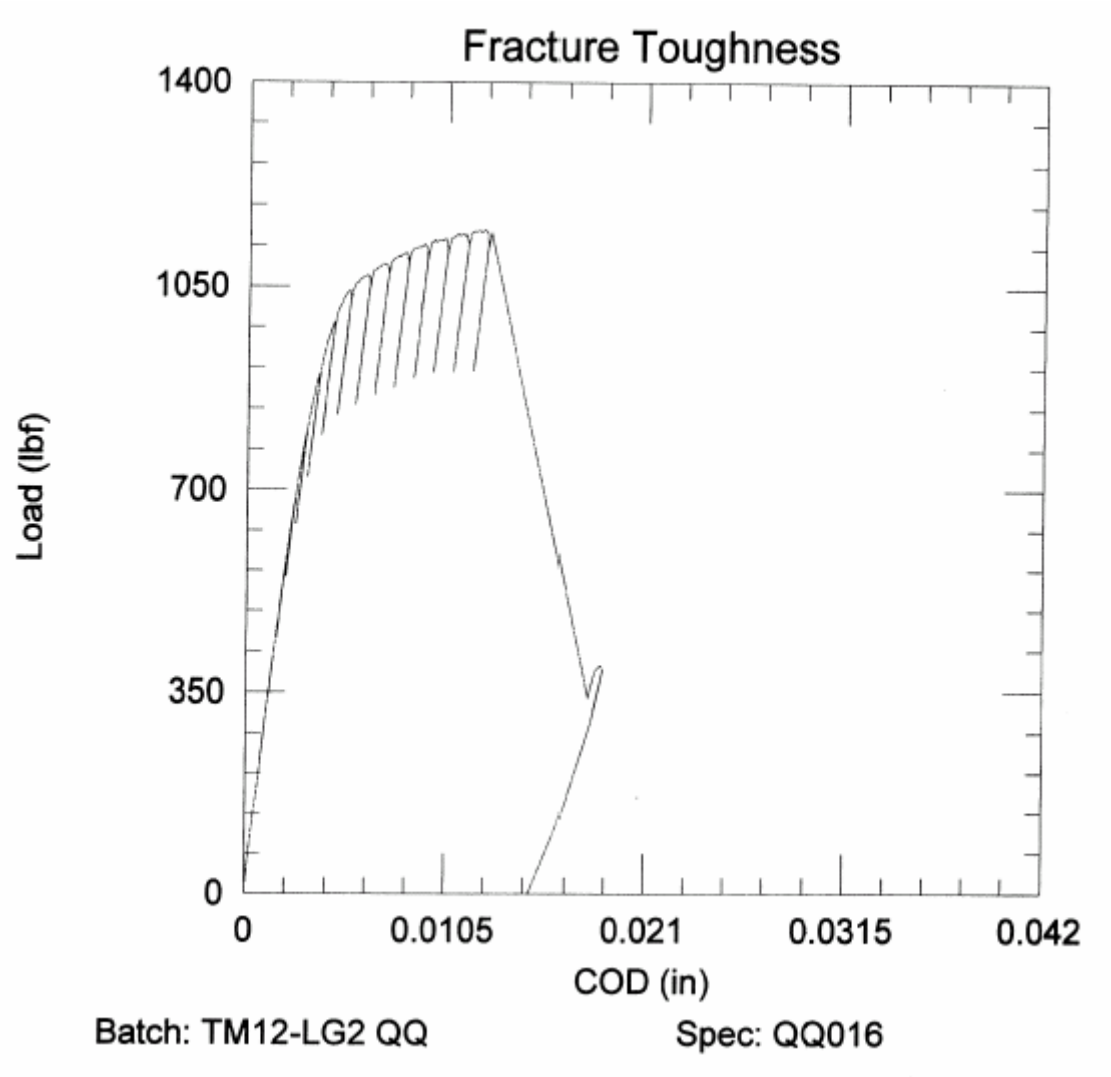

Figure B-23. Load-COD Plot for WF-25(6) PCS Toughness Specimen QQ017 (130 °F)

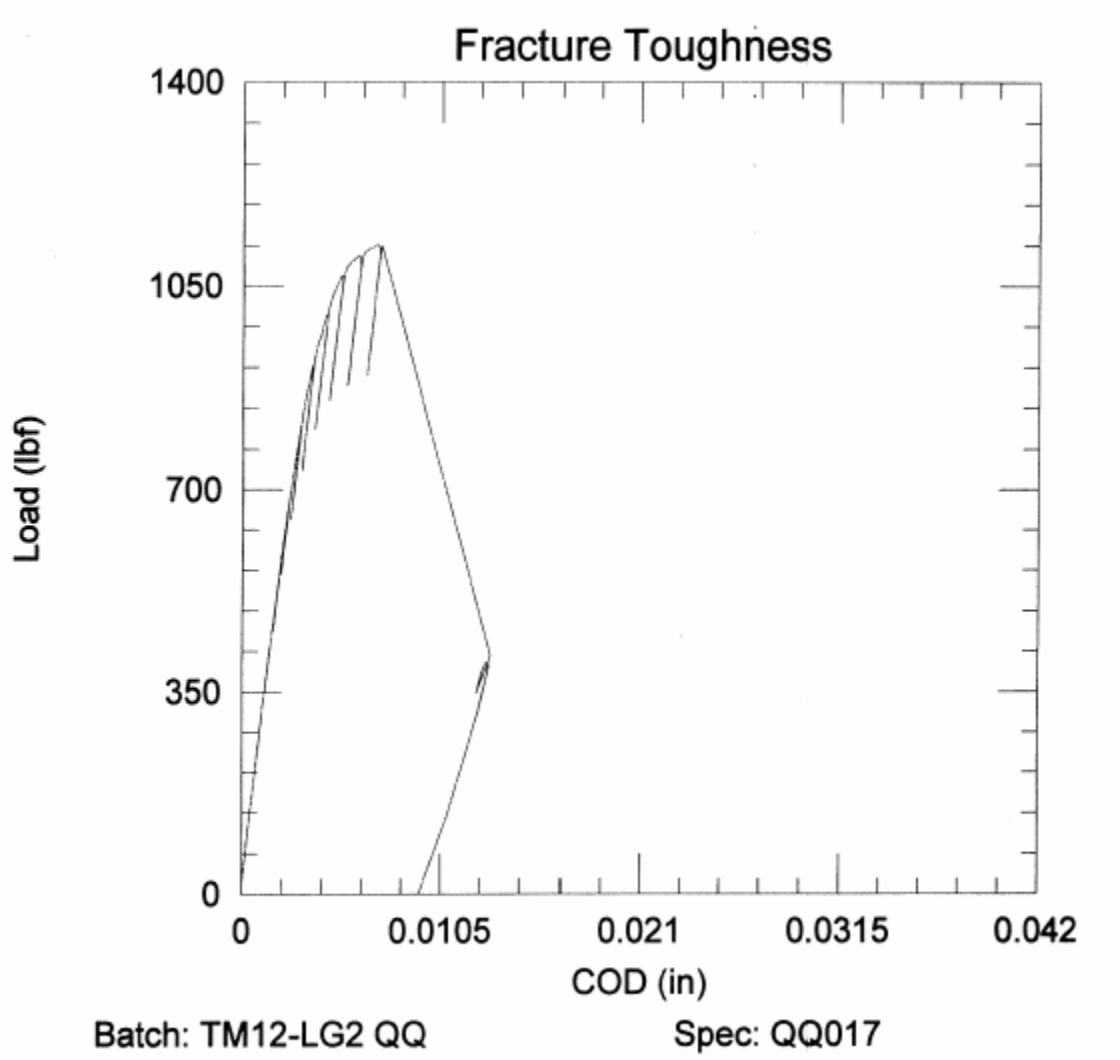

Figure B-24. Load-COD Plot for WF-25(6) PCS Toughness Specimen QQ018 (100 °F)

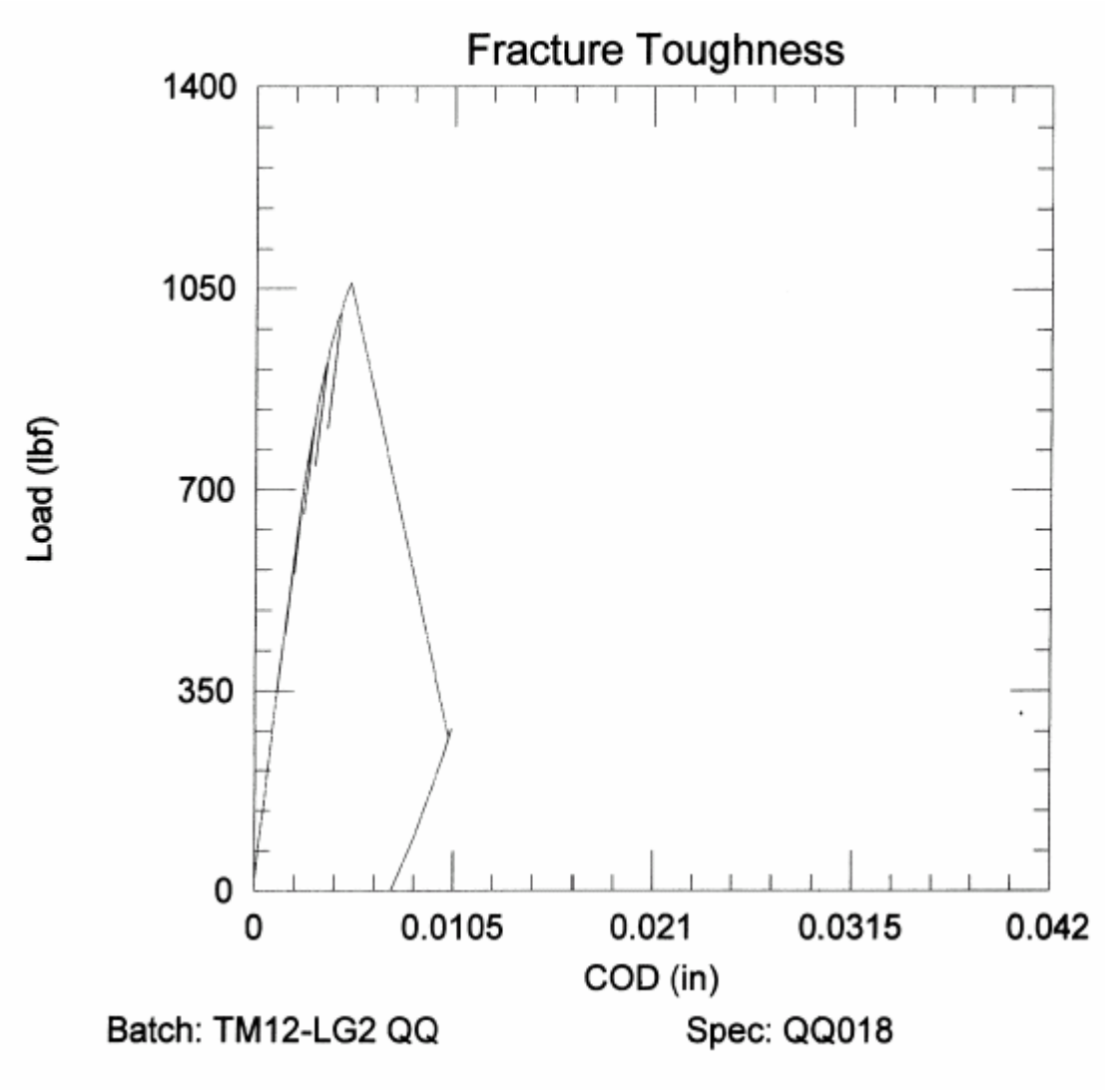

Figure B-25. Load-COD Plot for WF-25(6) PCS Toughness Specimen QQ019 (100 °F)

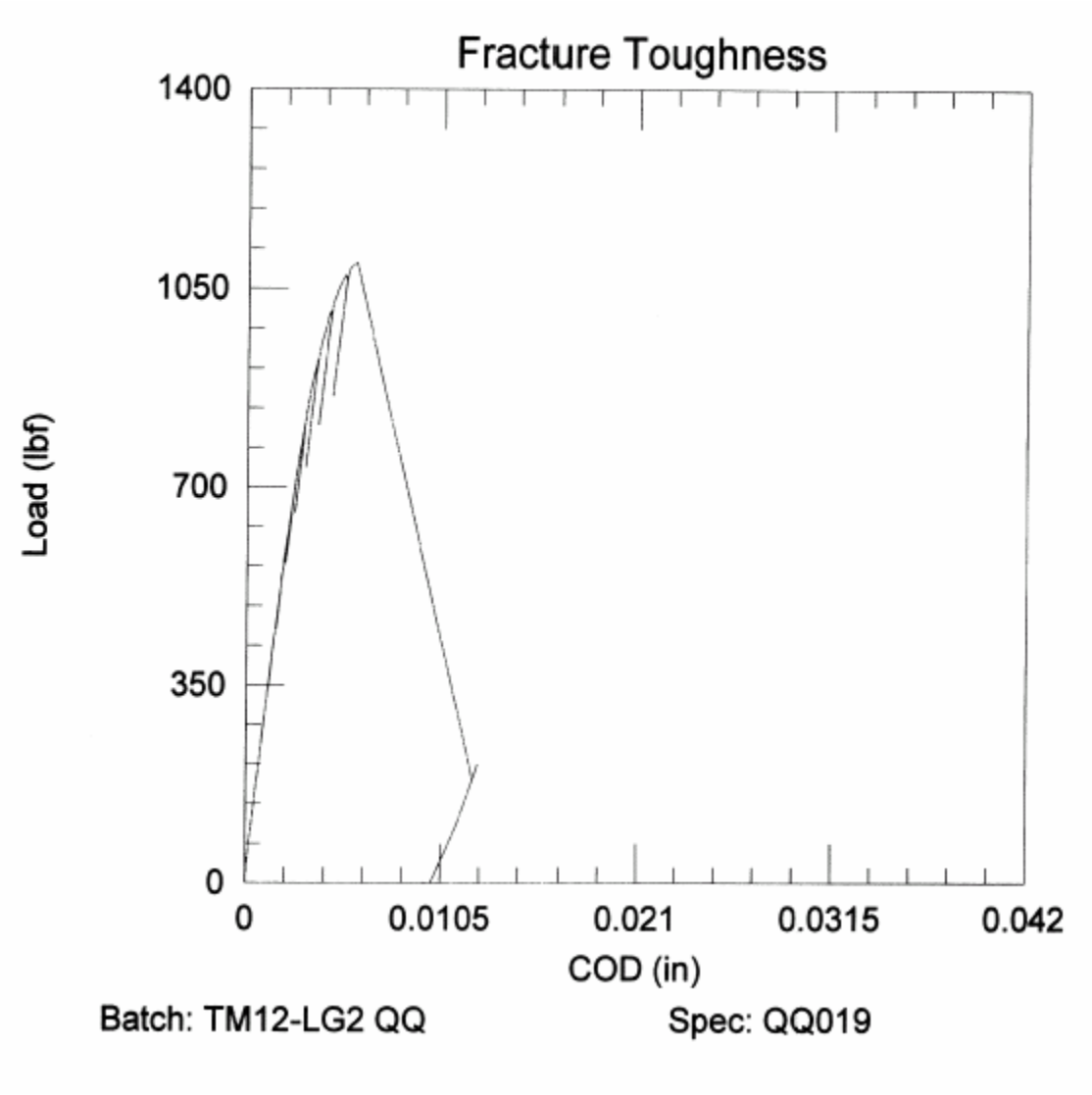

Figure B-26. Load-COD Plot for WF-25(6) PCS Toughness Specimen QQ020 (130 °F)

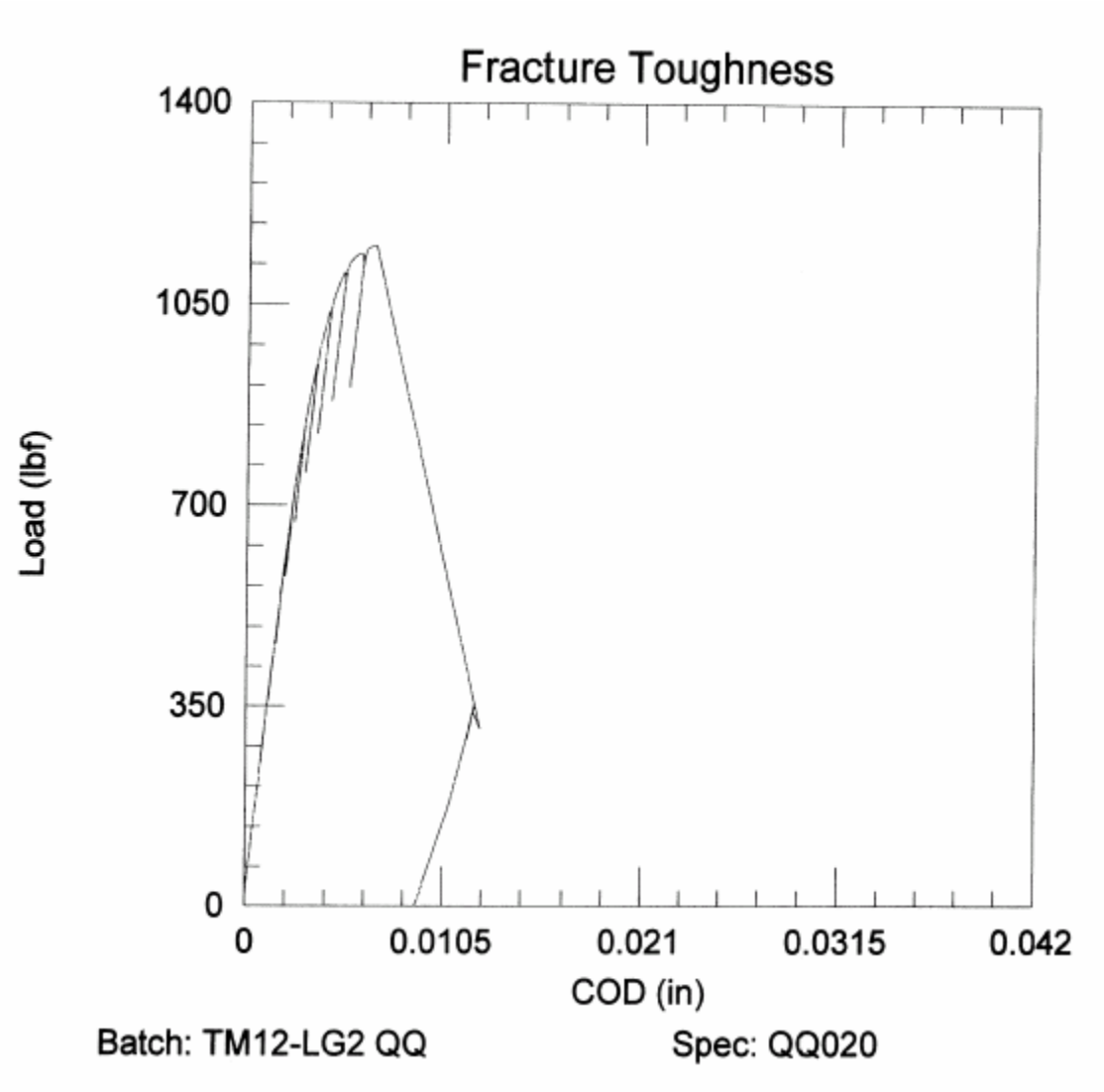

Figure B-27. Load-COD Plot for WF-25(6) PCS Toughness Specimen QQ021 (130 °F)

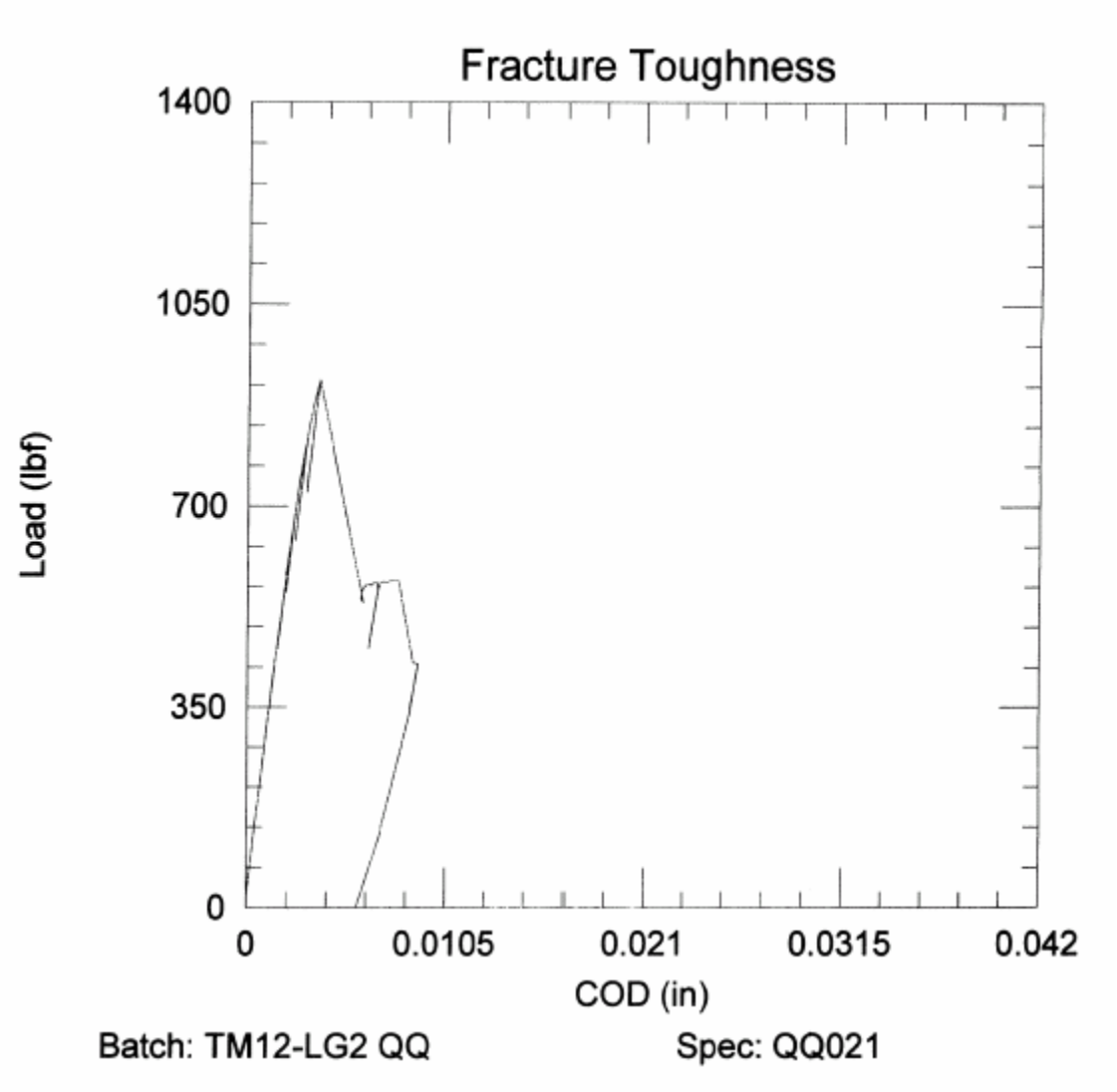

Figure B-28. Load-COD Plot for WF-25(6) 0.5 TC(T) Toughness Specimen QQ002 (170 °F)

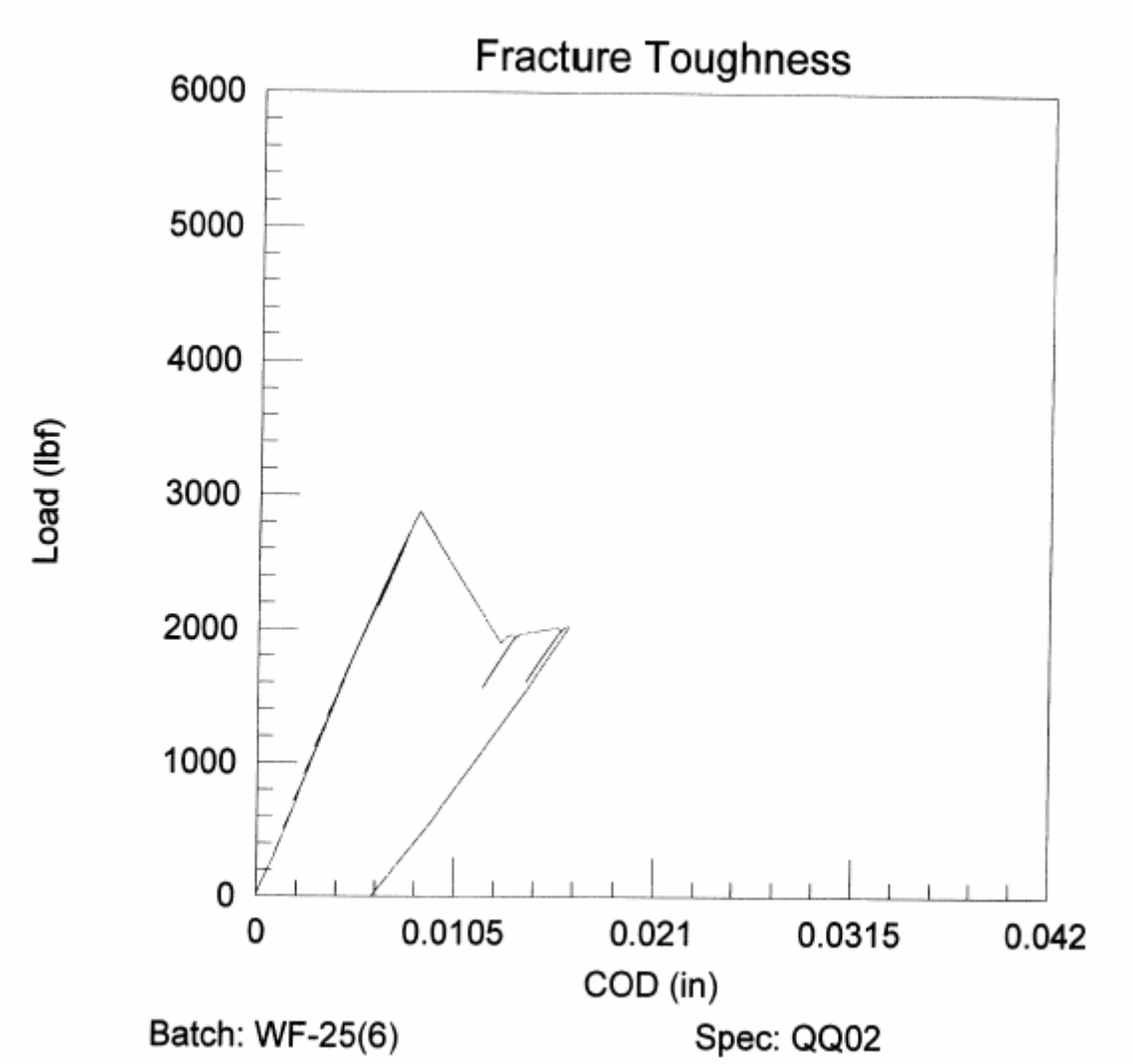

Figure B-29. Load-COD Plot for WF-25(6) 0.5 TC(T) Toughness Specimen QQ003 (170 °F)

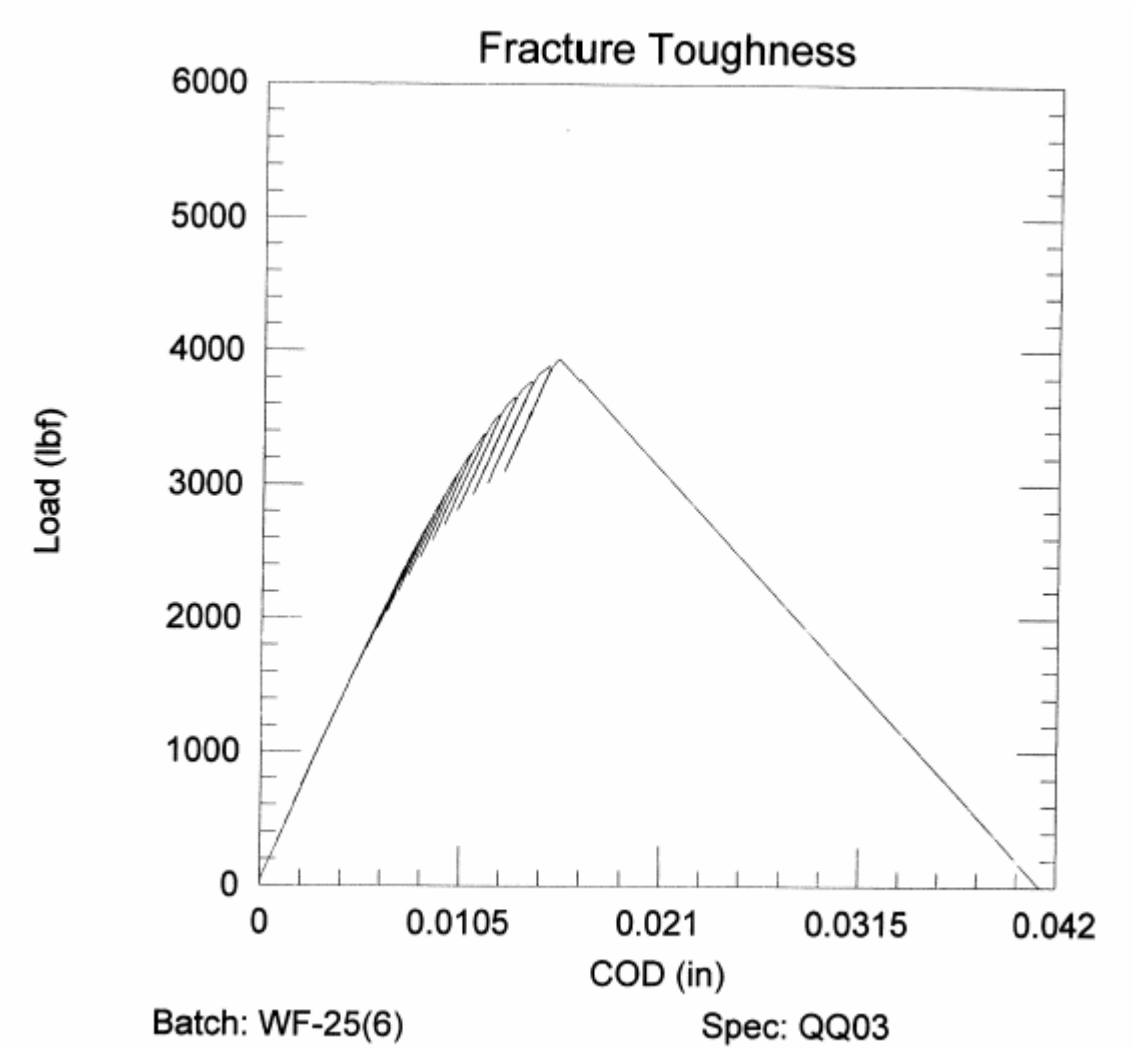

Figure B-30. Load-COD Plot for WF-25(6) 0.5 TC(T) Toughness Specimen QQ005 (170 °F)

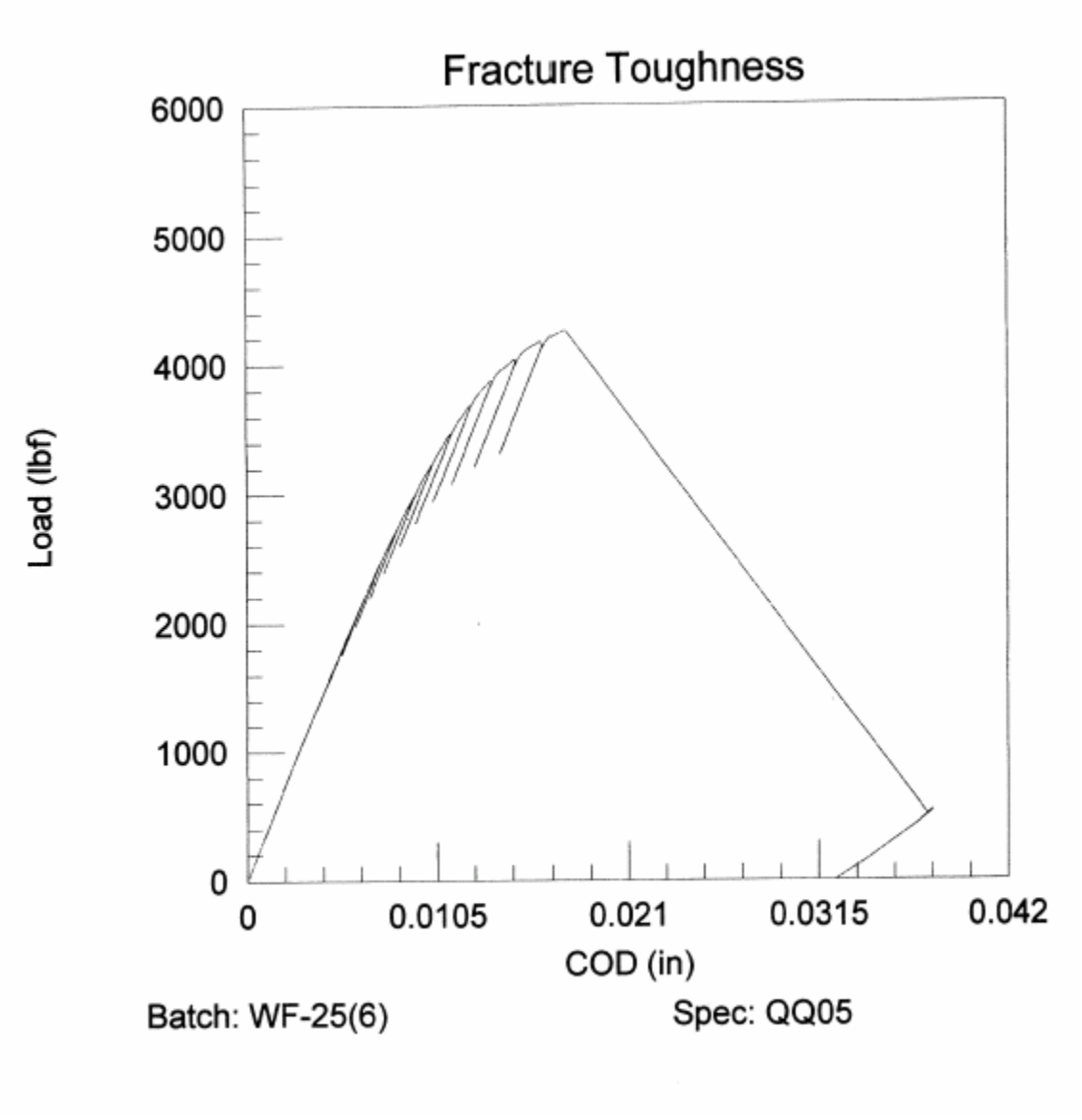

Figure B-31. Load-COD Plot for WF-25(6) 0.5 TC(T) Toughness Specimen QQ008 (170 °F)

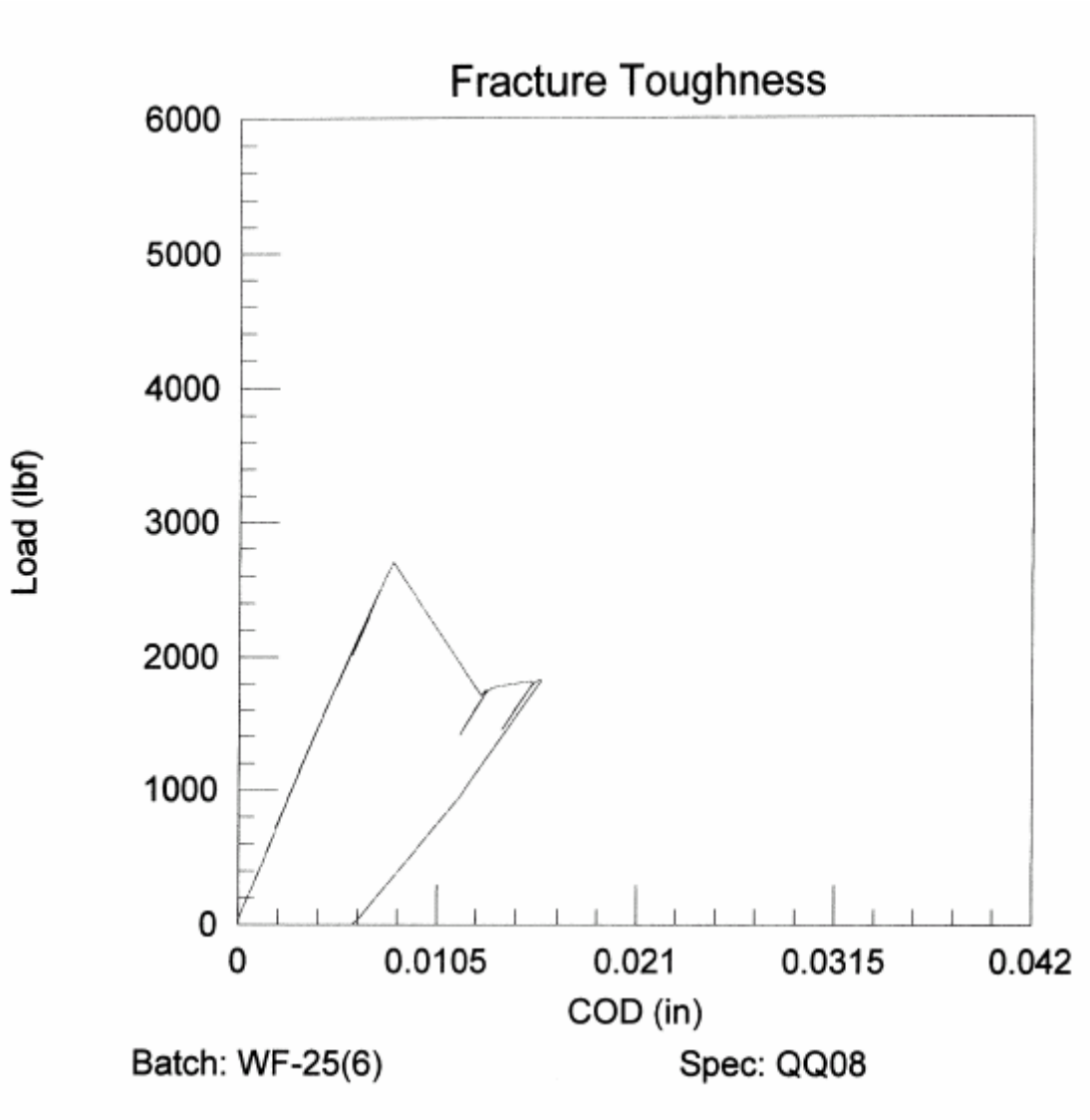

Figure B-32. Load-COD Plot for WF-25(6) 0.394 TC(T) Toughness Specimen QQ001 (170 °F)

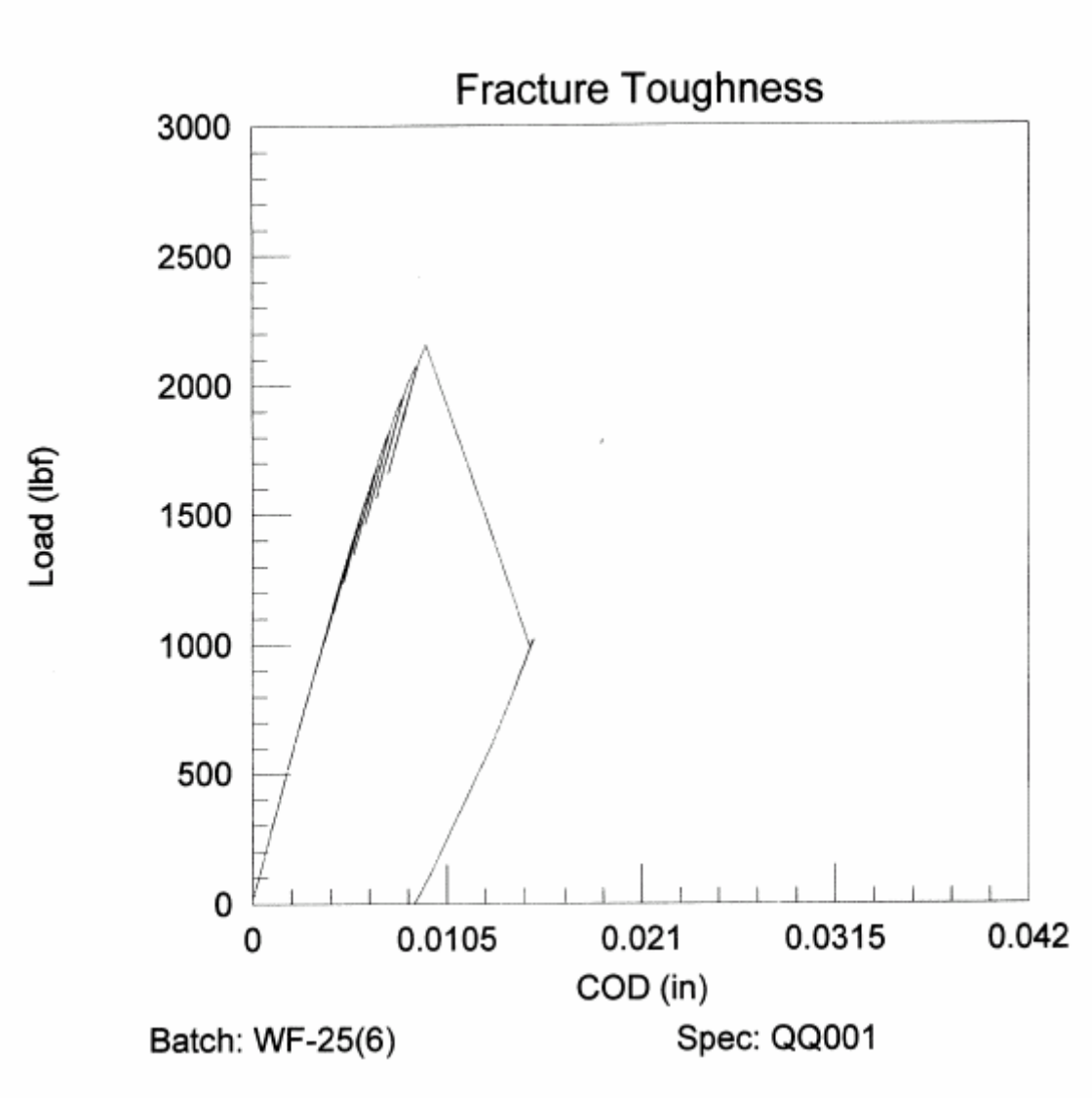

Figure B-33. Load-COD Plot for WF-25(6) 0.394 TC(T) Toughness Specimen QQ002 (170 °F)

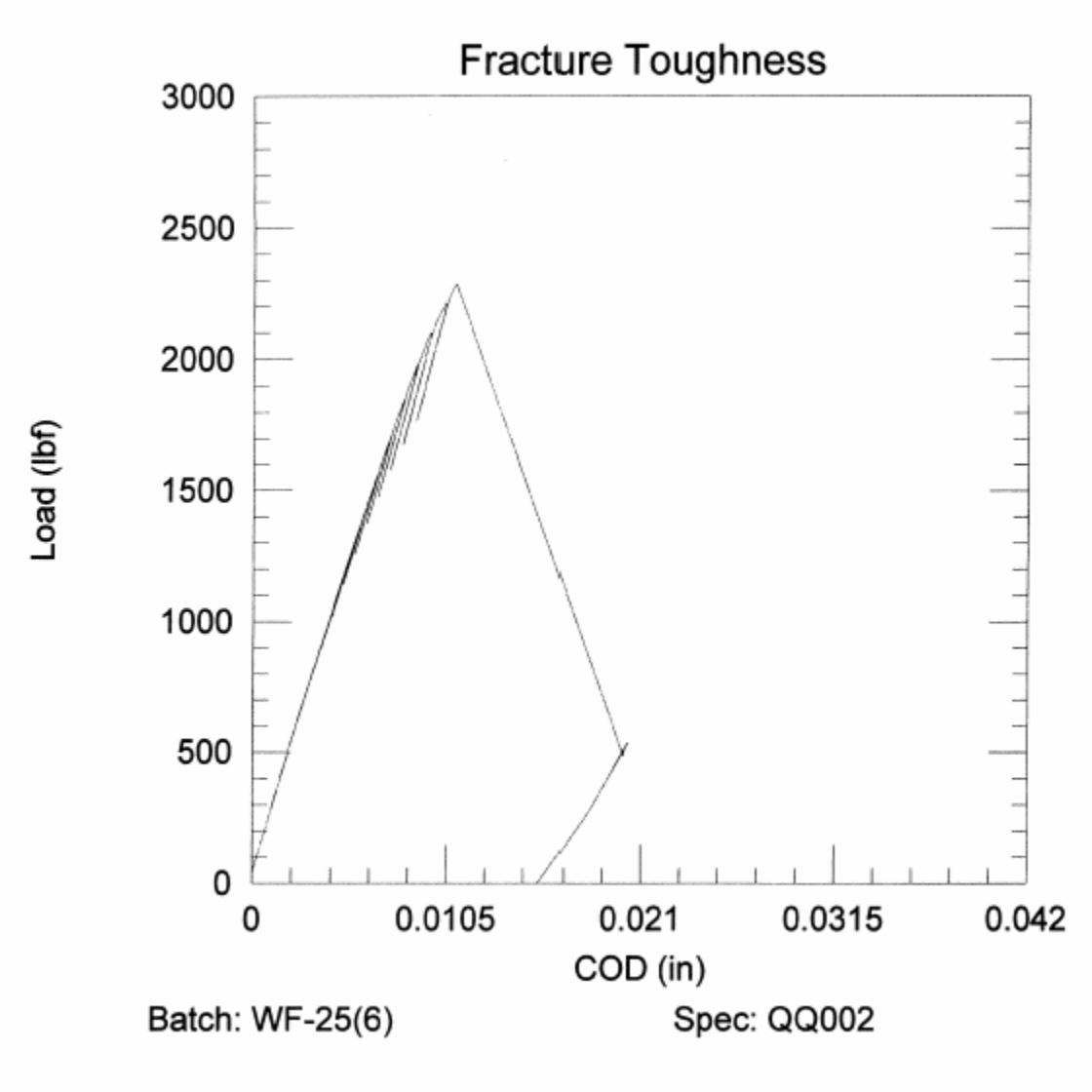

Figure B-34. Load-COD Plot for WF-25(9) PCS Toughness Specimen JJ001 (100 °F)

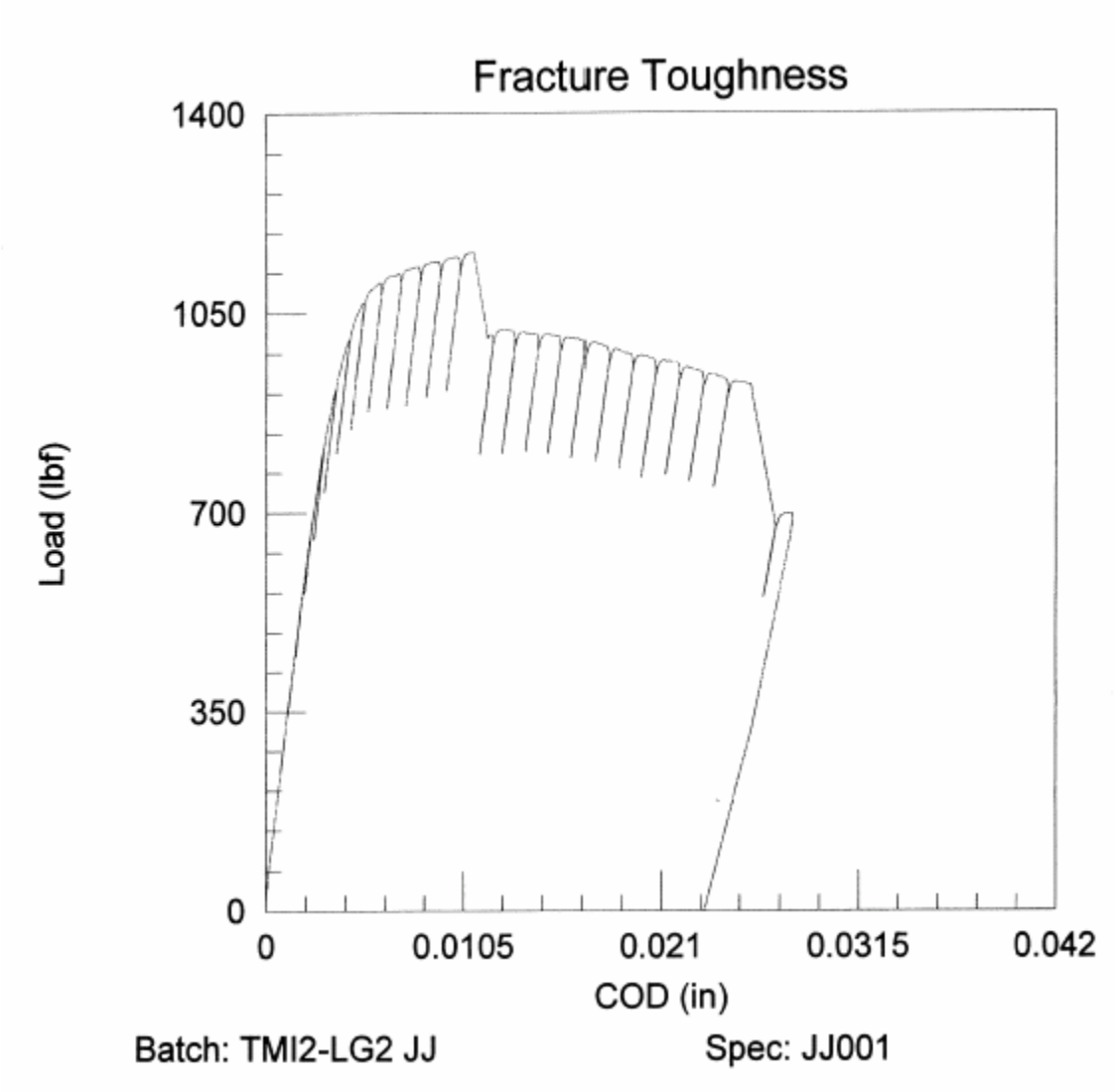

Figure B-35. Load-COD Plot for WF-25(9) PCS Toughness Specimen JJ002 (100 °F)

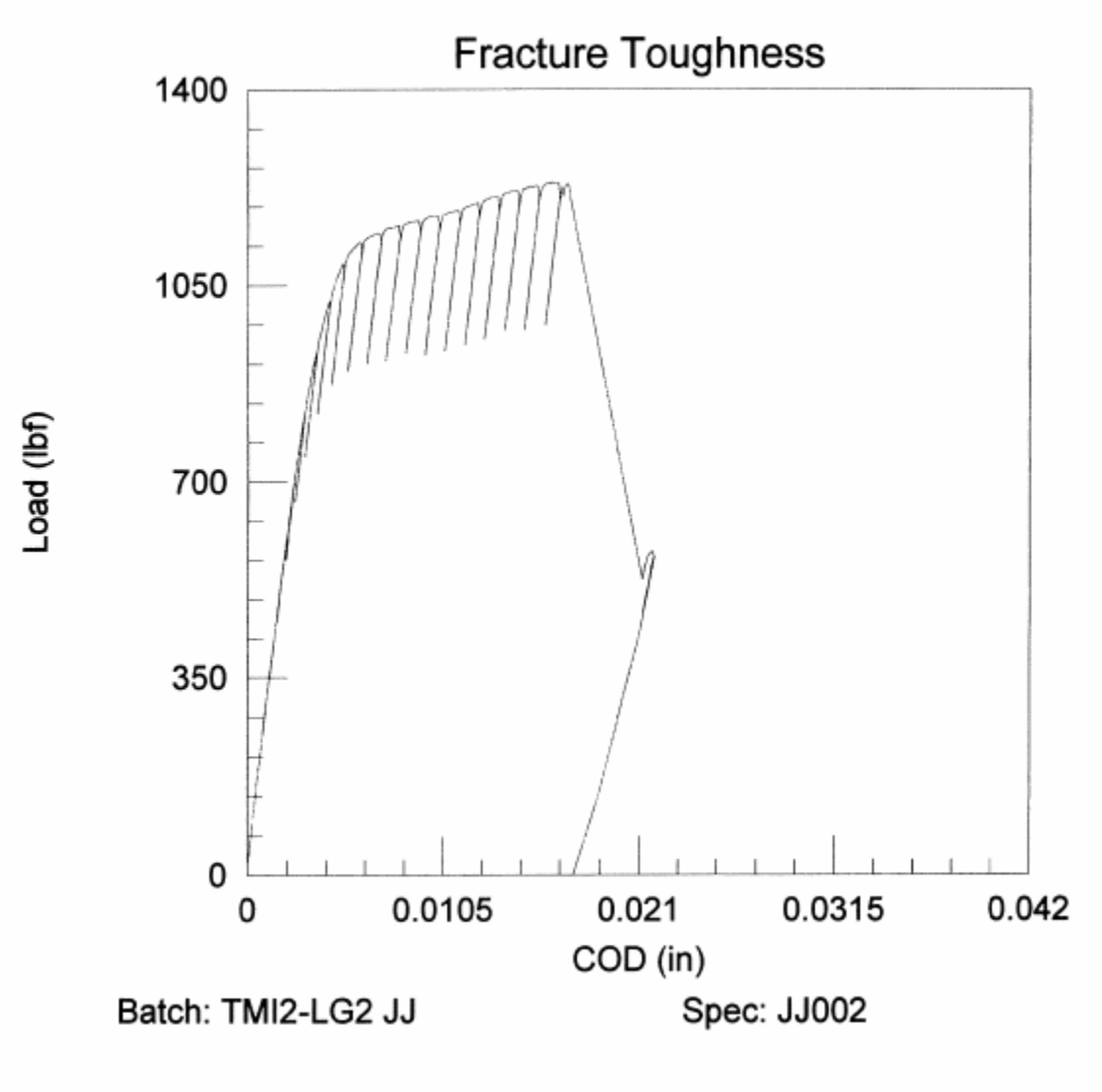

Figure B-36. Load-COD Plot for WF-25(9) PCS Toughness Specimen JJ003 (100 °F)

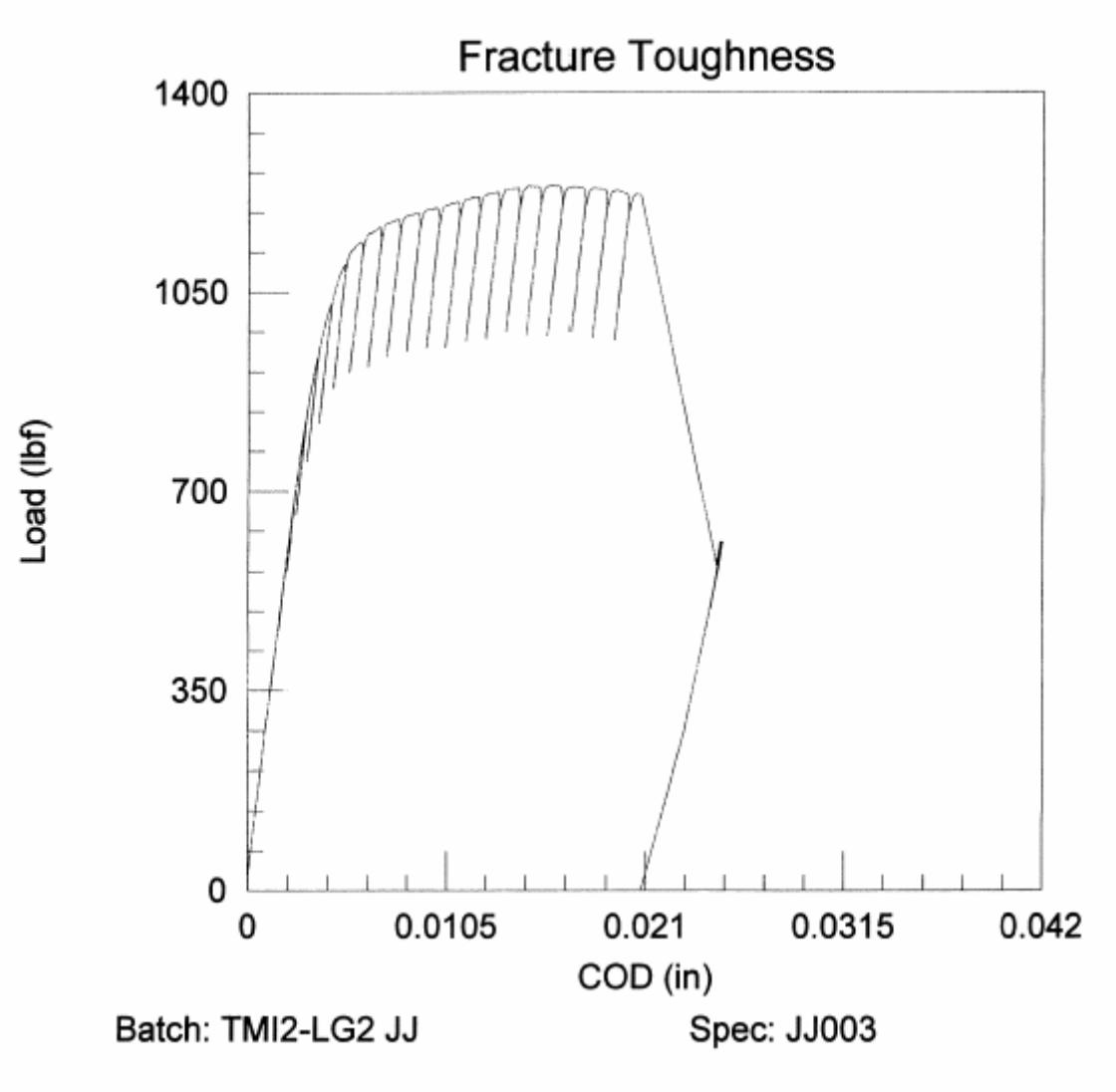

Figure B-37. Load-COD Plot for WF-25(9) PCS Toughness Specimen JJ004 (100 °F)

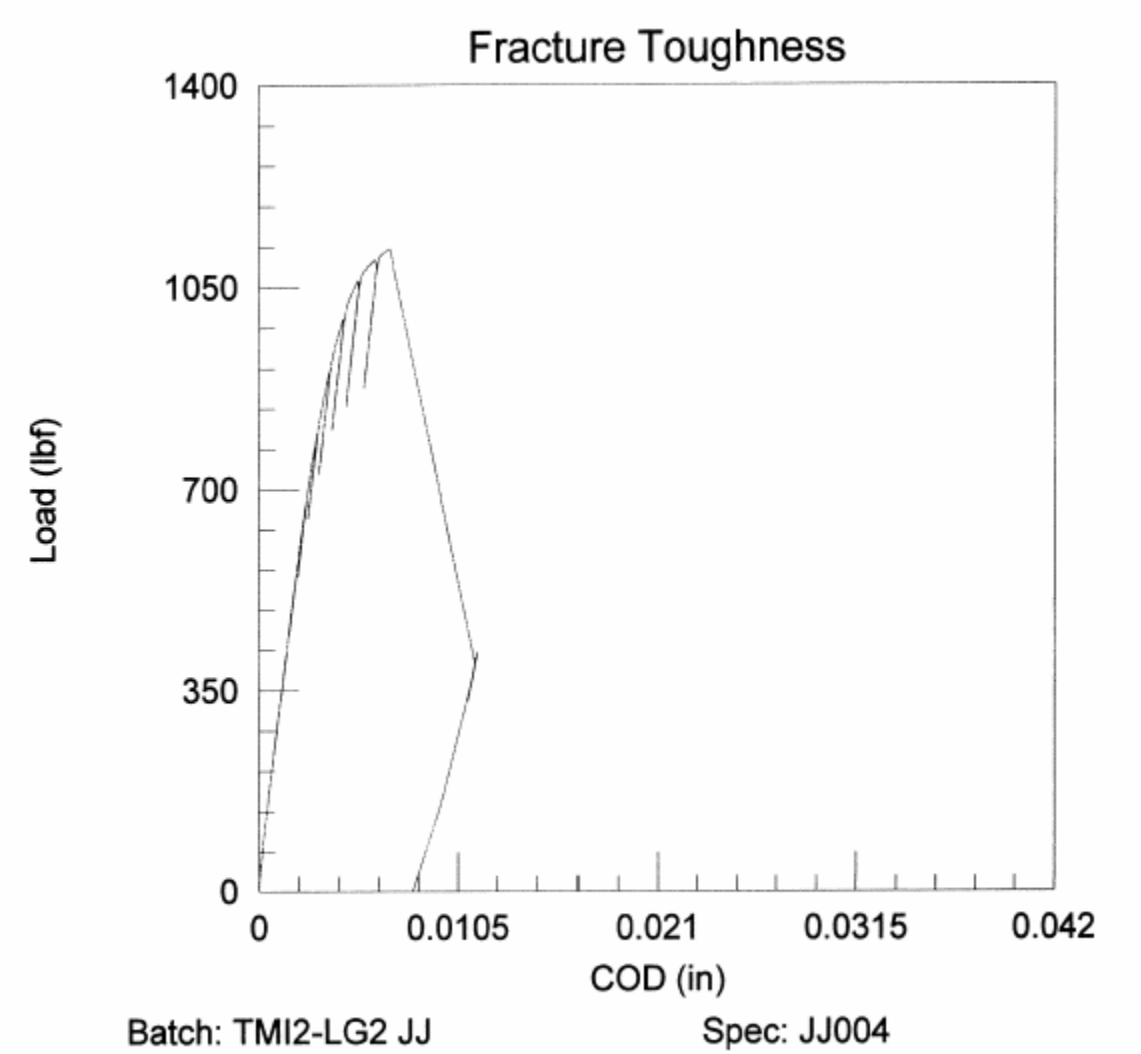

Figure B-38. Load-COD Plot for WF-25(9) PCS Toughness Specimen JJ005 (100 °F)

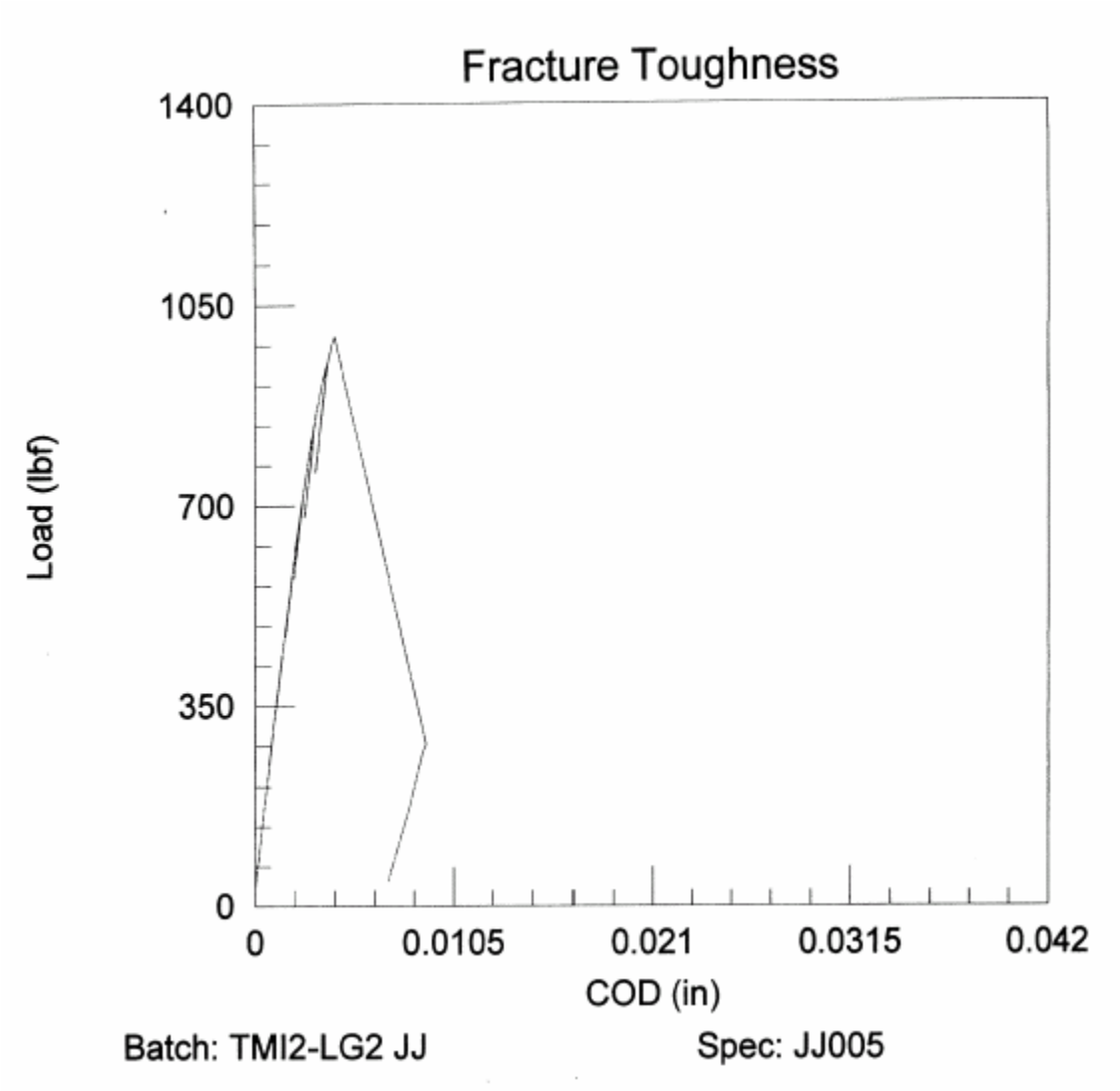

Figure B-39. Load-COD Plot for WF-25(9) PCS Toughness Specimen JJ006 (130 °F)

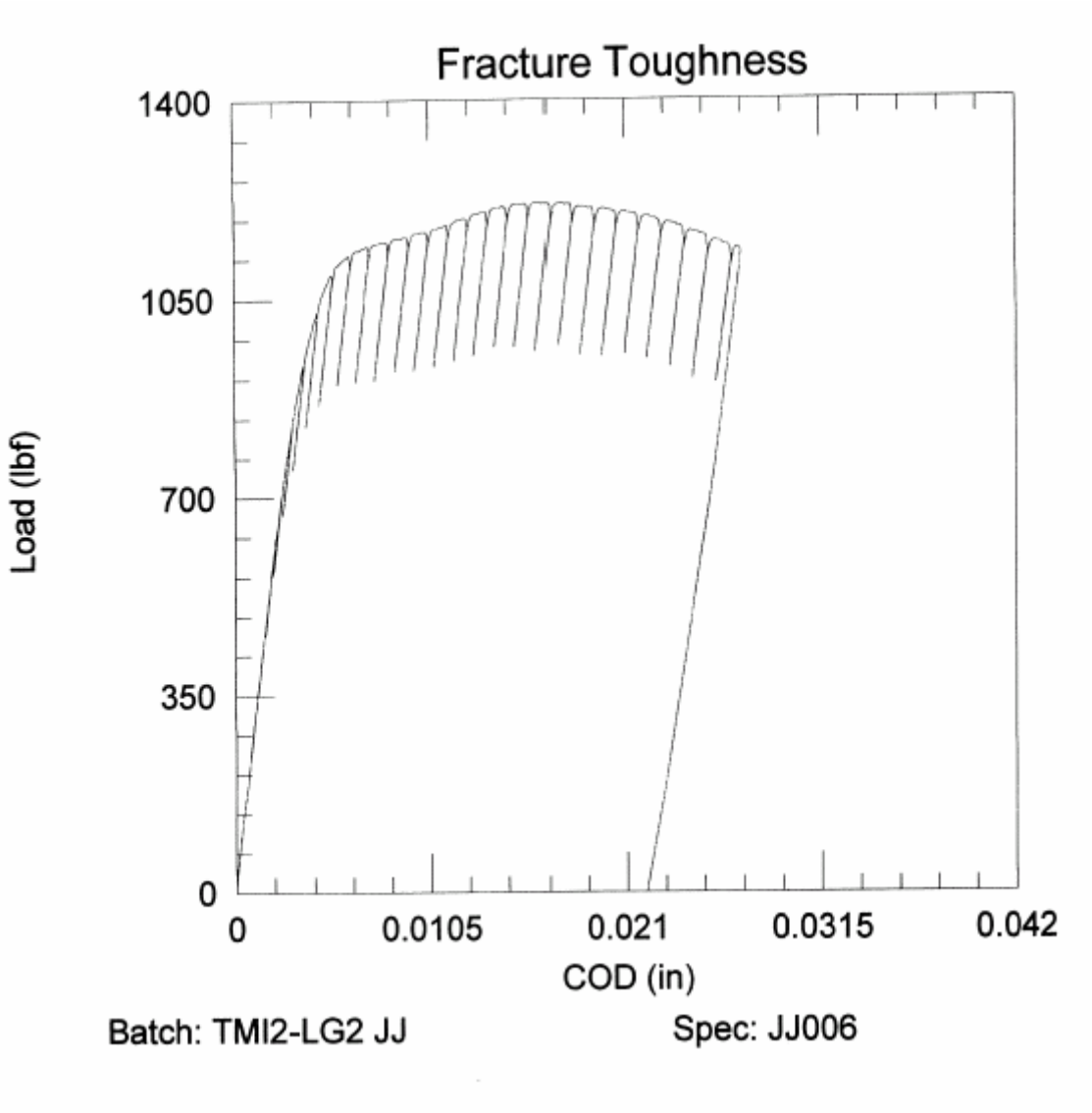

Figure B-40. Load-COD Plot for WF-25(9) PCS Toughness Specimen JJ007 (100 °F)

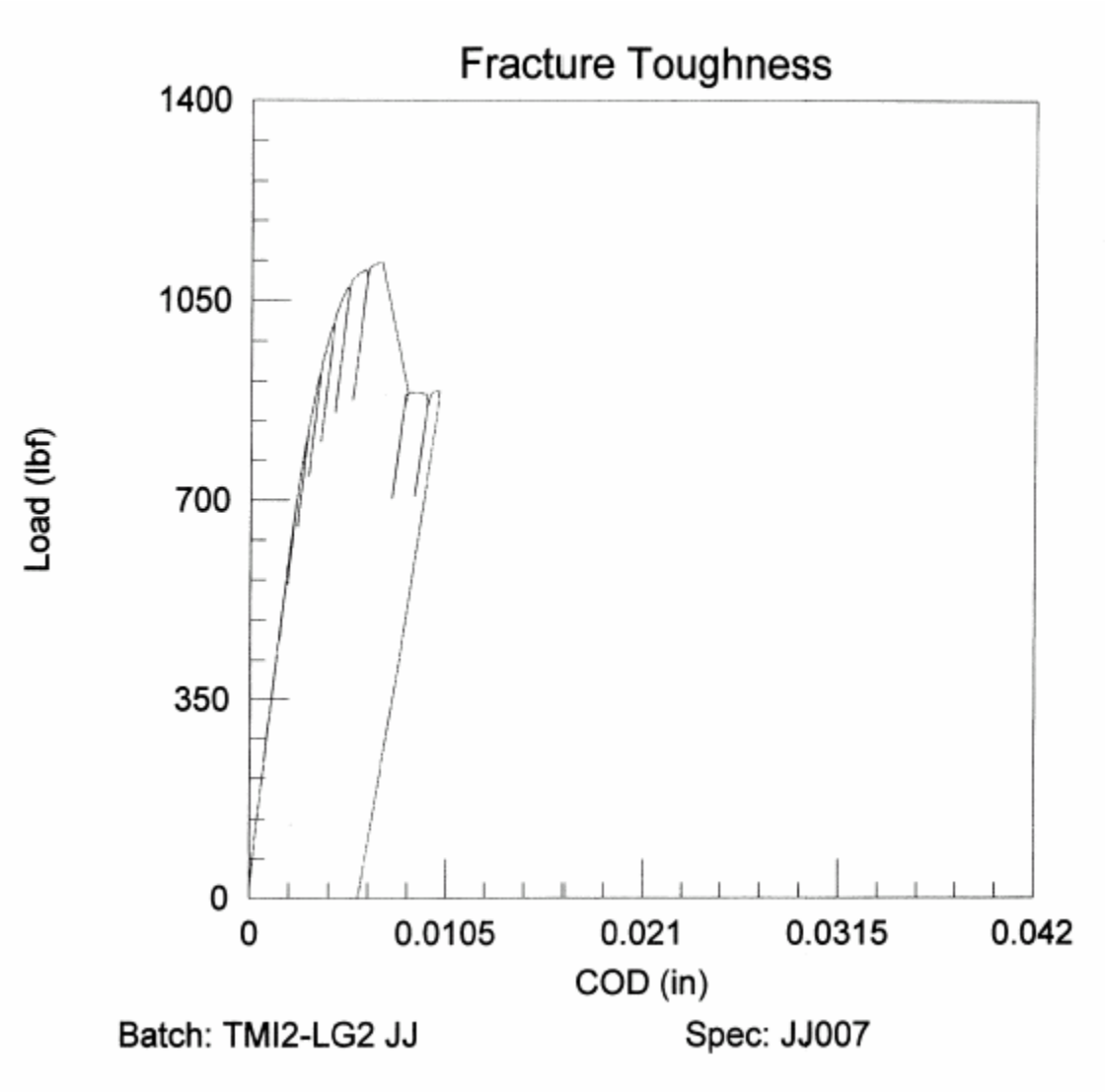

Figure B-41. Load-COD Plot for WF-25(9) PCS Toughness Specimen JJ008 (100 °F)

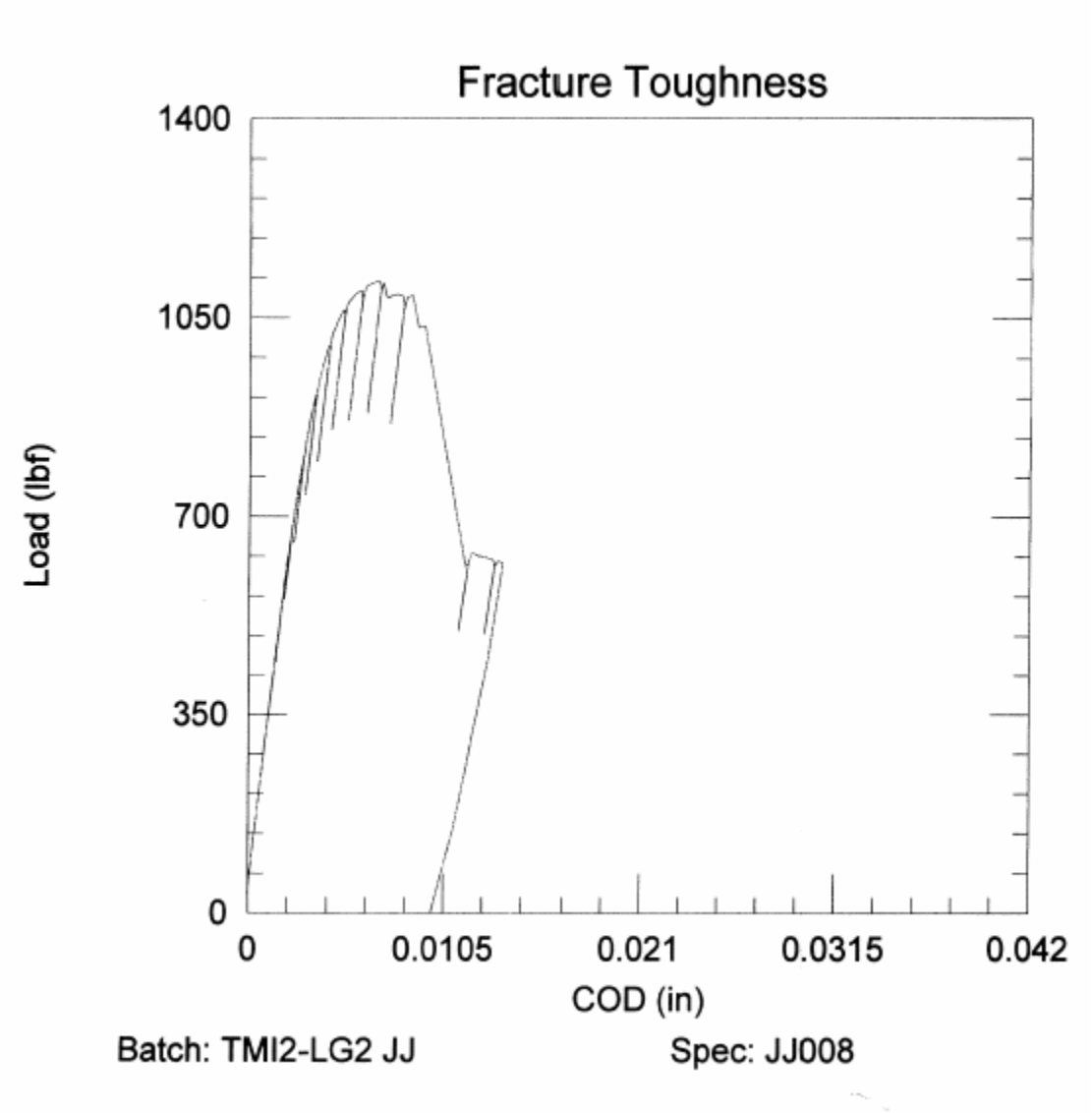

Figure B-42. Load-COD Plot for WF-25(9) PCS Toughness Specimen JJ010 (100 °F)

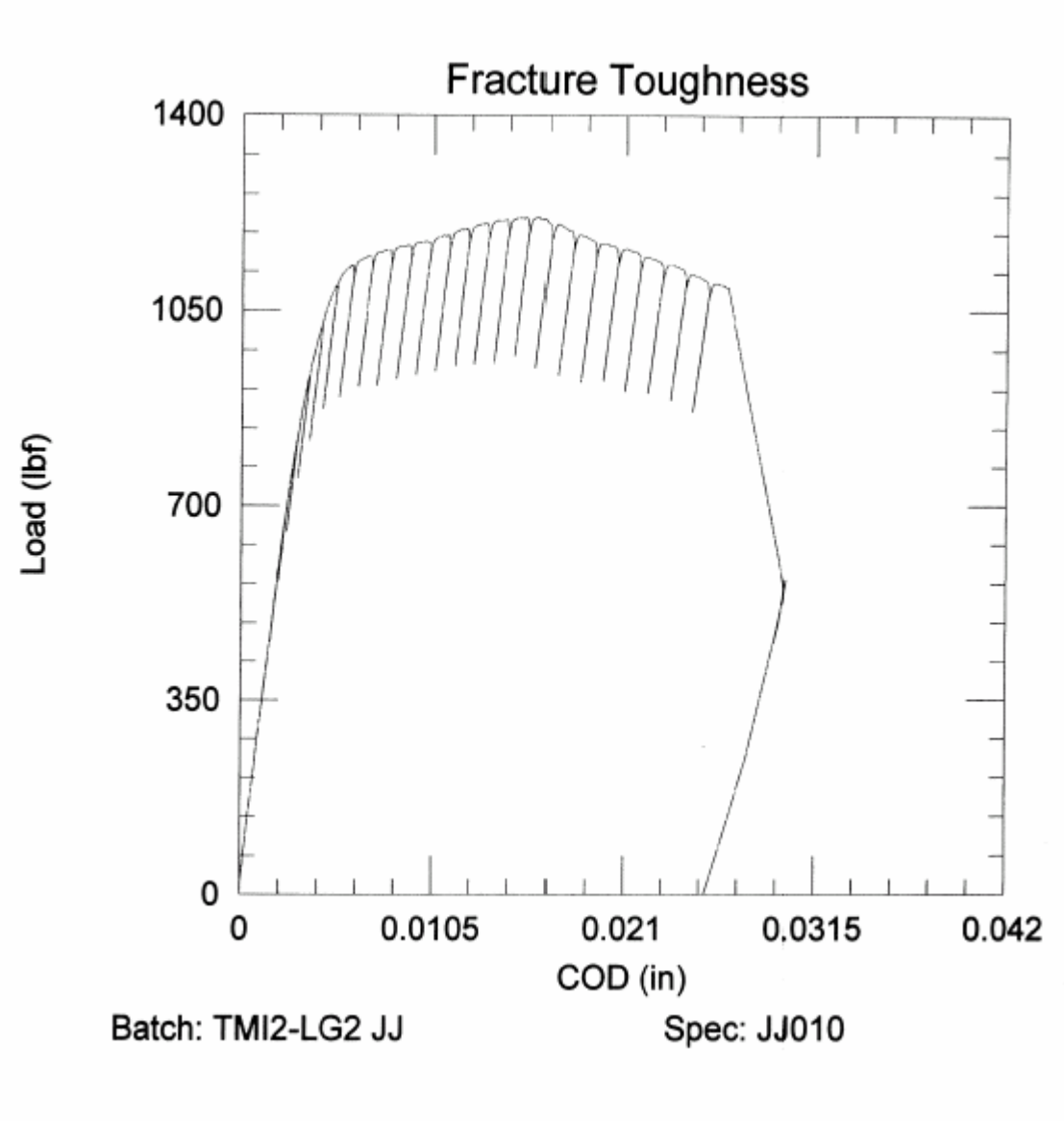

Figure B-43. Load-COD Plot for WF-25(9) 0.5 TC(T) Toughness Specimen JJ004 (110 °F)

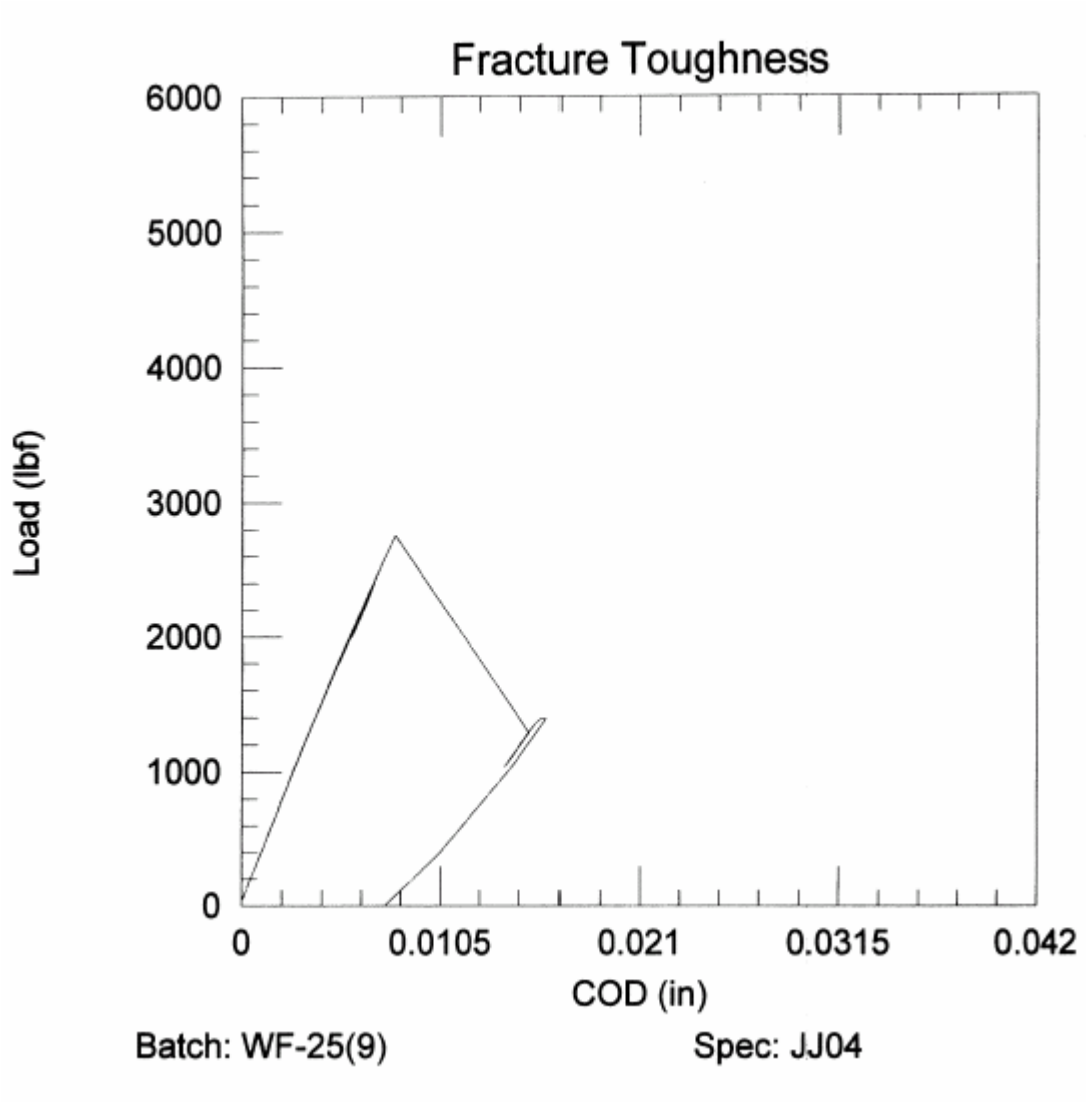

Figure B-44. Load-COD Plot for WF-25(9) 0.5 TC(T) Toughness Specimen JJ005 (110 °F)

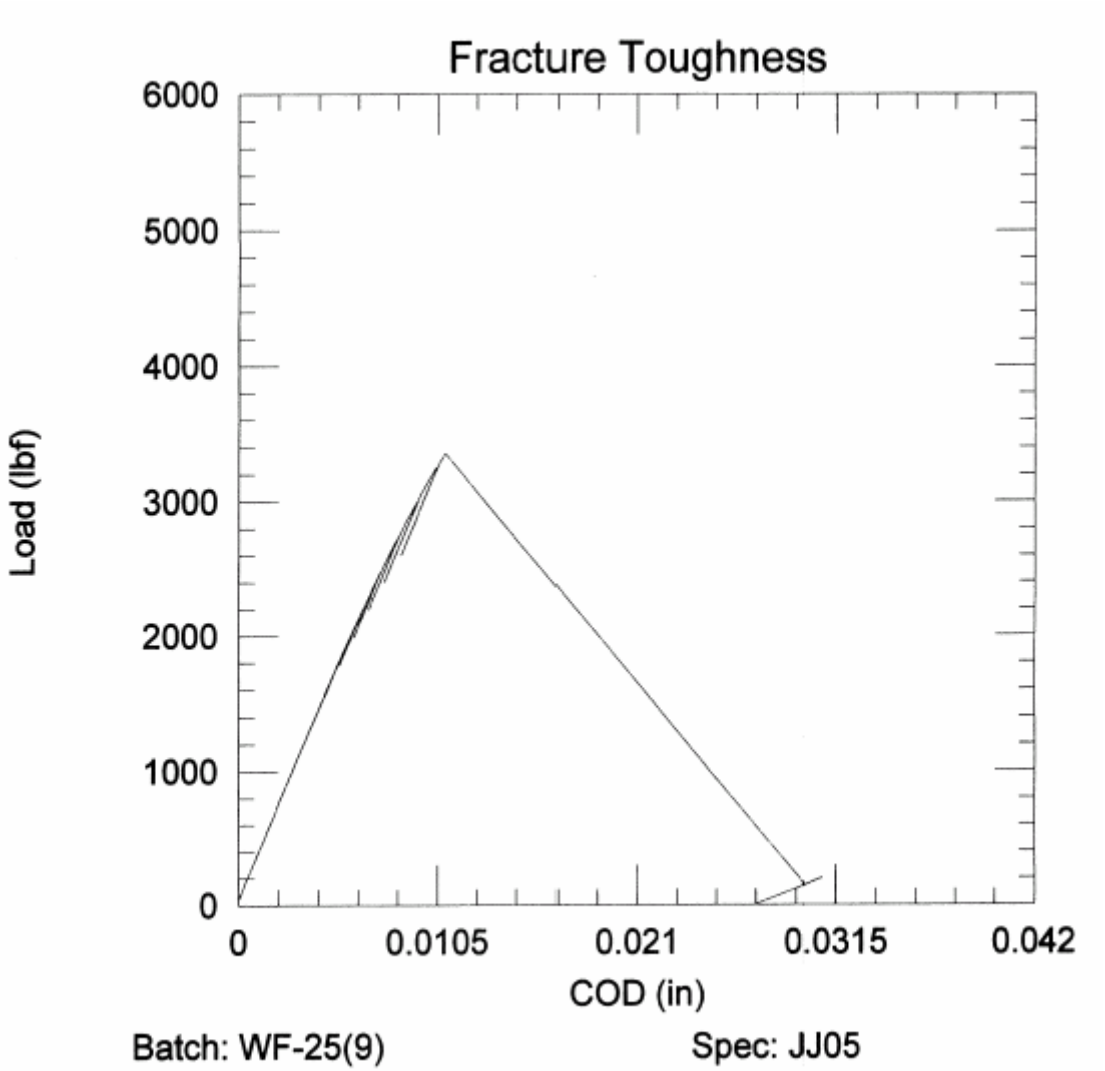

Figure B-45. Load-COD Plot for WF-25(9) 0.5 TC(T) Toughness Specimen JJ006 (110 °F)

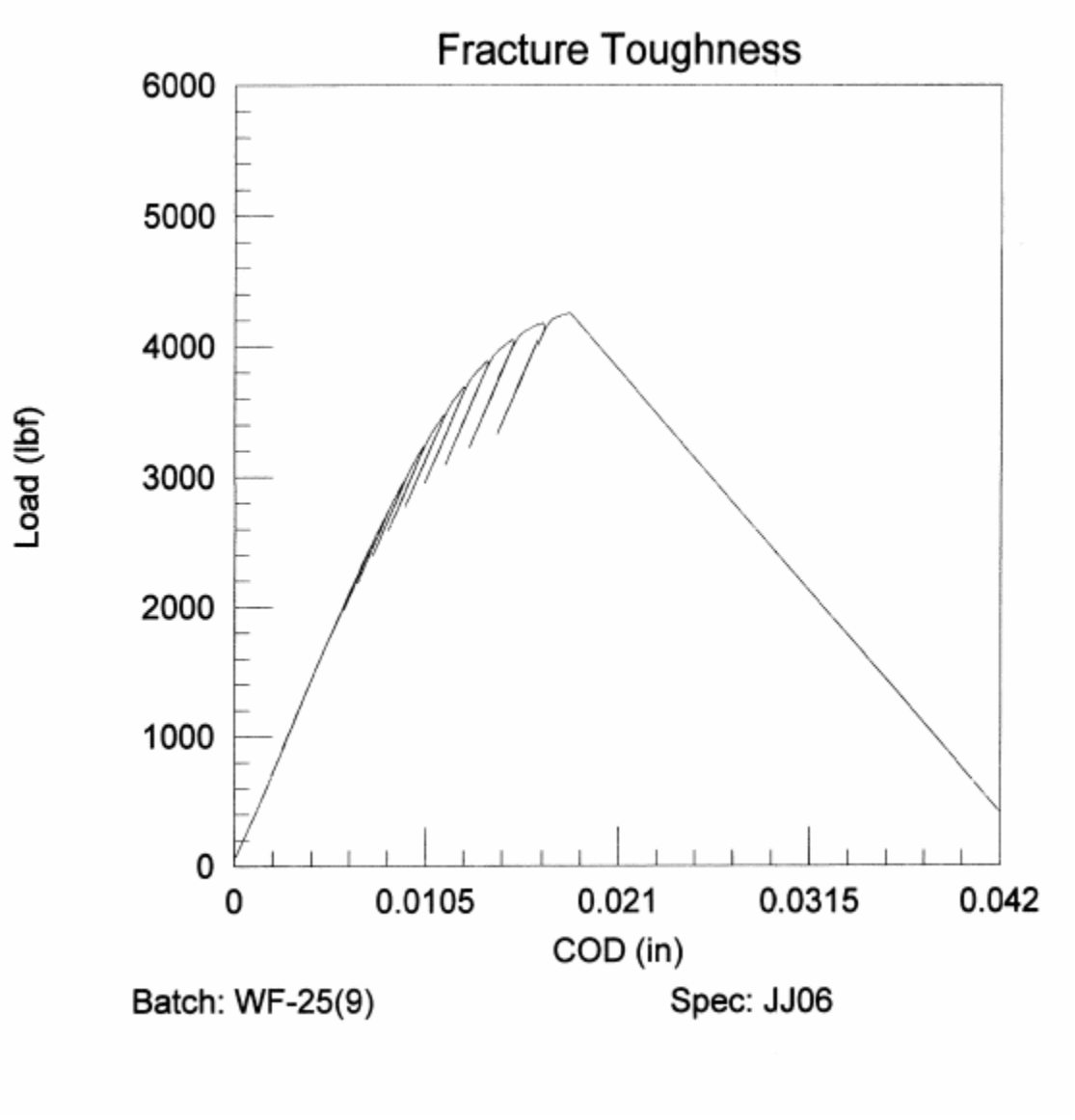

Figure B-46. Load-COD Plot for WF-25(9) 0.5 TC(T) Toughness Specimen JJ007 (110 °F)

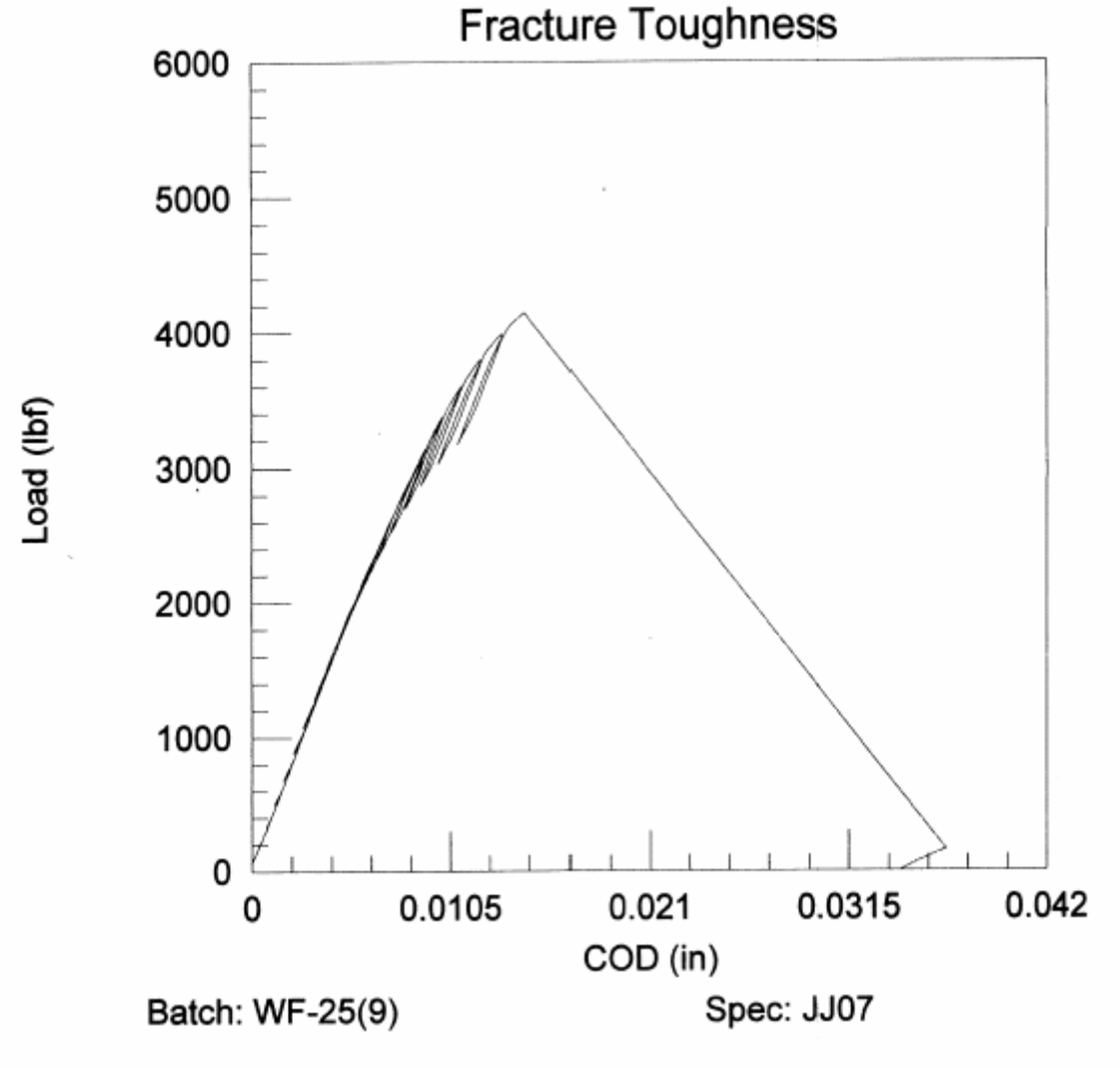

Figure B-47. Load-COD Plot for WF-25(9) 0.394 TC(T) Toughness Specimen JJ007 (110 °F)

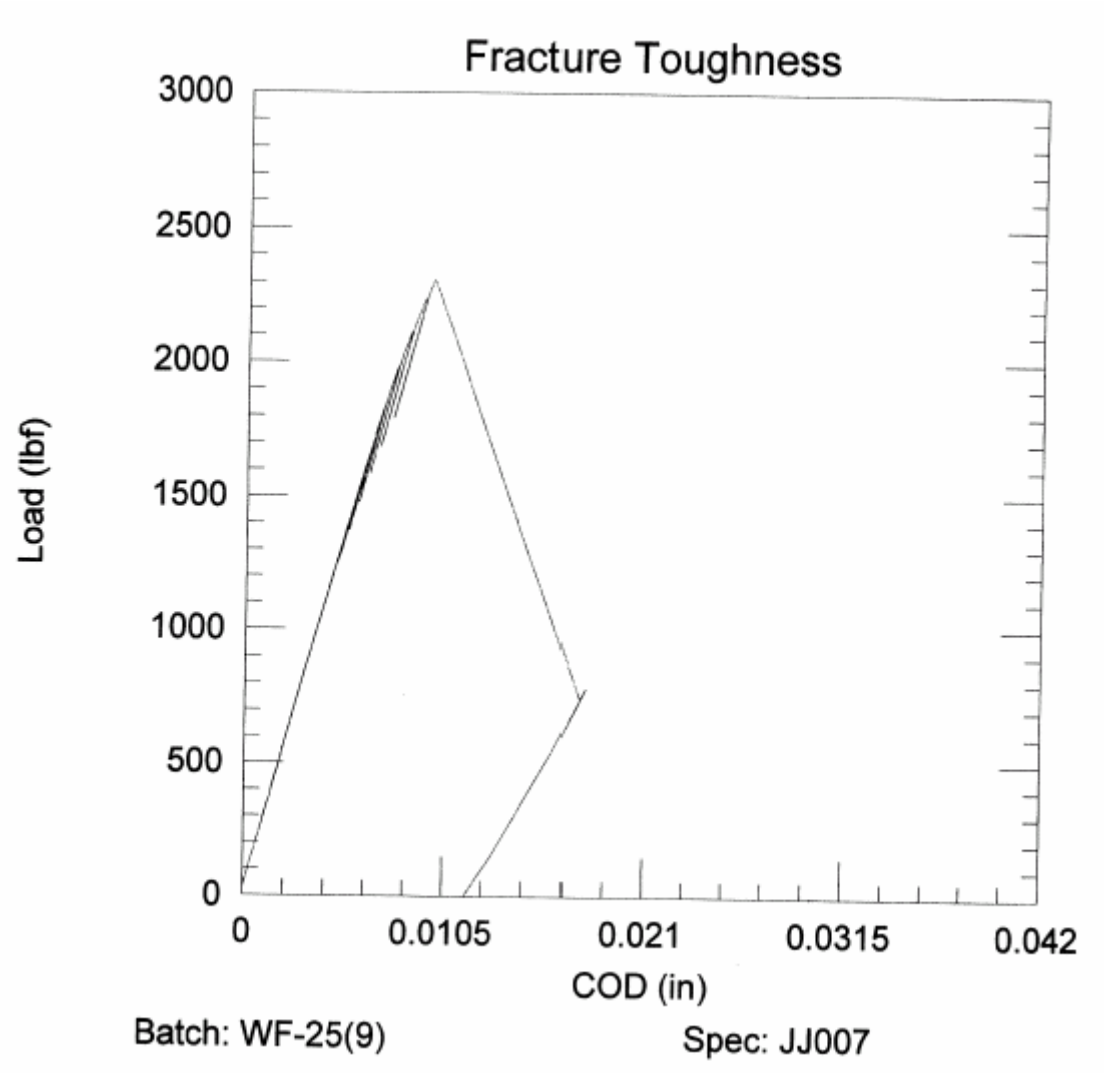

Figure B-48. Load-COD Plot for WF-25(9) 0.394 TC(T) Toughness Specimen JJ010 (110 °F)

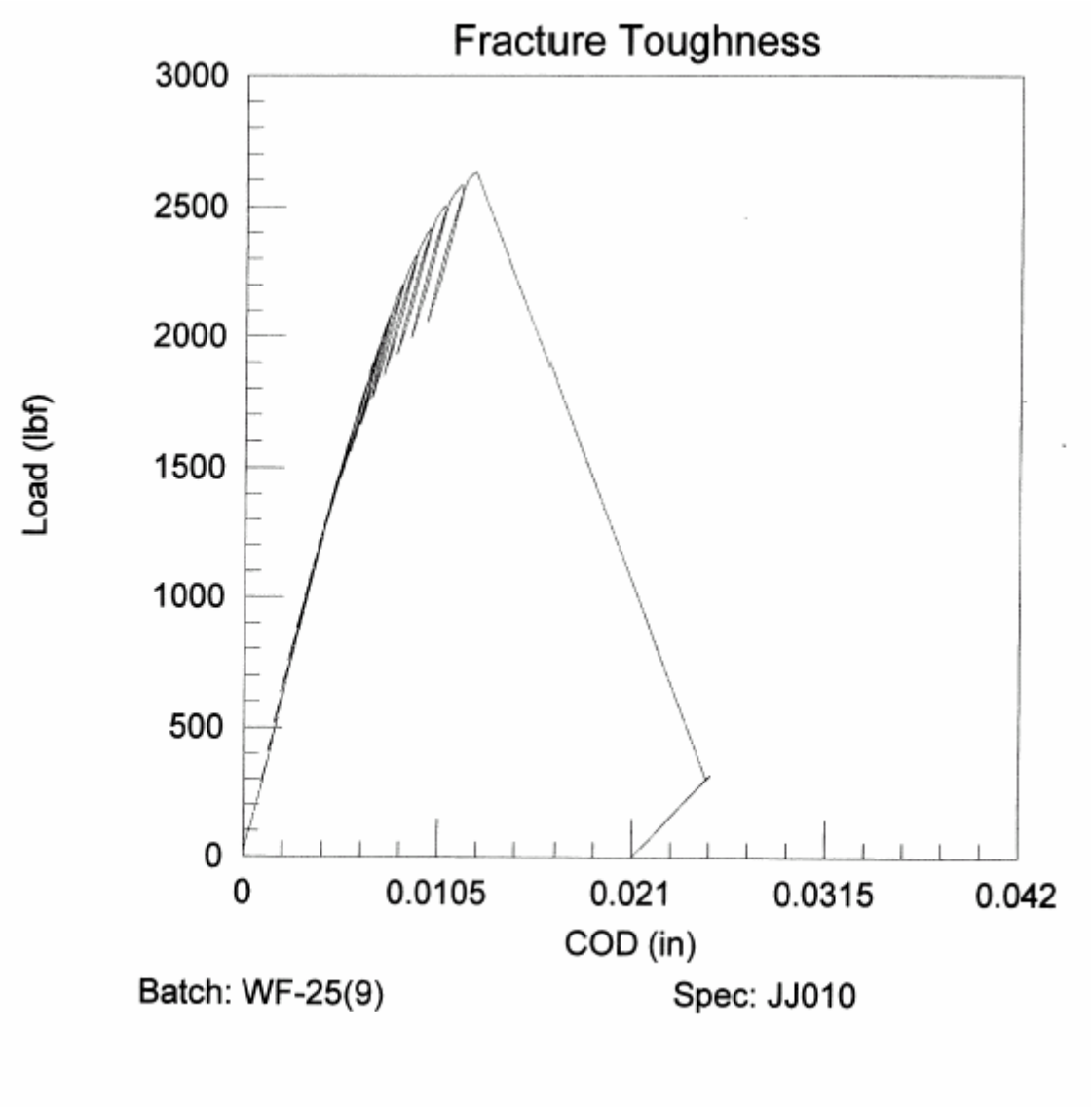

APPENDIX C

Fluence Analysis Methodology

C.1. Introduction

The primary tool used in the determination of the flux and fluence exposure to the capsule dosimetery is the two-dimensional discrete ordinates transport code DORT.[C-1]

The TMI2-LG2 capsule was located at 10.9° (off of the major axis) for cycles 7 through 12. The power distributions in the cycle 7-12 irradiation were symmetric both in θ and Z. That is, the axial power shape is roughly the same for any angle and, conversely, that the azimuthal power shape is the same for any height. This means that the neutron flux at some point (R, θ, Z) can be considered to be a separable function of (R, θ) and (R, Z). Therefore, the cycle 7-12 irradiation can be modeled using the standard Framatome ANP synthesis procedures.[C-2]

Figure C-1 depicts the analytical procedure that is used to determine the fluence accumulated over each irradiation period. As shown in the figure, the analysis is divided into seven tasks: (1) generation of the neutron source, (2) development of the DORT geometry models, (3) calculation of the macroscopic material cross sections, (4) synthesis of the results, and (5-7) estimation of the calculational bias, the calculational uncertainty, and the final fluence. Each of these tasks is discussed in greater detail in the following sections.

C.2. Generation of the Neutron Source

The time-averaged space and energy-dependent neutron sources for cycles 7-12 were calculated using the SORREL[C-3] code. The effects of burnup on the spatial distribution of the neutron source were accounted for by calculating the cycle average fission spectrum for each fissile isotope on an assembly-by-assembly basis, and by determining the cycle-average specific neutron emission rate. This data was then used with the normalized time weighted average pin-by-pin relative power density (RPD) distribution to determine the space and energy-dependent neutron source. The azimuthally averaged, time averaged axial power shape in the peripheral assemblies was used with the fission spectrum of the peripheral assemblies to determine the neutron source for the axial DORT run. These two neutron source distributions were input to DORT as indicated in Figure C-1.

C.3. Development of the Geometrical Models

The system geometry models for the mid-plane (R, θ) DORT were developed using standard Framatome ANP interval size and configuration guidelines. The Rθ model for the cycle 7-12

analysis extended radially from the center of the core to 2 feet into the concrete shield, and azimuthally from the major axis to 45°. The axial model extended from core plate to core plate, and from the center of the core out into the concrete shield. The geometrical models either met or exceeded all guidance criteria concerning interval size that are provided in Reg Guide-1.190.[C-4] In all cases, cold dimensions were used. The geometry models were input to the DORT code as indicated in Figure C-1.

C.4. Calculation of Macroscopic Material Cross Sections

In accordance with Reg Guide 1.190, the BUGLE-93[C-5] cross section library was used. The GIP code[C-6] was used to calculate the macroscopic energy-dependent cross sections for all materials used in the analysis – from the core out through the cavity and into the concrete and from core plate to core plate. The ENDF/B6 dosimeter reaction cross sections were used to generate the response functions that were used to calculate the DORT-calculated "saturated" specific activities.

The cross sections, geometry, and appropriate source were combined to create a set of DORT models (Rθ and RZ) for the cycle 7-12 analysis. Each Rθ and RZ DORT run utilized a cross section Legendre expansion of three (P_3), seventy directions (S_{10}), with the appropriate boundary conditions. A theta-weighted flux extrapolation model was used, and all other requirements of Reg Guide 1.190 that relate to the various DORT parameters were either met or exceeded for all DORT runs.

Figure C-1. Fluence Analysis Methodology for TMI2-LG2 Capsule DORT Analyses

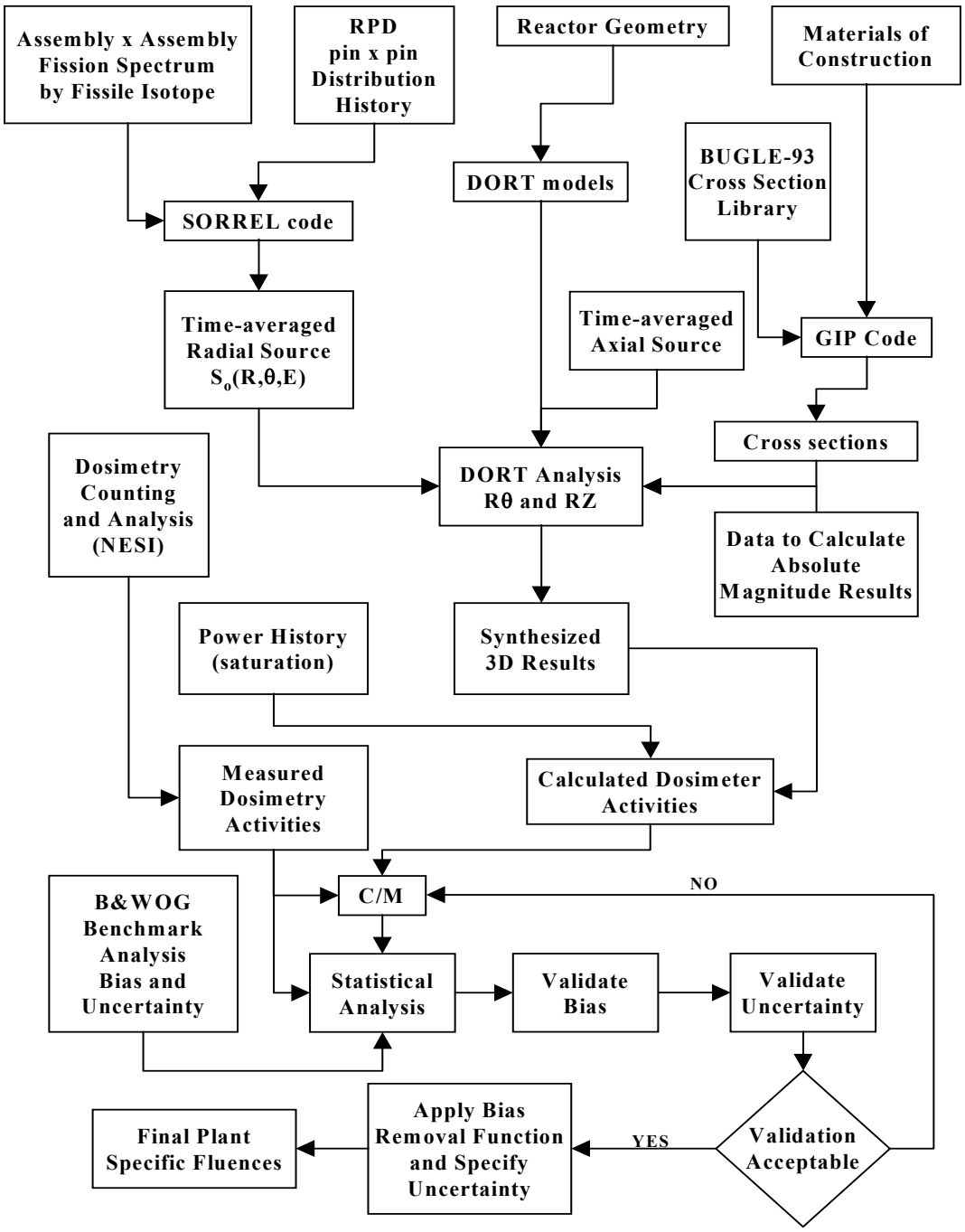

C.5. Synthesized Three Dimensional Results

The DORT analyses produced two sets of two-dimensional flux distributions, one for a vertical cylinder and one for the radial plane for each set of dosimetry. The vertical cylinder, which will be referred to as the RZ plane, is defined as the plane bounded axially by the upper and lower grid plates and radially by the center of the core and a vertical line within the concrete shield. The horizontal plane, referred to as the Rθ plane, is defined as the plane bounded radially by the center of the core and a point located 2 m into the concrete shield, and azimuthally by the major axis and the adjacent 45° radius. The vessel flux, however, varies significantly in all three cylindrical-coordinate directions (R, θ , Z). This means that if a point of interest is outside the boundaries of both the R-Z DORT and the R-θ DORT, the true flux cannot be determined from either DORT run. Under the assumption that the three-dimensional flux is a separable function,[C-2] both two-dimensional data sets were mathematically combined to estimate the flux at all three-dimensional points (R, θ, Z) of interest. The synthesis procedure outlined in Reg Guide 1.190 forms the basis for the Framatome ANP flux-synthesis process.

C.6. Calculated Activities and Measured Activities

The calculated activities for each dosimeter type "d" were determined using the following equation:

$$C_d = \sum_{g=1}^{G} \phi_g(\vec{r}_d) \times RF_g^d \times B_d \times NSF$$

where

C_d	…	calculated specific activity for dosimeter "d" in μCi of product isotope per gram of target isotope
$\phi_g(\vec{r}_d)$	…	three dimensional flux for dosimeter "d" at position $\vec{r}_d$ for energy group "g"
RF_g^d	…	dosimeter response function for dosimeter "d" and energy group "g"
B_d	…	bias correction factors for dosimeter "d"
NSF	…	non-saturation correction factor (NSF).

The bias correction factors (B_d) in the specific activity calculation above are listed in Table C-1.

Table C-1. Bias Correction Factors

Dosimeter Type	Bias
Activation	Short Half Life
Fission	Photofission
	Impurities

A photofission factor was applied to correct for the fact that some of the ^{137}Cs atoms present in the dosimeter were produced by (γ, f) reactions and were not accounted for in DORT analysis. Short half-life corrections were applied to the Fe and Ni dosimeter calculations, while impurity correction factors were insignificant and were not applied.

C.7. C/M Ratios

The following explanations will define the meanings of the terms "measurements" (M) and "calculations" (C) as used in this analysis:[C-2]

- Measurements: The meaning of the term "measurements" as used by Framatome ANP and the B&WOG is the measurement of the physical quantity of the dosimeter (specific activity) that responded to the neutron fluence, not to the "measured fluence." For the example of an iron dosimeter, a reference to the measurements means the specific activity of ^{54}Mn in μCi/g, which is the product isotope of the dosimeter reaction:

$$^{54}Fe + {}^{1}_{0}n \rightarrow {}^{54}Mn + p^{+}$$

- Calculations: The calculational methodology produces two primary results – the calculated dosimeter activities and the neutron flux at all points of interest. The meaning of the term "calculations" as used by Framatome ANP and the BWOG is the calculated dosimeter activity. The calculated activities are determined in such a way that they are directly comparable to the measurement values, but without recourse to the measurements. That is, the calculated values are determined by the DORT calculation and are directly comparable to the measurement values. ENDF/B6 based dosimeter reaction cross sections[C-7] and response functions were used in determining the calculated values for each individual dosimeter. In summary, it should be stressed

that the calculation values in the Framatome ANP approach[C-2] are independent of the measurement values.

C.8. Uncertainty

The TMI2-LG2 fluence predictions are based on the methodology described in the Framatome ANP "Fluence and Uncertainty Methodologies" topical report, BAW-2241P-A.[C-2] The time-averaged fluxes, and thereby the fluences throughout the reactor, and vessel are calculated with the DORT discrete ordinates computer code using three-dimensional synthesis methods. The basic theory for synthesis is described in Section 3.0 of the topical and the DORT three-dimensional synthesis results are the bases for the fluence predictions using the Framatome ANP "Semi-Analytical" (calculational) methodology.

The uncertainties in the TMI2-LG2 fluence values have been evaluated to ensure that the greater than 1.0 MeV calculated fluence values are accurate (with no discernible bias) and have a mean standard deviation that is consistent with the Framatome ANP benchmark database of uncertainties. Consistency between the fluence uncertainties in the updated calculations for the TMI2-LG2 capsule, and those in the Framatome ANP benchmark database ensures that the vessel fluence predictions are consistent with the 10 CFR 50.61, Pressurized Thermal Shock (PTS) screening criteria and the Regulatory Guide 1.99[C-8] embrittlement evaluations.

The verification of the fluence uncertainty for the TMI2-LG2 capsule includes:

- estimating the uncertainties in the TMI2-LG2 dosimetry measurements,
- estimating the uncertainties in the TMI2-LG2 capsule benchmark comparison of calculations to measurements,
- estimating the uncertainties in the cycles TMI2-LG2 specimen fluences, and
- determining if the specific measurement and benchmark uncertainties of the TMI2-LG2 capsule is consistent with the Framatome ANP database of generic uncertainties in the measurements and calculations.

The embrittlement evaluations in Regulatory Guide 1.99 and those in 10 CFR 50.61 for the PTS screening criteria apply a margin term to the reference temperatures. The margin term includes the product of a confidence factor of 2.0 and the mean embrittlement standard deviation. The factor of 2.0 implies a very high level of confidence in the fluence uncertainty as well as the uncertainty in the other variables contributing to the embrittlement. The dosimeter measurements from the TMI2-LG2 analysis would not directly support this high level of

confidence. However, the dosimeter measurement uncertainties are consistent with the Framatome ANP database. Therefore, the calculational uncertainties in the updated fluence predictions for TMI2-LG2 are supported by 728 additional dosimeter measurements and thirty-nine benchmark comparisons of calculations to measurements as shown in Appendix A of the topical.[C-2] The calculational uncertainties are also supported by the fluence sensitivity evaluation of the uncertainties in the physical and operational parameters, which are included in the vessel fluence uncertainty.[C-2] The dosimetry measurements and benchmarks, as well as the fluence sensitivity analyses in the topical are sufficient to support a 95 percent confidence level, with a confidence factor of ±2.0, in the fluence results from the "Semi-Analytical" methodology.

The Framatome ANP generic uncertainty in the dosimetry measurements has been determined to be unbiased and has an estimated standard deviation of 7.0 percent for the qualified set of dosimeters. The TMI2-LG2 dosimetry measurement uncertainties were evaluated to determine if any biases were evident and to estimate the standard deviation. The dosimetry measurements were found to be appropriately calibrated to standards traceable to the National Institute of Standards and Technology and are thereby unbiased by definition. The mean measurement uncertainties associated with the TMI2-LG2 capsule is as follows:

5.113% for TMI2-LG2.

These values were determined from Equation 7.6 in the topical and indicate that there is consistency with the Framatome ANP database. Consequently, when the Framatome ANP database is updated, the TMI2-LG2 capsule dosimetry measurement uncertainties may be combined with the other 728 dosimeters. Since the TMI2-LG2 measurements are consistent with the Framatome ANP database, it is estimated that the capsule dosimeter measurement uncertainties may be represented by the Framatome ANP database standard deviation of 7.0 percent. Based on the Framatome ANP database, there appears to be a 95 percent level of confidence that 95 percent of the TMI2-LG2 dosimetry measurements, for fluence reactions above 1.0 MeV, are within ±14.2 percent of the true values.

The Framatome ANP generic uncertainty for benchmark comparisons of dosimetry calculations relative to the measurements indicates that any benchmark bias in the greater than 1.0 MeV result is too small to be uniquely identified. The estimated standard deviation between the calculations and measurements is 9.9 percent. This implies that the root mean square deviation between the Framatome ANP calculations of the TMI2-LG2 dosimetry and the measurements should be approximately 9.9 percent in general and bounded by ±20.04 percent for a 95 percent confidence interval with thirty-nine independent benchmarks.

The weighted mean values of the ratio of calculated dosimeter activities to measurements (C/M) for TMI2-LG2 have been statistically evaluated using Equation 7.15 from the topical. The standard deviations in the benchmark comparisons are as follows:

$$\sigma_{\frac{C}{M}} = 6.512\% \text{ for TMI2-LG2.}$$

This standard deviation indicates that the benchmark comparisons are consistent with the Framatome ANP database. Consequently, when the Framatome ANP database is updated, the TMI2-LG2 benchmark uncertainties may be included with the other thirty-nine benchmark uncertainties in the topical. The consistency between the capsule's benchmark uncertainties and those in the Framatome ANP database indicates that the fluence calculations for the specimens within the TMI2-LG2 capsules has no discernible bias in the greater than 1.0 MeV fluence values. In addition, the consistency indicates that the fluence values can be represented by the Framatome ANP reference set, which includes a calculational standard deviation of 7.0 percent at the dosimetry locations. That is:

$$\sigma_{CapsuleFluence} =\leq 7.00\%$$

C.9. References

C-1. Rutherford, M. A., N. M. Hassan, et. al., Eds., *"DORT, Two Dimensional Discrete Ordinates Transport Cod,."* BWNT-TM-107, Framatome Technologies, Inc., Lynchburg, Virginia, May 1995.*

C-2. Worsham, J.R., et al., "*Fluence and Uncertainty Methodologies*," BAW-2241P-A, Revision 1, Framatome Technologies, Inc., Lynchburg, Virginia, April 1999.*

C-3. Hassler, L. A., and N. M. Hassan, *"SORREL, DOT Input Generation Code User's Manual*," NPGD-TM-427, Revision 10, Framatome ANP, Lynchburg, Virginia, May 2001.*

C-4. U.S. Nuclear Regulatory Commission, "*Calculational and Dosimetry Methods for Determining Pressure Vessel Neutron Fluence*," Regulatory Guide 1.190, March 2001.

C-5. Ingersoll, D. T., et. al., "*BUGLE-93, Production and Testing of the VITAMIN-B6 Fine Group and the BUGLE-93 Broad Group Neutron/photon Cross-Section Libraries Derived from ENDF/B-VI Nuclear Data*," ORNL-DLC-175, Radiation Safety Information Computational Center, Oak Ridge National Laboratory, Oak Ridge, Tennessee, April 1994.

C-6. Hassler, L. A. and N. M. Hassan, "*GIP User's Manual for B&W Version, Group Organized Cross Section Input Program*," NPGD-TM-456, Revision 11, Framatome Technologies, Inc., Lynchburg, Virginia, August 1994.*

C-7. Worsham, J. R., "*BUGLE-93 Response Functions*," FTG Document Number 32-1232719-00, Revision 0, Framatome Technologies, Inc., Lynchburg, Virginia, June 1995.*

C-8. U.S. Nuclear Regulatory Commission, *"Radiation Embrittlement of Reactor Vessel Materials*," Regulatory Guide 1.99, Revision 2, May 1998.

*- Available from Framatome ANP, Lynchburg, Virginia.

APPENDIX D

Fracture Toughness Specimen Dimensions and Pre-crack Length

Table D-1. Fracture Toughness Specimen Dimensions and Precrack Length for Irradiated SA-1526 Specimens

Specimen Identification	Thickness (in)	Net Thickness (in)	Width (in)	Precrack Length (in)	Specimen Geometry
Specimen Fluence: 1.812 x 10^{19} n/cm^2 (E>1 MeV)					
PP014	0.394	N/A	0.394	0.204	PCS[(a)]
PP015	0.394	N/A	0.394	0.204	PCS
PP016	0.394	N/A	0.394	0.207	PCS
PP017	0.394	N/A	0.394	0.207	PCS
PP018	0.394	N/A	0.394	0.208	PCS
PP019	0.394	N/A	0.394	0.205	PCS
PP020	0.394	N/A	0.394	0.206	PCS
PP021	0.394	N/A	0.394	0.209	PCS
PP022	0.394	N/A	0.394	0.202	PCS
Specimen Fluence: 1.548 x 10^{19} n/cm^2 (E>1 MeV)					
PP006	0.500	N/A	1.000	0.524	0.5TC(T)
PP009	0.500	N/A	1.000	0.518	0.5TC(T)
PP013	0.500	N/A	1.000	0.517	0.5TC(T)
PP015	0.500	N/A	1.000	0.517	0.5TC(T)
Specimen Fluence: 1.787 x 10^{19} n/cm^2 (E>1 MeV)					
PP007	0.394	N/A	0.788	0.416	0.394TC(T)
PP010	0.394	N/A	0.788	0.403	0.394TC(T)
Specimen Fluence: 1.585 x 10^{19} n/cm^2 (E>1 MeV)					
PP004	0.936	0.749	1.871	1.179	0.936TDC(T)

(a) Precracked Charpy-size single edge notch bend, SE(B), specimen.

Table D-2. Fracture Toughness Specimen Dimensions and Precrack Length for Irradiated WF-25(6) Specimens

Specimen Identification	Thickness (in)	Net Thickness (in)	Width (in)	Precrack Length (in)	Specimen Geometry
Specimen Fluence: 1.595 x 10^{19} n/cm^2 (E>1 MeV)					
QQ013	0.394	N/A	0.394	0.207	PCS[(a)]
QQ014	0.394	N/A	0.394	0.214	PCS
QQ015	0.394	N/A	0.394	0.208	PCS
QQ016	0.394	N/A	0.394	0.211	PCS
QQ017	0.394	N/A	0.394	0.204	PCS
QQ018	0.394	N/A	0.394	0.207	PCS
QQ020	0.394	N/A	0.394	0.206	PCS
QQ021	0.394	N/A	0.394	0.204	PCS
QQ019	0.394	N/A	0.394	0.203	PCS
Specimen Fluence: 1.557 x 10^{19} n/cm^2 (E>1 MeV)					
QQ002	0.500	N/A	1.000	0.536	0.5TC(T)
QQ003	0.500	N/A	1.000	0.526	0.5TC(T)
QQ005	0.500	N/A	1.000	0.508	0.5TC(T)
QQ008	0.500	N/A	1.000	0.522	0.5TC(T)
Specimen Fluence: 1.258 x 10^{19} n/cm^2 (E>1 MeV)					
QQ001	0.394	N/A	0.788	0.404	0.394TC(T)
Specimen Fluence: 1.787 x 10^{19} n/cm^2 (E>1 MeV)					
QQ002	0.394	N/A	0.788	0.414	0.394TC(T)
Specimen Fluence: 1.585 x 10^{19} n/cm^2 (E>1 MeV)					
QQ002	0.936	0.749	1.871	1.139	0.936TDC(T)

(a) Precracked Charpy-size single edge notch bend, SE(B), specimen.

Table D-3. Fracture Toughness Specimen Dimensions and Precrack Length for Irradiated WF-25(9) Specimens

Specimen Identification	Thickness (in)	Net Thickness (in)	Width (in)	Precrack Length (in)	Specimen Geometry
Specimen Fluence: 1.235 x 10^{19} n/cm^2 (E>1 MeV)					
JJ001	0.394	N/A	0.394	0.205	PCS[(a)]
JJ002	0.394	N/A	0.394	0.204	PCS
JJ003	0.394	N/A	0.394	0.207	PCS
JJ004	0.394	N/A	0.394	0.209	PCS
JJ005	0.394	N/A	0.394	0.206	PCS
JJ007	0.394	N/A	0.394	0.207	PCS
JJ008	0.394	N/A	0.394	0.206	PCS
JJ010	0.394	N/A	0.394	0.206	PCS
JJ006	0.394	N/A	0.394	0.209	PCS
Specimen Fluence: 1.565 x 10^{19} n/cm^2 (E>1 MeV)					
JJ004	0.500	N/A	1.000	0.510	0.5TC(T)
JJ005	0.500	N/A	1.000	0.519	0.5TC(T)
JJ006	0.500	N/A	1.000	0.531	0.5TC(T)
JJ007	0.500	N/A	1.000	0.520	0.5TC(T)
Specimen Fluence: 1.258 x 10^{19} n/cm^2 (E>1 MeV)					
JJ007	0.394	N/A	0.788	0.402	0.394TC(T)
JJ010	0.394	N/A	0.788	0.413	0.394TC(T)
Specimen Fluence: 1.585 x 10^{19} n/cm^2 (E>1 MeV)					
JJ002	0.936	0.749	1.871	1.168	0.936TDC(T)

(a) Precracked Charpy-size single edge notch bend, SE(B), specimen.